



# Antimicrobial properties of a Strontium-rich Hybrid System for bone regeneration

---

Dissertation for Master degree in Bioengineering

---

**LUÍS DANIEL MENDES BAPTISTA**

**PORTO, 2016**

**Supervisor:** Cristina Ribeiro, PhD

**Co-supervisor:** Inês Gonçalves, PhD



*“We are not going in circles, we are going upwards.  
The path is a spiral; we have already climbed many steps.”*

**Hermann Hesse, Siddhartha**



## Acknowledgements

I would like to show my gratitude to Dr<sup>a</sup>. Cristina Ribeiro and Dr<sup>a</sup>. Inês Gonçalves for the opportunity of being part of this project and for all the guidance provided everyday throughout this work.

To my work colleagues and friends whose presence and support was essential in the accomplishment of this journey. Yes, it was not just about work! I found great friendship and amazing people during this period with who I spend priceless moments. So, I give a special thanks to Andreia, Cláudia, Cláudia Monteiro, Daniel, Diana, Fabíola, Filipa, Inês, João, Micaela, Patricia, Ritinha, Zé. Also, my gratitude goes to the INEB team, especially to Ricardo Vidal for his willingness to help me on my work whenever I needed.

Finally, I will refer to the most important people in my life which accompanied me not only during my Dissertation but during all my life, so, to my brother Joãozito; cousins: Monica, Tiagão, Raquel, Tiago, and little M; parents: Mã and Pai; and uncles: Tia Dida and Tio Mané, for everything...

This work was financially supported by Project POCI-01-0145-FEDER-007274 - Institute for Research and Innovation in Health Sciences, funded by FEDER funds through COMPETE2020 - Programa Operacional Competitividade e Internacionalização (POCI) – and by national funds through FCT - Fundação para a Ciência e a Tecnologia.



## Abstract

The technological evolution brought an increase in life expectancy leading to the rise of “age related diseases”. Only in European Union., 27.5 million people, mostly elderly, suffer from osteoporosis which involves enormous costs both for patients and to the National Health Service as 3.5 million new fragility fractures with cost over € 37 billion, occur every year. So far, common healthcare treatment includes surgical implantation of bone grafts or bone substitutes, procedures which are related with some drawbacks. For instance, implant-related infections during surgery are still a major threat and, only in USA, costs \$1.2 billion, each year. Opportunistic pathogenic *S. aureus* and *S. epidermidis* are usually associated to bone infections during surgery comprising over 66% of the orthopaedic implant associated infections which treatment comprises the misuse of antibiotics directly related with the appearance of multi-drug resistant bacterial pathogenic strains. According to the previously stated, there is an urge to develop a new class of biomaterials that can both promote the bone regeneration and exhibit antimicrobial properties.

The enthusiastic alternative presented is based on the incorporation of strontium in both alginate discs and ceramic materials microspheres, which comprises a strontium-rich Injectable Hybrid System (HIS) of alginate polymeric matrix cross-linked *in situ* with Sr, and reinforced with Sr-rich microspheres. In this sense, the antimicrobial properties of strontium alone and comprised in alginate discs (Ca and Sr rich) and different type of ceramic microspheres ( $\mu$ HAp,  $\mu$ SrHAp – micrometric HAp; nHAp, nSrHAp – nanometric HAp; and SrTriP - strontium phosphate) were assessed against *S. aureus* and *S. epidermidis*.

The exposure of both *S. aureus* and *S. epidermidis* bacteria to strontium alone (as strontium chloride) revealed that strontium may be used as an effective inhibitory and bactericidal agent. Thus, MIC of 512 and 1024  $\mu$ g/mL and MBC of 1792 and 1536  $\mu$ g/mL were determined, respectively, for *S. aureus* and *S. epidermidis*.

Extracts of the discs towards *S. aureus* revealed that strontium was successfully released (maximum concentration of 114.36  $\mu$ g/mL after 72 hr), which is in agreement with an antimicrobial leaching system. Generally, the alginate discs exhibited low activity against both *S. epidermidis* and *S. aureus*, as no metabolic activity inactivation and no reduced culturability were achieved. Despite that, high metabolic activity reduction was achieved for *S. epidermidis* when exposed to ND extract (in PBS) of Sr rich alginate discs.

The produced microspheres were characterized in terms of morphology, surface porosity and elementary composition recurring to SEM/EDS analysis. SrTriP microspheres revealed the highest percentage of strontium incorporation – 65.4% wt (29.3% At); followed by the nSrHAp – 7.4% wt (2.1% At) and the  $\mu$ SrHAp – 4.3% wt (1.2% At). Microspheres

formulated with micrometric and nanometric HAp presented a completely different surface microarchitecture. As a result, the micrometric HAp presented a network structure with higher porosity and surface area than nanometric HAp. Extracts of the microspheres revealed also successful release of the strontium ions over time with a maximum release of 107.12 µg/mL for SrTriP microspheres after 21 days.

Concerning the experiments with microspheres and powders extracts, nHAp, nSrHAp, SrTriP and pSrTriP presented the best metabolic inactivations (total inactivation for SrTriP extract) and culturability reductions, despite a maximum of 23% bacterial killing (for SrTriP extract). Regarding the strontium rich ceramic microspheres experiments in direct contact, nHAp, nSrHAp and SrTriP presented good antimicrobial properties against *S. aureus*. Generally, high metabolic activity reductions were obtained for these microspheres, with a maximum of 100% for both nSrHAp and SrTriP. Moreover, good culturability reductions were attained, exhibiting a maximum of 52% for SrTriP after 6 hours exposure which presented, generally, better results than 24 hours exposure.

From a general perspective, there is a direct correlation between the incorporated strontium in the microspheres and its antimicrobial activity. As said, an increase in strontium, reveals an increase in metabolic and culturability reduction of *S. aureus*. According to the results obtained, the dual combination of Sr-rich alginate with Sr-rich microspheres could exhibit high potential in the implant biomaterials development for bone regeneration and bacterial infection prevention, and should be further analysed.

Overall, the acquired results highlight the potential of IHS as an emergent strategy for preventing bone surgery related infections and its drawbacks, namely *S. aureus* and *S. epidermidis*, as well as to enhance the osteogenic regeneration.



## Resumo

O rápido desenvolvimento tecnológico é responsável pelo aumento da esperança média de vida que leva ao aparecimento de doenças relacionadas com a idade. Só na União Europeia, 27.5 milhões de pessoas, na sua maioria idosos, sofrem de osteoporose situação que envolve enormes custos tanto para o paciente como para os Serviços nacionais de Saúde sendo que 3.5 milhões de novas fracturas patológicas ocorrem todos os anos com custos que ultrapassam os € 37 mil milhões. Até à data, o tratamento comum para este tipo de patologia inclui a implantação cirúrgica de enxertos ósseos ou materiais substitutos do osso. No entanto, estes procedimentos têm desvantagens, nomeadamente, o aparecimento de infeções relacionadas com implantes que é ainda uma grande preocupação nos dias de hoje. Só nos EUA, custam cerca de \$ 1.2 mil milhões, por ano. Bactérias patogénicas oportunistas como *S. aureus* e *S. epidermidis* estão geralmente associadas a este tipo de infeções do osso (66 % dos casos). O uso descontrolado de antibióticos no tratamento corrente de infeções destas estirpes tem levado a ao aparecimento de bactérias patogénicas multi-resistentes. Assim, é necessário o desenvolvimento de uma nova classe de biomateriais que tenham a capacidade de, para além de promoverem a regeneração óssea, exibirem propriedades antimicrobianas.

A nova alternativa apresentada baseia-se na incorporação de estrôncio em discos de alginato e em microesferas cerâmicas, num Sistema Híbrido Injectável (IHS). Este sistema é composto por uma matriz polimérica de alginato reticulada *in situ* com estrôncio e reforçada com microesferas ricas em estrôncio. Neste sentido, foram avaliadas as propriedades antimicrobianas do estrôncio por si só e incorporado em discos de alginato (ricas em cálcio e em estrôncio) e em diferentes tipos de microesferas cerâmicas ( $\mu$ HAp,  $\mu$ SrHAp – HAp micrométricas; nHAp, nSrHAp – HAp nanométricas; e SrTriP –fosfato de estrôncio), contra a *S. aureus* e a *S. epidermidis*.

A análise da exposição de *S. aureus* e de *S. epidermidis* ao estrôncio, sob a forma de cloreto de estrôncio, revelou que o estrôncio tem propriedades inibitórias e bactericidas. Assim, foi obtida MIC de 512 e 1024  $\mu$ g/mL, e também MBC de 1792 e 1536  $\mu$ g/mL, para a *S. aureus* e *S. epidermidis*, respectivamente.

Os extractos de discos contra a *S. aureus* revelaram que o estrôncio foi libertado com sucesso (concentração máxima de 114.36  $\mu$ g/mL após 72h), o que está de acordo com um sistema antimicrobiano de “leaching”. De uma forma geral, os discos de alginato exibiram reduzida actividade contra as duas estirpes, de tal forma que não foram obtidas redução significativa da actividade metabólica e redução na culturabilidade. No entanto,

elevada redução da actividade metabólica foi conseguida para a *S. epidermidis* quando exposta ao extracto ND (em PBS) dos disco de alginato ricos em estrôncio.

As microesferas produzidas foram caracterizadas em termos de morfologia, porosidade de superfície e composição elementar com recurso a análise SEM/EDS. As microesferas de SrTriP revelaram a maior percentagem de incorporação de estrôncio – 65.4 % wt (29.3% At); seguida por nSrHAp – 7.4% wt (2.1% At) e ainda  $\mu$ SrHAp – 4.3% wt (1.2% At). As microesferas formuladas com HAp micrométrica e nanométrica apresentaram uma microarquitECTURA de superfície completamente diferente. Deste modo, a microesfera de HAp micrométrica apresentou uma rede estrutural com maior porosidade e área de superfície do que a HAp nanométrica. Os extractos das microesferas revelaram também libertação de estrôncio ao longo do tempo com uma libertação máxima de 107.12  $\mu$ g/mL para microesferas de SrTriP ao fim de 21 dias.

Tendo em conta os ensaios com extractos de microesferas e de pós, nHAp, nSrHAp, SrTriP e pSrTriP apresentaram as melhores inactivações metabólicas (inactivação total para o extracto de SrTriP) e melhores reduções de culturabilidade, apesar de ser obtido um máximo de apenas 23 % para os extractos de SrTriP. Relativamente aos ensaios com microesferas cerâmicas ricas em estrôncio em contacto directo, nHAp, nSrHAp e SrTriP exibiram boa actividade antimicrobiana contra a *S. aureus*. De uma forma geral, foram obtidas elevadas reduções da actividade metabólica para estas microesferas com um máximo de 100% para tanto nSrHAp como SrTriP. Para além disso, foram também obtidas reduções a culturabilidade significativas, com um máximo de 52 % para o SrTriP após 6 h de exposição o que, no geral, apresentaram melhores resultados do que para 24 h de exposição.

Numa perspectiva global, pode ser verificada uma relação directa entre a incorporação de estrôncio nas microesferas e a sua actividade antimicrobiana. Deste modo, um aumento de estrôncio revelou um aumento nas reduções da actividade metabólica e culturabilidade contra *S. aureus*. Tendo em conta os resultados obtidos, a combinação dupla de alginato rico em estrôncio com as microesferas ricas em estrôncio poderá ter um elevado potencial no desenvolvimento de biomateriais para implantes destinados à regeneração óssea, e, por isso, devem ser meticolosamente revistos.

De uma forma geral, os resultados obtidos evidenciam o potencial do IHS como uma estratégia emergente na prevenção de infeções relacionadas com a cirurgia óssea, bem como os seus inconvenientes, nomeadamente no caso da *S. aureus* e da *S. epidermidis*, bem como na potenciação da regeneração osteogénica.

## Table of contents

<b>Acknowledgements</b> .....	<b>v</b>
<b>Abstract</b> .....	<b>vii</b>
<b>Resumo</b> .....	<b>ix</b>
<b>List of tables</b> .....	<b>xiii</b>
<b>List of figures</b> .....	<b>xv</b>
<b>Glossary</b> .....	<b>xix</b>
<b>Chapter 1   Work outline</b> .....	<b>1</b>
1. Background and project presentation.....	1
1.1. Research objectives .....	2
3. Thesis organization.....	4
<b>Chapter 2   Literature review</b> .....	<b>5</b>
1. The need for bone implant materials – socioeconomic background .....	5
2. Bone structure and properties (an overview).....	7
3. Synthetic bone substitutes .....	8
3.1. Alginate based biomaterials .....	8
3.2. Bioceramics.....	11
3.4. Osteoinduction, osteoconduction and osseointegration .....	13
4. Infection after surgery .....	15
5. Pathogenic <i>Staphylococcus aureus</i> and <i>Staphylococcus epidermidis</i> .....	18
6. Prevention of bacterial infection: the window of opportunity before biofilm development .....	19
7. Antimicrobial systems: contact and leaching.....	21
8. Metal ions as antimicrobial agents and its incorporation in biomaterials.....	23
9. The potential of Strontium .....	24
9.1. Strontium incorporation and distribution in bone .....	24
9.2. Effects of strontium in modified biomaterials.....	25
9.3. Strontium activity in bone regeneration.....	26
9.4. Strontium cytotoxicity .....	28
9.5. Strategies using strontium as antimicrobial.....	29
9.6. Strontium antimicrobial mechanism of action.....	35
<b>Chapter 3   Materials and Methods</b> .....	<b>37</b>
3.1. Strontium chloride solutions .....	37
3.1.1. Preparation of the strontium chloride solutions. ....	37
3.2. Ca- and Sr-rich alginate discs.....	37
3.2.1. Ca- and Sr-rich alginate discs production .....	37
3.2.2. Preparation of Ca- and Sr-rich alginate discs' extracts.....	38
3.2.3. Ca and Sr release from the Ca- and Sr-rich alginate discs.....	39
3.3. Ca- and Sr-rich microspheres.....	39

3.3.1. Ca- and Sr-rich microspheres preparation .....	39
3.3.2. Ca- and Sr-rich microsphere characterization .....	40
3.3.2.3. Zeta Potential analysis .....	41
3.3.3. Preparation of Ca- and Sr-rich microsphere and powders extract .....	41
3.3.4. Ca and Sr release from the microspheres and powders .....	41
3.4. Antimicrobial assessment .....	41
3.4.1. Bacterial strains and growth conditions.....	41
3.4.2. Minimum inhibitory concentration (MIC) and minimum bactericidal concentration (MBC) .....	42
3.4.3. Direct exposure of microspheres and powders .....	44
3.5. Statistical analysis.....	45
<b>Chapter 4   Results and Discussion .....</b>	<b>47</b>
4.1. Bactericidal activity of SrCl <sub>2</sub> solutions .....	47
4.2. Characterization and antimicrobial activity of the injectable hybrid system.....	53
4.2.1. Characterization of the Ca- and Sr-rich alginate discs extracts.....	53
4.2.2. Bactericidal activity of the Ca- and Sr-rich alginate discs extracts.....	54
4.2.3. Characterization of the Ca- and Sr-doped microspheres and powders and its extracts .....	59
4.2.4. Bactericidal activity of the Ca- and Sr-doped microspheres and powders and its extracts.....	65
<b>Chapter 5  Concluding remarks and future perspectives .....</b>	<b>73</b>
5.1. General conclusions .....	73
5.2. Future research perspectives.....	75
<b>References .....</b>	<b>77</b>
<b>Appendix .....</b>	<b>I</b>
Appendix 1 – SEM/EDS analysis. Size (diameter) and EDS analysis of the produced microspheres .....	II
Appendix 2 – MIC after challenging <i>S. aureus</i> to 72h microspheres and powders extracts.....	IV
Appendix 3 – Antimicrobial evaluation of the 21 days microspheres extracts towards <b><i>S. aureus</i></b> .....	V
Appendix 4 - Gradual changes in turbidity of the medium after 24h direct exposure .... towards <i>S. aureus</i> .....	VII

## List of tables

<b>Table 1.</b> Type, place and application of ionic substitutions on the HAp structure. ....	13
<b>Table 2.</b> Metal and metalloids used as antimicrobials (elements presented by their chemical symbol).....	24
<b>Table 3 –</b> Percentages of metabolic activity inhibition and percentage of death for <i>S. epidermidis</i> and <i>S. aureus</i> after exposure to several SrCl <sub>2</sub> solution concentrations. ....	50
<b>Table 4 –</b> MIC and MBC values for <i>S. epidermidis</i> and <i>S. aureus</i> after exposure to SrCl <sub>2</sub> solutions. ....	50
<b>Table 5 –</b> Percentages of metabolic activity inhibition and percentages of death for <i>S. epidermidis</i> and <i>S. aureus</i> after exposure to 48 hr and 72 hr Sr-rich and Ca-rich alginate discs extracts and its dilutions.....	58
<b>Table 6 –</b> Zeta potential (ZP) analysis of the produced microspheres.....	62
<b>Table 7 -</b> Percentages of metabolic activity inhibition and percentages of death for <i>S. aureus</i> after exposure to 72 hr extracts of the microspheres and powders. ....	68
<b>Table 8-</b> Percentages of metabolic activity inhibition and percentages of death for <i>S.aureus</i> after direct exposure of 6 hr and 24 hr to the microspheres and powders .....	72



## List of figures

<b>Figure 1</b> - Graphical abstract. Separated components of the injectable hybrid system and its antimicrobial dynamics. ....	3
<b>Figure 2 – Representation of the alginate structure. A –</b> Representation of the 1,4-linked $\beta$ -D.mannuronic acid (M) and of $\alpha$ -L guluronic acid (G) residues (adapted from <sup>30</sup> ). <b>B –</b> Representation of the alginate chemical structure. The three different forms of polymer segment arrangement are presented (in the figure it is represented the sodium alginate structure). ....	9
<b>Figure 3 –</b> Schematic representation of alginate cross-linking by $M^{2+}$ metal cations – “egg box” model where four G subunits are bound by one $M^{2+}$ ion. <sup>27</sup> (adapted from <sup>36</sup> ).....	10
<b>Figure 4.</b> Frequency of main pathogenic species found in clinical isolates from orthopaedic implant-associated infections (adapted from <sup>77</sup> ). ....	19
<b>Figure 5 –</b> Scheme of the potential strontium antimicrobial mechanisms of action <sup>148</sup> .....	36
<b>Figure 6–</b> Schematic representation of the production of the Ca- and Sr-alginate discs. .	38
<b>Figure 7 –</b> Schematic representation of the discs extracts preparation.....	38
<b>Figure 8 –</b> Schematic representation of the droplet extrusion method setup. Paste preparation and paste extrusion.....	40
<b>Figure 9 – Strontium chloride solution against <i>S. epidermidis</i> grown on TSB (A) and MHB (B).</b> A1 and B1 – Metabolic activity evaluation. Relative fluorescence units (RFU) are presented as a function of $SrCl_2$ concentration. A2, A3 and B2 – Bacteria culturability. CFUs count is presented as a function of $SrCl_2$ concentration. <i>S. epidermidis</i> represents the negative control (no treatment). Mean values $\pm$ standard deviation are illustrated. Bars marked with * are statistically different from the control and bars marked with (*) and brackets are statistically different between them ( $P < 0.05$ ). ....	48
<b>Figure 10 – Strontium chloride solutions against <i>S. aureus</i> grown on TSB.</b> A1 – Metabolic activity evaluation. Relative fluorescence units (RFU) are presented as a function of $SrCl_2$ concentration. A2 – Bacteria culturability. CFUs count is presented as a function of $SrCl_2$ concentration. <i>S. aureus</i> represents the negative control (no treatment). Mean values $\pm$ standard deviation are illustrated. Bars marked with * are statistically different from the control and bars marked with (*) and brackets are statistically different between them ( $P < 0.05$ ). ....	49
<b>Figure 11 –Strontium and calcium release from the alginate discs over time.</b> 1 hr, 24 hr, 48 hr, 72 hr and 7 days discs extracts (in TSB) were quantified regarding Sr (A) and Ca (B) composition ( $\mu g/mL$ ) by ICP-AES.....	53

**Figure 12 – Antimicrobial activity of Sr-rich discs extracts (in PBS) towards *S. epidermidis* grown on TSB (A) and MHB (B).** A1 and B1 – Metabolic activity evaluation. Relative fluorescence units (RFU) are presented as a function of extracts dilutions. A2 and B2 – Bacteria culturability. CFUs count is presented as a function of SrCl<sub>2</sub> concentration. *S. epidermidis* represents the negative control (no treatment). Mean values ± standard deviation are illustrated. Bars marked with \* are statistically different from the control (P < 0.05). .....55

**Figure 13 – Antimicrobial activity of the Ca- and Sr-rich alginate discs extracts (in TSB) towards *S. aureus*.** Sr-rich (A) and Ca-rich (B) discs, *S. aureus* grown on TSB. A1 and B1 – Metabolic activity evaluation. Relative fluorescence units (RFU) are presented as a function of extracts dilutions. A2 and B2 – Bacteria culturability. CFUs count is presented as a function of the discs extracts. *S. aureus* represents the negative control (no treatment). Mean values ± standard deviation are illustrated. Bars marked with \* are statistically different from the control and bars marked with (\*) and brackets are statistically different between them (P < 0.05).....56

**Figure 14 – SEM micrographs of the μHAp (A), μSrHAp (B), nHAp (C), nSrHAp (D) and SrTriP (E) microspheres.** Increasing magnification is presented from left to right (1. 100x; 2. 400x; 3. 2000x; 4. 10000x; 5. 20000x and 6. 50000x) revealing the porous microarchitecture of the microspheres. ....60

**Figure 15 – SEM micrographs of nHAp (A) and nSrHAP (B) microspheres. A1 and A2** with increasing magnifications (left to right, 50000x, 100000x and 100000, respectively) revealing the interior of the microspheres and the nanometric grain and **B** the nanometric grain (100000x).....61

**Figure 16 – FTIR-ATR spectra of A – nanometric (blue line) and micrometric (red line) HAp powders; B – micrometric HAp powders (red line), μHAp microspheres (dark blue line) and μSrHAp microspheres (pink line); C – nanometric HAp powders (black line), nHAp microspheres (pink line) and nSrHAP microspheres (purple line); D – strontium phosphate powders (green line) and SrTriP microspheres (pink line).**.....62

**Figure 17 – Strontium and calcium release from the microspheres (A) and powders (B) over time.** 3 days, 10 days and 21 days microspheres and powder extracts were quantified in Sr (1) and Ca (2) composition (μg/mL) by ICP-AES. (For the nHAp only the 21 days' time-point was done given to material restriction). .....64

**Figure 18 – Antimicrobial evaluation of 72 hr microspheres extracts towards *S. aureus*.** A1 – Metabolic activity evaluation. Relative fluorescence units (RFU) are presented as a function of extracts dilutions. A2 – Bacteria culturability. CFUs count is presented as a function of the extracts dilutions. *S. aureus* represents the negative control (no treatment). Mean values ± standard deviation are illustrated. Bars marked with (\*) are statistically



different from the control and bars marked with (\*) and brackets are statistically different between them ( $P < 0.05$ ). No statistical analysis is presented for nHAp extracts as only one sample was used, given to material restrictions. ....66

**Figure 19 – Bactericidal evaluation of the powders extracts.** 72 hr extracts against *S. aureus*. **A1** – Metabolic activity evaluation. Relative fluorescence units (RFU) are presented as a function of extracts dilutions. **A2** – Bacteria culturability. CFUs count is presented as a function of the extracts dilutions. *S. aureus* represents the negative control (no treatment). Mean values  $\pm$  standard deviation are illustrated. Bars marked with \* are statistically different from the control ( $P < 0.05$ ). ....67

**Figure 20 - Bactericidal evaluation of the direct exposure of microspheres to S. aureus.** 6h (A) and 24h (B) exposure against *S. aureus*. **A1** and **B1** – Metabolic activity evaluation. Relative fluorescence units (RFU) are presented as a function of the masses of powders used. **A2** and **B2** – Bacteria culturability. CFUs count is presented as a function of the masses of microspheres used. *S. aureus* represents the negative control (no treatment). Mean values  $\pm$  standard deviation are illustrated. Bars marked with (\*) are statistically different from the control and bars marked with (\*) and brackets are statistically different between them ( $P < 0.05$ ). ....69

**Figure 21 - Bactericidal evaluation of the direct exposure of powders to S. aureus.** 6h (A) and 24h (B) exposure against *S. aureus*. **A1** and **B1** – Metabolic activity evaluation. Relative fluorescence units (RFU) are presented as a function of the masses of powders used. **A2** and **B2** – Bacteria culturability. CFUs count is presented as a function of the masses of microspheres used. *S. aureus* represents the negative control (no treatment). Mean values  $\pm$  standard deviation are illustrated. Bars marked with (\*) are statistically different from the control ( $P < 0.05$ ). ....71



## Glossary

ATCC	American type culture collection
BCP	Biphasic calcium phosphate
BGs	Bioactive glasses
BMD	Bone mineral density
BMPs	Bone morphogenic proteins
CACC	copper alginate-cotton cellulose
CaPs	Calcium phosphate
CaSR	Calcium sensing receptor
CDHA	Calcium deficient hydroxyapatite
CPC	Calcium phosphate cements
ECM	Extracellular matrix
EU	European union
FDA	U.S. Food and Drug Administration
FGF	Fibroblast growth factor
FTIR	Fourier transform infrared spectroscopy
G	$\alpha$ -L guluronic acid
GDL	D-(+)-Gluconic acid $\delta$ -lactone
GIC	Glass ionomer cements
HAp	Hydroxyapatite
HIS	Injectable hybrid system
ICP-AES	Inductive coupled plasma - atomic emission spectroscopy
IGF	Insulin-like growth factor
M	1,4-linked $\beta$ -D.mannuronic acid
MBC	Minimum bactericidal concentration
MDR	Multidrug-resistant
MHB	Müller Hinton Broth
MIC	Minimum inhibitory concentration
MRSA	Methicillin-resistant Staphylococcus aureus
MScs	Mesenchymal stem cells
MW	Molecular weight
NLRs	NOD-like receptor
OD	Optical density
o/n	Overnight
OPG	Osteoprotegerin

PDGF	Platelet-derived growth factor
PEG	Poly(ethylene glycol)
RANKL	Receptor activator of nuclear kB ligand
RGR	Arginylglycyaspartic acid
RMGIC	Resin modified glass ionomer cements
ROS	Reactive oxygen species
SEM/EDS	Scanning electron microscopy/ Electron Backscattered Diffraction
SCPP	Strontium-doped calcium polyphosphate
SSI	Surgical site infection
STF	Strontium titanate ferrite metal oxide
TCP	Tricalcium phosphate
TLRs	Toll-like receptor
ZP	Zeta potential
TGF- $\beta$	Transforming growth factor $\beta$
TSA	Tryptic Soy Agar
TSB	Tryptic Soy Broth
VEGF	Vascular endothelial growth factor

# Chapter 1

---

## Work outline

### 1. Background and project presentation

Besides the incredible fast expansion of the human knowledge, it is clear the existence of problems that persist without a definitive solution and, therefore, are still very present in the nowadays medical community without an effective resolution. In fact, the contradictory happens when the knowledge achieved so far is able to perpetuate human life beyond limits but, at the same time, is still not sufficient to deal with all the problems that comes with this benefit. An example of this is age. We are allowed to live longer, but our comprehension is not enough to resolve effectively all the problems that start to appear with elderliness. The fact that the healthy balance of the bones is severely compromised by factors such as age conduces to the occurrence of osteoporosis and fragility fractures. Other causes may appear which are not specifically connected to elderliness as bone major defects also occur in young and adults. In all causes and whatever the cause, this leads to major bone defects that need to be treated by surgical implantation of either grafts (either auto-, allo- or xenografts) or osteoinductive biomaterials. In both cases, surgical site infection (SSI) is a major threat that besides the human costs comes with a huge economic burden. The standard approach to resolve infection is the systemic administration of potent antibiotics which over usage is being related with the creation of multidrug-resistant (MDR) bacterial strains. Other current treatment alternatives include second surgery for implant removal or, in more severe cases, amputation of the limb. Therefore, there is an urge to find better solution to fight infection that don't compromise either the patient's health or the ability to effectively eradicate the infection.

Our group has developed an injectable hybrid system composed by a Strontium-rich alginate matrix (vehicle: reticulates *in situ* in the presence of Strontium) reinforced by Strontium-rich calcium phosphate microspheres. This system was firstly design based in the osteogenic properties of a gradual and local release of Strontium (leaching system) given by the alginate and microspheres degradation. Concordantly, Strontium is already well known to induce osteoblast stimulation and osteoclast inhibition promoting bone formation. Additionally to this osteogenic activity, preliminary works have used Strontium as antimicrobial agent which shown interesting antimicrobial activity. Thus, the interest of this

work is focused on the study of this same delivery of Strontium ions ( $\text{Sr}^{2+}$ ) to truly assess the potential of this injectable hybrid system in the prevention of infection after surgery. Few information of the strontium antimicrobial properties and mechanism of action is available in literature. In fact, this is the first study of strontium rich microspheres and alginate, to our knowledge. Bone implant-related infections are usually associated with infection by *Staphylococcus aureus* (*S. aureus*) and *Staphylococcus epidermidis* (*S. epidermidis*) and, therefore, these were the bacterial strains chosen to address the antibacterial properties of the system developed by our group.

### 1.1. Research objectives

The main objective of the present work is to evaluate the antimicrobial properties of the injectable hybrid system developed by our group against two major pathogenic bacteria, *S. aureus* and *S. epidermidis*. This opportunistic bacteria are usually associated to nosocomial infections, such as medical devices and implants infections, being one of the most problematic bone infections, which is further addressed in this study.

Firstly, this work aims to determine the strontium concentration required for the complete eradication or, at the least, the inhibition of the bacterial growth. Therefore, the antimicrobial potential of strontium was assessed by microdilution method exposing the bacteria to  $\text{SrCl}_2$  solutions at several concentrations. In this sense, the minimum inhibitory concentration (MIC) and the minimum bactericidal concentration (MBC) were determined for both strains.

Subsequently, the antimicrobial properties of the Injectable Hybrid System (IHS) were evaluated. As the HIS comprehends different components, it is of great interest to comprehend which is the antimicrobial contribute of each part of this system, and, therefore, fully understand its dynamic. To accomplish the previously stated, the IHS was sub-divided into its two main components: the Sr-rich alginate (the vehicle) in discs; and the Sr- rich microspheres, as the structural reinforcement of the IHS. This research would lead to future optimizations of the HIS and, consequently, to better address bone infections mainly associated to bone implants/defects and osteogenic regeneration.

Regarding the antimicrobial properties of the alginate discs and Sr- rich microspheres, the concentration of strontium present in the two main components and the extent of leaching to the surrounding environments were carefully analysed. Moreover, the evaluation of the ions release kinetic is of the greatest interest as the present system aims for bacterial prevention purposes on the potential site of infection during and after the implementation of IHS in bone surgery. The disks extracts obtained were added to both

bacterial strains and quantified in terms of metabolic inactivation and culturability on solid medium.

Concerning the potential effect of the type of ceramic used in the microspheres constitution in its antimicrobial properties, several ceramic materials were used to extrude the microspheres, as well as two powders. As said, five different ceramic materials were used in the microspheres comprehending: micrometric hydroxyapatite ( $\mu\text{HAp}$ ), nanometric hydroxyapatite ( $\text{nHAp}$ ), strontium phosphate ( $\text{SrTriP}$ ), Sr- rich micrometric hydroxyapatite ( $\mu\text{SrHAp}$ ), Sr- rich nanometric hydroxyapatite ( $\text{nSrHAp}$ ); and two different powders were used namely, strontium phosphate ( $\text{pSrTriP}$ ) and strontium carbonate ( $\text{pSrCO}_3$ ). The microspheres were carefully characterized using Scanning Electron Microscopy (SEM/EDS) and Fourier Transformed Infra-red spectroscopy (FTIR). *S. aureus* was then exposed to the microspheres, either by direct contact or through extracts, and two methods for quantification were performed, including reduction of metabolic activity (alamar blue assay) and cells culturability on solid medium (CFUs counting).

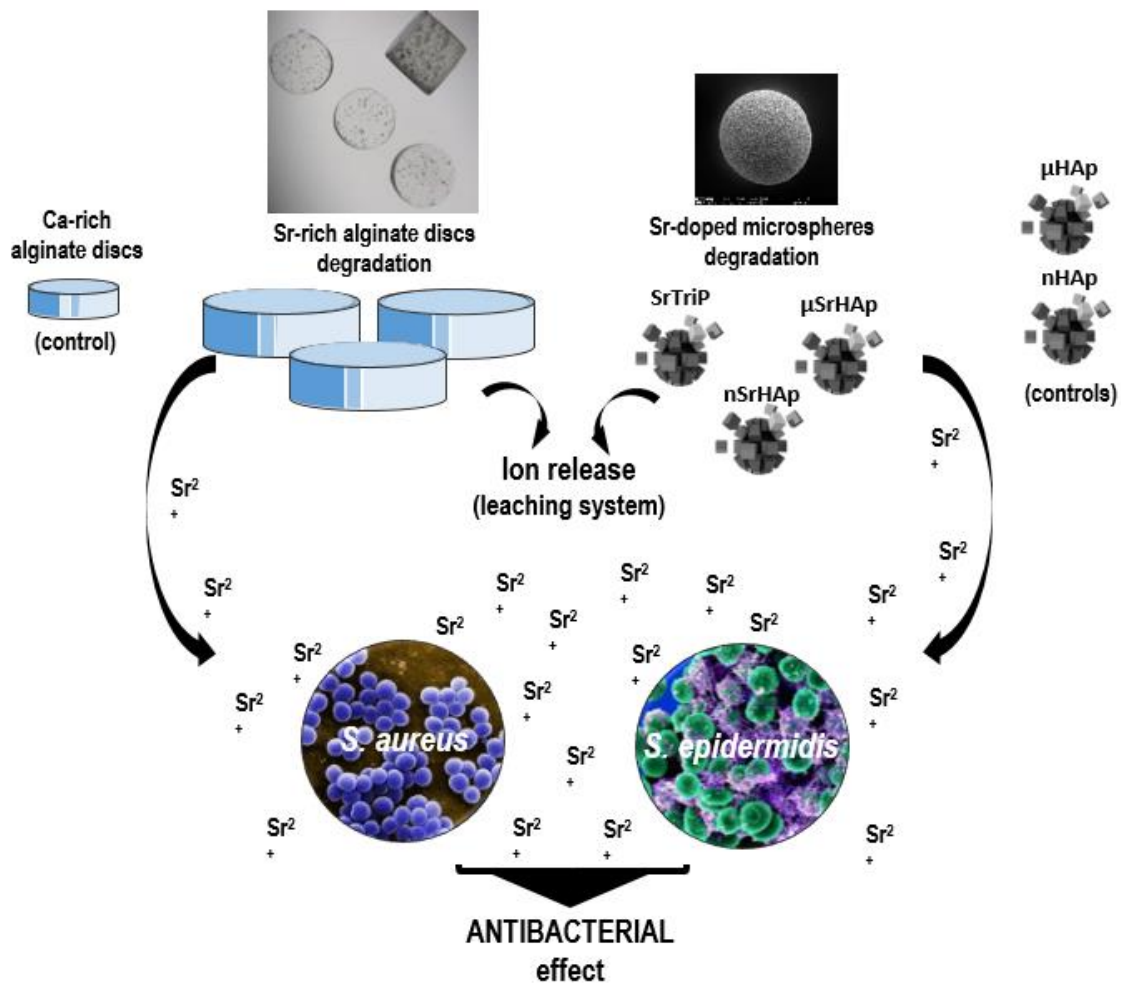


**Figure 1** - Graphical abstract. Separated components of the injectable hybrid system and its antimicrobial dynamics.

### 3. Thesis organization

This thesis is divided in 5 Chapters. In Chapter 1, the context, main goals and guidelines of the work described in the next Chapters are briefly presented.

Chapter 2 presents a review of the literature. The socioeconomic impact of bone infections, bone structure and its particular properties, as well as synthetic bone substitutes are briefly discussed. Moreover, a short review of the surgery associated infections and the prevention of bacterial colonization on the site of procedure are also addressed. Due to the importance of the opportunistic pathogens *S. aureus* and *S. epidermidis* in nosocomial infections associated to medical devices and implants, important features of these two strains, including its virulence factors, biofilm formation and preferential sites of infection are also described, as well as the problematic of multidrug resistance. Furthermore, antimicrobial systems of contact and leaching types are also analysed. Subsequently, there is a short discussion about the antimicrobial properties of metal ions including strontium and its incorporation in biomaterials.

Chapter 3 focuses on the materials and methods required for the present study, including the, preparation of strontium rich alginate discs and microspheres, its extracts, bacterial strains cultivation and maintenance and the methods applied for antimicrobial properties evaluation.

Chapter 4 centres on the results obtained for the different methods used as well as on a brief discussion of the most important results obtained.

At last, Chapter 5 presents an overview of the thesis, with emphasis on the main concluding remarks and future research perspectives.



# Chapter 2

---

## Literature review

### 1. The need for bone implant materials – socioeconomic background

Given the fast technological evolution observed through the last decades the population is being allowed to live longer which gives rise to an increasing demand for bone substitutes <sup>1</sup>.

The health of the bones, its strength and integrity, relies in the maintenance of a delicate balance between bone formation by osteoblasts and bone resorption by osteoclasts. This equilibrium is difficult to maintain especially with age and when suffering certain bone diseases. Once the equilibrium bone formation/resorption is broken, the osteoclast's activity tends to exceed the one of the osteoblast resulting in an unbalanced system that, consequently, may lead bone to become brittle and prone to fracture <sup>2</sup>. Normally, age and disease are intimately connected and, given the observed increase in life expectancy, the cases of osteoporosis are becoming more and more numerous <sup>3</sup>. In EU (European Union) an estimate made in 2010 have revealed that there are 22 million women and 5.5 million men diagnosed with osteoporosis, which is responsible for the occurrence of about 3.5 million new fragility fractures. Besides the individual costs associated, fragility fractures represent also a huge economic burden that, only in UE in 2010, was estimated at € 37 billion <sup>4</sup>.

The treatment of bone defects normally passes by the surgical implantation of either grafts: autografts (transplantation of patient's own tissue), allografts (transplantation of tissue from other individuals of the same specie) or xenografts (transplantation of tissue from individuals of different species) or osteoinductive biomaterials <sup>5-7</sup>. From the two, bone grafting still represents the standard approach for the treatment of major bone defects once they already contain osteogenic bone cells, marrow cells and an osteoconductive collagen matrix. Actually, in bone surgery allo- and autografts represent 95% of the overall used bone grafts whereas synthetic materials represent only 5% <sup>8</sup>. In both auto- and allo-grafts, the traditional grafts used are of cancellous bone which is obtained from the fibula and iliac crest <sup>6</sup>. Nevertheless, with all these advantages come also some drawbacks that can compromise the final outcome, as it will be discussed further <sup>9</sup>. Considering the described approaches, they all have to deal with different challenges and therefore, they all present

specific advantages and complications. Thus, despite the fact that these are the standard procedures, there are still significant concerns about the shortcomings related with their usage. Respectively, limited amount available and donor site morbidity; viral transmission and potential immune response; potential transmission of animal-derived pathogens and the possibility of immunogenic rejection; highly invasive procedures and systemic risks related with the surgery and prolonged postoperative recovery<sup>5</sup>. Furthermore, it is well known that there can be significant post operative infections at donor and graft sites that severely impairs the bone inductive factors<sup>6</sup>. All these graft-related issues constitute, therefore, a real obstacle to a fast and complete healing.

Infection has still a straight relation with bone implant surgery and, for instance, only in United States, \$1.2 billion are spent annually to treat such cases. This economic burden is due to the high costs associated to the whole process of healing required that can easily reach \$100.000 per case of implant-related infection<sup>10</sup>. Also worrying is the systematic use of antibiotics to fight these infections<sup>11</sup>. It is known that the overuse of antibiotics is gradually making microbes such as bacteria more resistant originating multidrug resistant strains. This leads antibiotics to be much less effective against implant-related infections what, ultimately, may result in the removal of the implant or even amputation<sup>12,13</sup>. Therefore, it is evident the necessity for the development of new treatment options in order to address this problem. An enthusiastic strategy is local drug delivery that, contrary to systemic administration, reduces the development of resistant bacteria and allows for high drug concentration at the infection site<sup>14</sup>.

Accordingly, nowadays we are still facing several issues related with bone disease/defects and bone surgery/implant and post operative infection which lead to an urge for innovative biomaterials. Injectable systems composed of *in situ* gelling hydrogels such as alginate are of great interest in what concerns major bone defects as they may be easily functionalised and implanted in a minimally invasive manner<sup>15</sup>. The development of bioceramics with specific characteristics such as anti-osteoporotic, anti-inflammatory and antimicrobial properties seems to represent a great option to achieve that goal<sup>1</sup>. Calcium phosphate materials have also been shown to be very versatile allowing for structural and composition alterations and incorporation of bioactive agents such as metal ions.

Strontium (Sr) has been first reported more than half a century ago by Shorr and Carter et al. to have a beneficial effect in the treatment of osteoporosis<sup>16</sup>. The potential of strontium had been neglected for several years probably given to confusions between its stable forms (<sup>84</sup>Sr, <sup>86</sup>Sr, <sup>87</sup>Sr and <sup>88</sup>Sr) and its harmful radioactive isotopes (<sup>85</sup>Sr, <sup>87m</sup>Sr, <sup>89</sup>Sr and <sup>90</sup>Sr)<sup>17</sup>. Nevertheless, several more recent studies have revealed that strontium substituted Ca-phosphate ceramics have great potential as bone and dental substitutes,

drug carrier and fillers<sup>18</sup>. Additionally, few studies have revealed that strontium shows also some relevant antimicrobial activity which makes its use very appealing in implant materials.

The bioengineering of a biomaterial consisting on a Strontium-rich alginate scaffold reinforced with Strontium-rich calcium phosphate ceramic microspheres may represent a promising injectable hybrid system to use as a filler in bone implants. The proposed value in this system is the possibility of creating a biomimetic material that is, by definition, a hybrid both in its composition: alginate hydrogel scaffold vs calcium phosphate microspheres; and in its biological activity: bone regeneration vs antimicrobial properties. With this system, we are fusing two very distinct materials, concerning its composition and mechanical properties, but whose distances are brought together in the establishment of a dynamic bone regenerative and infection preventive environment in a symbiosis that has as common element the presence of Strontium. In the end, the objective is to promote a material able to effectively induce bone healing while preventing/modulating inflammatory reactions by reducing implant-related infections after surgery<sup>13,19</sup>. In this work it will be addressed the potential antimicrobial properties of strontium in the development of more efficient osteoconductive implants with a special emphasis in the bactericidal properties of strontium-based biomaterials for bone replacement and repair.

## 2. Bone structure and properties (an overview)

The human body is composed by a large diversity of bones that act as support for all the surrounding tissues that compose our bodies.<sup>20</sup> Thus, our skeleton is continually being subjected to different types of forces which reveal high strength and fracture toughness that are only possible given the distinct structure and mechanical properties of the bone tissue.<sup>21</sup> In a broad perspective, bone mechanical properties are strongly defined by three important aspects: the relative amount of its main components (mineral, water and organics: essentially type-I collagen); and the quality and resultant spatial arrangement of these components in a material.<sup>22</sup>

Like all tissue within the body, bone has also a defined hierarchical organisation of its structure which expands over several orders of magnitude.<sup>20</sup> Various levels of the hierarchical organisation have been described: (1) the macrostructure - bone is arranged in two different configurations either in a cancellous pattern (trabecular bone) or in a compact pattern (cortical bone), these two types of bone construct being more easily differentiated by their level of porosity and density; (2) the microstructure; (3) the sub-microstructure; (4) the nanostructure; and (5) the sub-nanostructure.<sup>20,23</sup>

Bone mineral mass is dominantly composed of nano-crystalline non-stoichiometric hydroxyapatite (HAp,  $\text{Ca}_{10}(\text{PO}_4)_6(\text{OH})_2$ ) and  $\beta$ -tricalcium phosphate ( $\beta$ -TCP,  $\beta\text{-Ca}_3(\text{PO}_4)_2$ ).

For these reasons hydroxyapatite and  $\beta$ -tricalcium phosphate have been widely used materials in surgical bone restoration because of their biocompatibility.<sup>24</sup> In fact, the prime factor in bone strength is its mineral density (BMD), however it's a very reductive approach to only consider the BMD, and aspects of also great impact such as shape, geometry, 3-dimensional microarchitecture, properties inherent to the matrix, possible micro-damages, and bone turnover shouldn't be neglected. For instance, for a better understanding, the bone matrix may be seen as a dual phase system where the mineral phase offers the stiffness, whereas collagen fibres provide the necessary ductility that allows for energy absorption preventing/decreasing occurrence of bone fracture<sup>25</sup>.

### 3. Synthetic bone substitutes

#### 3.1. Alginate based biomaterials

A diversity of biomaterials from natural ones to synthetic have been applied in regenerative medicine. From those, the polymers of natural origin are a very appealing option due to their biological activity, chemical versatility and resemblance to the natural occurring ECM. Therefore, these materials are believed to be good cell supportive matrices<sup>26</sup>.

Alginic acid, or commonly known alginate, is a hydrophilic and anionic polysaccharide and an example of a naturally occurring polymer. It is U.S. Food and Drug Administration (FDA)-approved and corresponds to one of the most biosynthesized material and is mainly obtained from brown seaweed and bacteria<sup>26,27</sup>. This polymer has gained the attention of researchers given its good accessibility, absence of toxicity, compatibility with both hydrophilic and hydrophobic molecules and easy manipulation of its adhesive and mechanical properties<sup>27</sup>. Alginate is a co-polymer composed from blocks of 1,4-linked  $\beta$ -D-mannuronic acid (M) and  $\alpha$ -L guluronic acid (G) residues (Figure 2.A) which are covalently bound and arranged in a linear fashion<sup>28</sup>. The blocks are normally arranged in three different forms in a polymer segment: consecutive G residues, consecutive M residues and alternating M and G residues (Figure 2.B).

Given its characteristics, alginate has been appointed for a large broad of applications particularly as a supporting matrix and/or delivery system in tissue repair and regeneration. Biocompatibility, non-antigenicity, biodegradability and chelating ability are some of the features that make alginate such an attractive material<sup>29</sup>. For instance, alginate has a pH-dependent anionic structure and therefore has the possibility to create interaction with proteoglycans and polyelectrolytes. Accordingly, cationic drugs and molecules can be incorporated in the alginate by simple electrostatic interactions<sup>26</sup>.

Depending on the production process and source, the molecular weight (MW) of the alginate may be comprehended between 10 to 600 kDa<sup>27</sup>. The MW is an important indicator that dictates, for instance, the degradation rate and mechanical properties of alginate-based

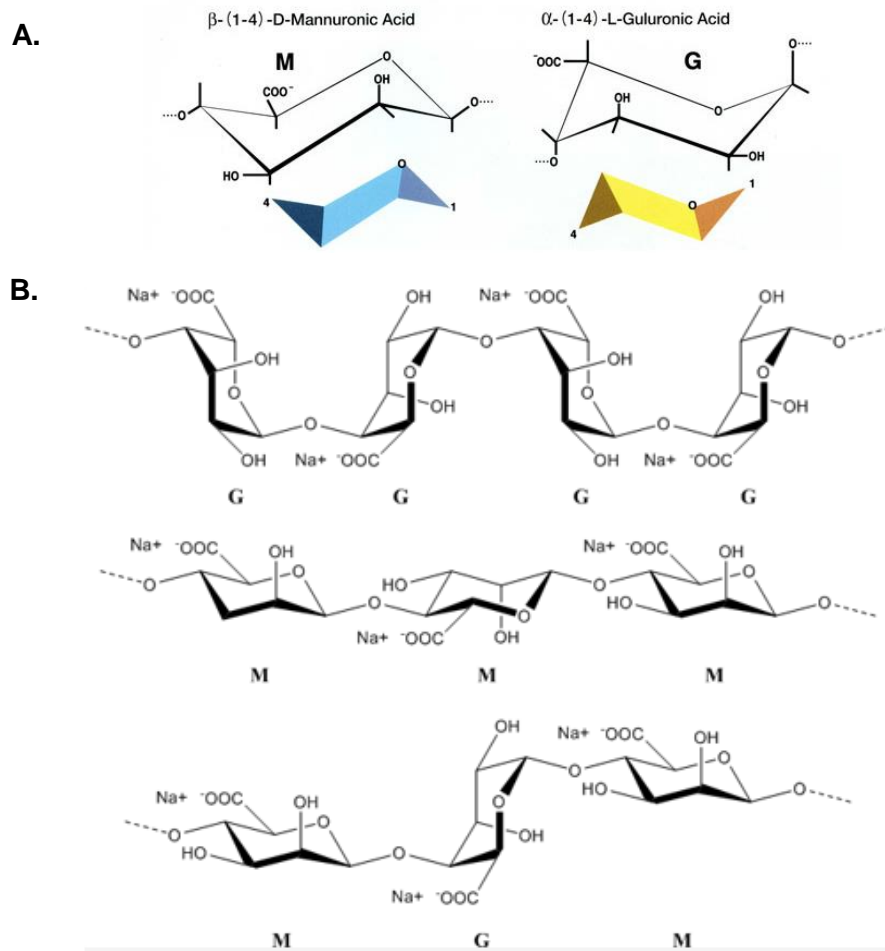


**Figure 2 – Representation of the alginate structure. A –** Representation of the 1,4-linked  $\beta$ -D.mannuronic acid (M) and of  $\alpha$ -L guluronic acid (G) residues (adapted from<sup>30</sup>). **B –** Representation of the alginate chemical structure. The three different forms of polymer segment arrangement are presented (in the figure it is represented the sodium alginate structure).

biomaterials. Essentially, there is an inverse relationship between the alginate MW and its degradability: the higher the MW, slower the degradation. This dynamics is given by the number of available locations for hydrolysis degradation which are decreased when the MW is increased. At the same time that the alginate degradation takes place, the alginate mechanical properties are altered given to structural changes that occur at the molecular and macroscopic levels. Besides MW influence in alginate behaviour, the site of implantation is also of significant importance. The biomaterial may be subjected to a diversity of pH-environments that can ultimately affect its mechanical and swelling behaviour also altering its degradation properties/rate<sup>26</sup>.

### 3.1.1. Alginate hydrogel production

Hydrogels may be defined as a three-dimensional cross-linked polymeric network obtained by the reaction between one or more monomers. The definition comprehends also that it's a polymeric structure that is able to swell and retain substantial quantities of water<sup>26,31</sup>. Its tissue-like water content, capability of providing an homogeneous encapsulation (of cells, particles as microspheres, for instance, among other), efficient mass transfer rate, possibility to tailoring its physical properties and its potential as injectable systems make hydrogels very promising in tissue engineering. Therefore in alginate hydrogels relies the possibility of creating biologically active biomaterials that can be delivery in a minimal invasive fashion to almost any size and shape defect<sup>32</sup>.

Respecting its gelation mechanism alginate hydrogels may be classified as physical or chemical gels, characterized by, respectively, physical association or covalent bonds between the polymeric chains<sup>32</sup>. Several approaches have been utilized in alginate hydrogel preparation which include the ionic cross-linking, covalent cross-linking, thermal gelation (phase transition) and cell cross-linking<sup>26,33</sup>.

Ionic cross-linking is the simplest and most common method applied in alginate hydrogel preparation and comprehends the combination between an aqueous solution and an ionic cross-linking agent – divalent metal cations<sup>27,33,34</sup>. Several ions such as  $Mg^{2+}$ ,  $Ca^{2+}$ ,  $Sr^{2+}$ ,  $Ba^{2+}$ ,  $Fe^{2+}$  and  $Cu^{2+}$  have been employed in alginate hydrogel formation<sup>26,35</sup>. This process takes place given the chelation of the metal cations played by the carboxylate groups of the 1,4-linked  $\beta$ -D-mannuronic acid (M), but principally of the 1,4-linked  $\alpha$ -L-guluronic acid (G) residues<sup>27,28</sup>. This preference by the guluronate blocks relies in its structure which permits a higher degree of coordination of the divalent cations. To form a gel, one polymer chain of guluronate blocks forms junctions with adjacent guluronate chains in a structural arrangement designated by “egg-box” model (Figure 3.)<sup>33</sup>.

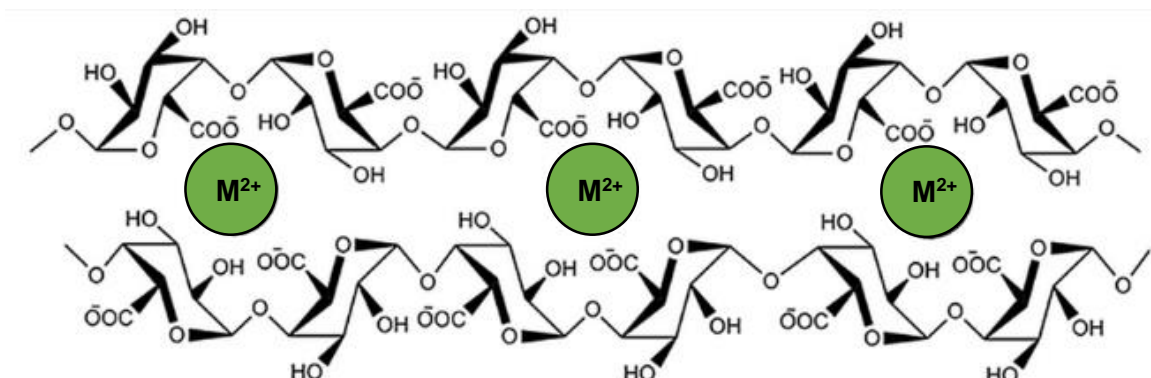


**Figure 3** – Schematic representation of alginate cross-linking by  $M^{2+}$  metal cations – “egg box” model where four G subunits are bound by one  $M^{2+}$  ion.<sup>27</sup> (adapted from<sup>36</sup>).

An important aspect in the gelation process is the rate at which it occurs. With a too fast gelation it is difficult to control gel uniformity and strength, while slower kinetics allow for a higher uniformity degree of the structures and therefore higher mechanical integrity of the hydrogel. For instance,  $\text{CaCl}_2$ , which is often used as cross-linking agent, promotes a poorly controlled gelation since it is highly soluble in aqueous solution making rapidly available the calcium ions to the alginate. To solve this problem it is possible to use buffers containing phosphate groups that will compete with the alginate carboxylate groups for the calcium ions. Other alternative is to take advantage of the low solubility of some compounds such as calcium sulphate ( $\text{CaSO}_4$ ), calcium carbonate ( $\text{CaCO}_3$ ) or strontium carbonate ( $\text{SrCO}_3$ ). As the cross-linking ions are less available, given its weak solubility, the gelation process is retarded and the working time of the alginate is enlarged<sup>33</sup>. As the solubility of carbonate, for instance, is so weak there is also the possibility to acidify the solution by the addition of D-(+)-Gluconic acid  $\delta$ -lactone (GDL). GDL hydrolysis occurs in a slow fashion providing an also slow but continuous lowering of pH, which proportionate a gradual dissociation of the cross-linking ions<sup>29,37</sup>. This working time enlargement also proves to be very useful in the surgical environment where the surgeon must have sufficient time to inject the material in the patient's defect before the occurrence of the alginate gelation.

### 3.2. Bioceramics

Bioceramics are a class of biomaterials that are utilized for replacing damaged or diseased portions of musculoskeletal structures. This category of materials may have a wide range of behaviour within the body. Accordingly, they can go from ceramics that are practically inert, like ceramic oxides, to its opposite where materials are bioresorbable. The calcium phosphates (CaPs) are the most commonly used bioceramics as they are biologically present in the inorganic phase of hard tissues as bones and teeth<sup>38</sup>. According to Dorozhkin et al., there are eleven different known non-ion-substituted calcium orthophosphates comprehending a molar ratio of Ca/P between 0.5 and 2.0<sup>39</sup>. Within the CaPs family, hydroxyapatites (HAp) are the most widely used material having a Ca/P molar ratio of 1.667<sup>38,40</sup>. Given its chemical similarity with the biological calcified tissues, calcium phosphates present an extraordinary biocompatibility and bioactivity.<sup>39</sup> However, HAp ceramics show to be virtually non-resorbable when applied as bone implant substitutes.<sup>41</sup> Additionally to hydroxyapatite, tricalcium phosphate (TCP) is also a commonly used bioceramics that is biodegradable, presenting the ability to dissolve in physiological media. Thus, TCP is a great option in those cases in which it is intended to replace the implanted material over time by natural occurring bone. Tricalcium phosphate may be found in four different polymorphs being the  $\alpha$ - and  $\beta$ - forms the most common. Taking into consideration

the mentioned characteristics of these two bioceramics, HAp and TCP, it would be desirable, in some situations, to merge both materials in one biphasic bioceramic forming the commonly known biphasic calcium phosphate (BCP). This is an exciting alternative, given the observed discrepancy between the solubility of the BCP's two phases (HAp and TCP) composition. This would be advantageous in cases where it would be required the implanted material to support the bone repair during time while being slowly resorbed and replaced by the natural forming bone tissue *in vivo*. To accomplish that, it is possible to match and adapt the rate of resorption of the BCP with the rate of bone regeneration by manipulating its content ratio in  $\beta$ -TCP and HAp. If happens that the solubility of the BCP is higher than the one of bone formation, then the usefulness of the implant will be limited. Accordingly, the higher the composition of TCP in BCP, the higher the rate of dissolution will be.<sup>40</sup> The discovery by Brown and Chow of the first Ca-P cement in the 80's by mixing CaP powders with water, that had the ability to harden with time at room temperature, has also opened up novel perspectives for innovative approaches in medicine, namely in the treatment of bone defects.<sup>42</sup> Calcium phosphate cements (CPC) present several biological properties that make this material very useful for bone treatments. For instance, CPC may be design to be injectable, biodegradable, osteoconductive and can be remodelled and replaced by new bone *in vivo*. In contrary to CPC that are expected to polymerise at low temperatures, other cements such as PMMA polymerise at high temperatures which leads to heat-induced osteonecrosis and impairments of healing as this exothermal reaction may severely injury the periosteal blood supply.<sup>43</sup> This is a great advantage in favour of CPC. Also an interesting approach to these ceramic materials is the ionic substitutions of calcium by other elements in the calcium phosphates structure as it will be discussed further. This substitution allows for several improvements of the material providing the possibility to modulate, for instance, its properties and its bioactivity.<sup>1</sup>

### 3.2.1. Ionic substitution

The structure of the HAp can accommodate a diversity of substitutions by replacing the calcium ( $\text{Ca}^{2+}$ ), phosphate ( $\text{PO}_4^{3-}$ ) and hydroxide ( $\text{OH}^-$ ) groups with other compatible ions. This can be done with the purpose of altering the mechanical and biological properties of a material. Thus, the use of different dopants, the combination of dopants and the variation of their concentration in the material structure, can be manipulated in order to influence the final mechanical strength, degradation profiles and cell-material interactions.<sup>44</sup> These ionic substitutions may also come with some alterations in the structure of the material. For instance, it may alter the crystal morphology, crystallinity, lattice parameters, solubility and the thermal stability of hydroxyapatite<sup>40</sup>.



According to the element or group that is being replaced, the substitutions may be classified as anionic or cationic. The first case corresponds to the substitutions which occur in the phosphate or in the hydroxyl positions while the second case corresponds usually to the locals occupied by the atoms of calcium. Many types of substitutions with different final application have been reported for the different possible substitutions places, information that can be found summarised in Table 1.

**Table 1.** Type, place and application of ionic substitutions on the HAp structure.

Type of substitution	Substitution place	Ion substitute	Application
Anionic substitutions	At phosphate- or hydroxyl-groups	Carbonates (CO <sub>3</sub> <sup>2-</sup> )	Reported effect over sinterability of calcium phosphate ceramics <sup>45</sup>
		Chlorides (Cl <sup>-</sup> )	Reported effect over promotion of biphasic mixtures of HAp and TCP upon calcination <sup>46</sup>
		Fluorides (F <sup>-</sup> )	Reported effect over mechanical properties, inhibition of phase decomposition and sintering of HAp <sup>47</sup>
		Silicates (SiO <sub>3</sub> <sup>2-</sup> )	Reported effect over skeletal development, integrity of ECM, and osteoblast and osteoclast activity <sup>38</sup>
		Sulphur (S <sup>2-</sup> ) and sulphates (SO <sub>4</sub> <sup>2-</sup> )	Reported effect over biological cement for building skin cell, hair, nails and cartilage <sup>38</sup>
		Selenium oxyanions	Reported effect on induction of cancer cell apoptosis, over pre-osteoblast proliferation and antibacterial activity <sup>48,49</sup>
Cationic substitutions	Normally at the calcium position	Lithium (Li <sup>+</sup> )	Reported effect over bone mineral density <sup>50</sup>
		Sodium (Na <sup>+</sup> )	Reported effect over thermal stability and delayed allotropic transformation of β- to α-TCP <sup>51</sup>
		Potassium (K <sup>+</sup> )	Reported effects over protein adsorption propensity and thermal stability of apatite <sup>52</sup>
		Silver (Ag <sup>+</sup> ), Copper (Cu <sup>2+</sup> ) and Zinc (Zn <sup>2+</sup> )	Reported to have antimicrobial activity <sup>53</sup>
		Strontium (Sr <sup>2+</sup> )	Reported to have effect both over bone formation and resorption and antimicrobial activity <sup>18,38,40</sup>

### 3.4. Osteoinduction, osteoconduction and osseointegration

Osteoinduction is the phenomenon by which primitive, undifferentiated and pluripotent cells are recruited and induced to mature into more differentiated cell lineages that are able to promote bone formation. These immature cells are, therefore, stimulated to develop from mesenchymal cells to osteoprogenitors. With the proper stimulus they can be conducted to differentiate into bone inductive cells such as the pre-osteoblasts that will give rise to osteoblasts which are responsible for the creation of new bone. Thus, this process may be seen as the combination of steps that lead to osteogenesis, a biological

phenomenon naturally occurring in every kind of bone healing and that is essential for a correct bone restoration and implant anchorage. The basis of the osteoinduction relies on the presence of osteoinductive agents that are, in fact, naturally released upon the occurrence of trauma in the bone such as bone morphogenic proteins (BMPs), which have been widely studied and are known to be bone inductive agents. This process of recruitment, induction and differentiation is essential in bone injury, as the already existing osteoblasts in the bone are considered insufficient to complete a proper healing once they only contribute in a small portion to the formation of the needed new bone. Despite the fact that there is the belief that Ca-P ceramics are not osteoinductive, there are several studies reporting ectopic osteogenesis, respectively in extraskeletal tissues.<sup>54</sup> Biodegradability, for instance, is an important factor as the dissolution of Ca and P enriches the environment favouring bone formation, however other aspects may also have a strong impact in ceramic-induced osteogenesis. For instance, induced bone was only present in porous structures what suggests that the maintenance of these structures after implantation is fundamental during osteogenesis. Thus, again emerges the debate about which is the best rate of biodegradation for an implant material<sup>55</sup>. Also alginate biodegradable biomaterials have been shown to be a very versatile and its functionalization with molecules such RGD have been proved to be capable to induce pre-osteoblast cell attachment, proliferation and differentiation<sup>56</sup>. Nevertheless, besides the importance of osteoinduction in bone healing, the discussion about whether a biomaterial is or not bone inductive has been described not to be the only key factor in bone repair, as the injury itself is already capable of recruiting undifferentiated bone cells.<sup>54</sup>

Another important feature in bone healing is the osteoconduction of the implanted material. This process is intimately related with the ability of the implant to allow bone to grow on its surface. Osteoconduction is actually dependent at some degree on the previously discussed osteoinduction. To afford bone conduction it is necessary the action of growth factors that induce both mitogenesis and angiogenesis in order to regulate the formation of bone tissue. Accordingly, an appropriate vascularization is a critical aspect in bone formation which allows for the needed blood supply phenomenon supported by growth factor such as: FGF, VEGF, IGF, TGF- $\beta$  and PDGF<sup>57</sup>. Despite the biological feature behind bone repair, the material itself and its behaviour within the body is also of great importance. For example, silver and copper materials cannot support bone to grow on its surfaces becoming impossible bone conduction. On the other hand, ceramic materials such as Sr-HAp have revealed to be able to grow both osteoprecursor and osteoblast cells on its surface. In fact, Sr-HAp demonstrated to enhance bone cells growth on its surface when compared to HAp alone.

Upon defining osteoinduction and osteoconduction it is inevitable to discuss about osseointegration. Several definitions to this phenomenon have been described being ones more simplistic than other. From a biomechanics point of view osseointegration represents “a process whereby clinically asymptomatic rigid fixation of alloplastic materials is achieved, and maintained, in bone during functional loading”. Understanding the definition of osseointegration it is to comprehend that this process is intimately related with the earlier discussed osteoinduction and osteoconduction. Without them, bone integration of the implant wouldn't be achieved. Nevertheless, despite this dependency in these two initial processes of bone induction and conduction, osseointegration implicates a continued bone fixation over time.<sup>54</sup>

#### **4. Infection after surgery**

Infection can be defined as the process in which occurs the invasion of the host organism's tissues by another organism that has the ability to promote its multiplication and cause disease. There is a wide range of microorganisms capable of causing infection and among them we may find bacteria, viruses, viroids, prions, parasites and fungi. In addition, infection is also comprised by the host's response to this attack, namely, both against the microorganisms and the toxin they produce and release. To combat these pathogenic invaders the host's organism resorts to its immune system, primarily by reacting with an innate response that normally comprises a process of inflammation and, secondly by developing an adaptive response that is specific for each pathogen. Thus, although an infection is usually associated with an inflammatory reaction, it is important to understand that the reverse may not be true, since the occurrence of inflammation does not directly mean that we are dealing with an infection.<sup>58</sup> Inflammation may be generally defined as being a complex biological reaction of vascularized living tissue to a harmful stimuli in a certain local. The purpose of inflammation is to provide a fast and robust non-specific immune response that can contain, neutralize and dilute the pathogenic origin of the injury.<sup>59</sup> This is done by a coordinate delivery of blood components to the local of injury or infection. Through primitive humoral, cellular and mechanical processes, “front-line” leucocytes such as neutrophils and eosinophils are stimulated and readily migrate, in a process of exudation, to the infected/injured site in order to eliminate the harmful agents.<sup>60</sup> This stimulus is accomplished by resident macrophages and mast cells that primarily mediate the recognition of the antigens from the intruders. This recognition is done by Toll-like receptors (TLRs) and NOD-like receptors (NLRs) which are receptors of the innate immune system. Upon recognition, the macrophages and mast cells produce and release a diversity of inflammatory components such as cytokines, vasoactive amines and chemokines that

mediate the process of exudation and neutrophil activation. Besides that, neutrophils are also stimulated by direct contact with pathogens and when activated they release their granules which are composed of toxic substances in order to kill the invading pathogens. These granules have in their constitution reactive oxygen (ROS) and nitrogen species, cathepsin, elastase and proteinase 3 which are very powerful substances. However, these components cannot discriminate the host from microbial invaders, thus there is inevitable collateral damage caused to the host tissues.<sup>61</sup> Therefore, since this is a non-specific process, this response must be regulated so that no further damage occurs to the tissue allowing the re-establishment of homeostasis. Thus, when the acute inflammation is effective and the threat is eliminated, it is put into motion a process that stops the release of pro-inflammatory mediator and promotes the release of the anti-inflammatory ones, inhibiting the pro-inflammatory signalling.<sup>62</sup> There is then a switch from inflammation to resolution where recruited monocytes start the removal of the dead cells initiating the process of tissue remodelling. If the acute inflammation is not successful, persistent pathogens may induce a chronic inflammation. Additionally, the presence of a non-degradable foreign body may also result in a chronic inflammation. In both cases macrophages continually try to phagocytose and destroy the pathogens which results in the formation of granulomas and tertiary lymphoid tissues.<sup>61</sup> In the adaptive response, specialized lymphocytes, like B and T cells, express on their surfaces an incredible selection of antigen-specific recognition receptors that allow for specific identification of pathogens. This identification then triggers the elimination of the invaders. Further, the adaptive immune response creates also a long-lasting immunological memory that offers protection against future reinfection by the same pathogens.<sup>62</sup>

Normally, if the defences of the host are unimpaired, it is relatively easy for the organism to eliminate the threat that means, to impede microbial contamination and subsequent colonization. Nevertheless, there are several predominant factors that may have a great impact in this process. For instance, if the microorganism inoculum surpasses a certain threshold, if host defences are low, if there is disruption of tissue surfaces or if there is the insertion of a foreign body. Thus, surfaces such as bone, traumatized tissue, cartilage and implant materials are not provided with an effective protective cellular layer or a shielding extracellular polysaccharide membrane (glycocalyx) and, therefore, are predisposed to contamination.<sup>63</sup> In fact, the major origins of microorganism triggering implant-related infections are the host skin and the physician themselves throughout the implant placement. For instance, bacteria is able to pass over host defences by migrating through the openings created by incisions and then to the surface of the implant devices in the host. Posterior propagation is susceptible to happen through haematogenous routes.<sup>13</sup> Thus, besides the uncertainty and diversity of causes for surgical site infection (SSI), it is

possible to define some risk factors related with its occurrence. Considering what has been discussed, the risk factor for SSI may be broadly divided into two different categories: patients' characteristics related and operative procedure related. Nevertheless, risk factor may change between different types of surgery. Regarding patients' characteristics, diabetes, malnutrition, anemia among other, have been related with the development of SSI. On the other hand, operative factors such as duration of surgery, emergency operations, contaminated and dirty surgery and type of incision also significantly influence the SSI occurrence. Sometimes, these are aspects that are not predictable and are difficult to control.<sup>64,65</sup> Therefore, in the case of surgical treatment involving implants, new strategies should be applied in the design of the material, respectively, the creation of biomaterials that are themselves antimicrobials.

Between the pathogens that are usually found to cause infection both in momentarily and permanently implanted devices, predominantly *Staphylococcus epidermidis* and *Staphylococcus aureus*, *Enterococcus spp.* and the yeast *Candida spp.* are the most common microorganisms.<sup>66</sup> The type of the implant material and place where it is located is preponderant in which is the microbiological profile in implant-related infections. For instance, infection of blood vessel catheters, cerebrospinal fluid shunts, arterial graft, endoprotheses and cardiac valves are commonly related with *Staphylococci*, *Enterococci*, *Enterobacteriaceae* and *Candida sp.*. In the other hand, *Enterobacteriaceae* and *Enterococci* usually colonize catheters utilized in the urinary tract.<sup>13</sup> In bone, *S. aureus*, for instance, is the leading bacteria causing osteomyelitis and septic arthritis, while coagulase-negative *staphylococci* are more common to be associated to prosthetic joint infection.<sup>67</sup> Thus, the material properties are definitely preponderant in the colonization of an implant once the bacterial adhesion, for instance, is the primary and probably the most relevant aspect in implant-related infections. This adhesion is facilitated by hydrophobic molecules, attractive Van der Waals forces and by the existing pilus and fimbriae in the surface of bacteria. Therefore, the binding of bacteria to an implant is determined by a variety of factors according to dipole-dipole attractions, atomic structure, oxidation number and also according to the single properties of each implant material as for example its topography.<sup>63</sup> Also, hydrophobic biomaterial surfaces potentiates high adherence to bacteria with hydrophobic cell surface since there is a decrease in the free surface energy. After adherence, bacteria begins to proliferate and to produce a polysaccharide "slime" that is excreted involving the colonies for protection and structural support. This process allows bacteria to strongly adhere to the implant material providing the appropriate environment for the aggregation of bacterial cells (cell-to-cell adhesion), as well as for the consolidation of the binding permitting the build-up of multi-layers of microorganisms – biofilm.<sup>13</sup> This biofilm formation is a critical problem in device related-infections as it provides significant

resistance to antibiotics, for instance, as well as a platform for further spreading of bacteria.<sup>68</sup> Finally, these resistance and prevalence of microbial infection can result in the maintenance of an inflammatory environment which, as described above, may strongly impair the tissue repair. Consequently, the required processes of osteoinduction, osteoconduction and lastly osseointegration for a complete bone healing after implant surgery will be highly affected and will have a severe delay in the final outcome.

## 5. Pathogenic *Staphylococcus aureus* and *Staphylococcus epidermidis*

Staphylococci are facultative anaerobic Gram-positive bacteria known by its spherical-shape morphology and clustering cocci arrangement with between 0.5 - 1.0  $\mu\text{m}$  in diameter. Being Gram-positive bacteria, they lack the outer membrane but they possess a thick peptidoglycan layer with low content in lipid and lipoprotein outside of the cell membrane. Cell wall of this type of bacteria is significantly more resistant than the one of Gram-negative (with a thin peptidoglycan layer) which is more susceptible of being compromised<sup>69</sup>. Staphylococci may further be divided into two main group: coagulase-positive and coagulase negative staphylococci (CoNS) bacteria<sup>70</sup>.

*Staphylococcus aureus*, coagulase positive bacteria, are known to naturally and perpetually colonize the moist squamous epithelium of the anterior nares which end up to be the main reservoir of this microorganism in the human body<sup>71</sup>. Other less significant body sites are also prone to *S. aureus* colonization comprehending mucous membranes such as vagina, pharynx and perianal area. Normally, an undamaged squamous epithelium do not provoke chronic colonization of *S. aureus*, nevertheless, the skin may support transient colonization providing to bacteria a way of being carried from one place to another within the body<sup>72</sup>. However, in some cases, this organism is able to promote minor superficial skin infection (as abscesses or impetigo, for instance) or in more severe cases of infectious invasion to cause endocarditis, septic arthritis and osteomyelitis<sup>73</sup>. Therefore, given its natural occurrence in the body and facility in carriage/transmission, *S. aureus* colonization and infection is a critical health community concern that is tremendously increased in patients who have been catheterized or gone through surgery<sup>71</sup>. The treatment of these infections is progressively becoming of more difficult resolution given the wide appearance of strains resistant to multiple antibiotics, largely known as methicillin-resistant *Staphylococcus aureus* (MRSA)<sup>71</sup>. Accordingly, MRSA has arisen as the single most common surgical-site infection pathogen in hospitals<sup>74</sup>.

Also *S. epidermidis* is a natural occurring and widely coloniser of the human epithelia being mostly found in the axillae, head and nares<sup>75</sup>. Contrary to *S. aureus*, *S. epidermidis* is a coagulase-negative bacteria and therefore the enzyme coagulase is not expressed<sup>70</sup>.

This microorganism is well-known to provoke nosocomial infections extremely easily, once more, given to its natural presence in the human skin and mucosa, fact that eases its entrance either by body injuries or by implanted devices <sup>76</sup>.

Both *S. aureus* and *S. epidermidis* are biofilm producer bacteria and therefore they have the ability to form biofilm within or on the surface of implant devices. The eradication of this biofilms rises great concern as they constitute a very effective way of bacterial to evade from the external mechanism directed to their kill. As described, these are two bacterial strain which naturally occur in our bodies being part of our intrinsic flora what turns these microorganisms a constant concern when dealing with cases of potential direct exposure such as in surgery. Accordingly, *S. aureus* and *S. epidermidis* are the most common opportunistic pathogens associated with orthopaedic infection as they are together responsible for the cause of around 66% of this cases (Figure 4.) <sup>77</sup>.

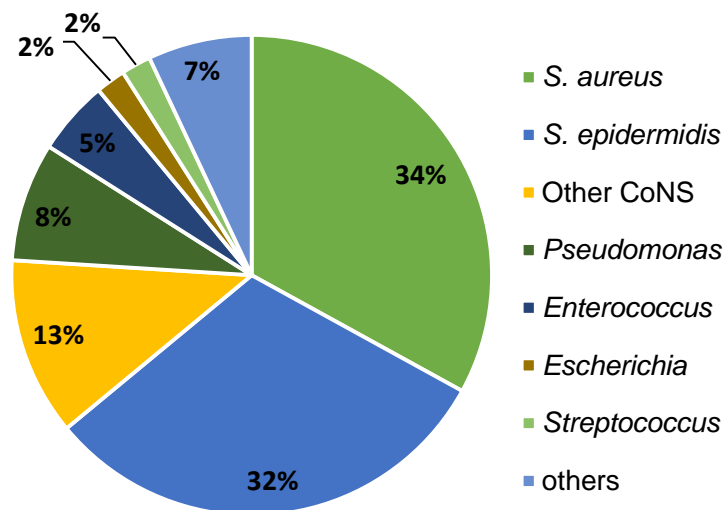


**Figure 4.** Frequency of main pathogenic species found in clinical isolates from orthopaedic implant-associated infections (adapted from <sup>77</sup>).

## 6. Prevention of bacterial infection: the window of opportunity before biofilm development

Bacteria may be found in two distinct states, either as planktonic or sessile cells. The planktonic cells are defined “as free flowing bacteria in suspension” whereas cells in the sessile state (ordinarily known as biofilm) are “structured community of bacterial cells enclosed in a self-produced polymeric matrix and adherent to an inert or living surface” <sup>78</sup>. These biofilm structures start to be formed when floating bacteria (planktonic bacteria) segregate endogenous signalling molecules coordinating the process of attachment in a phenomenon called quorum sensing <sup>79</sup>. The biofilms can be formed not only attached to a

surface but also either suspended as flocks in fluid or as pellicles in air-liquid interfaces and take typically around 10 days to reach full structural maturity<sup>80</sup>.

The correct development of a bacterial biofilm may be conditioned by a diversity of factors comprehending the type of bacterial strains involved, the properties of the material surface, environment parameters (as pH, nutrients and temperature) as well as the hydrodynamic conditions once bacteria phenotypically react to different shear stress<sup>81</sup>. During biofilm formation, there are also mechanisms such as cell surface aggregation by the rearrangement of attached cells through bacterial motility, the binary division of the attached cells which allows new cells to spread into different directions creating clusters and the recruitment of planktonic cells which are essential in the biofilm success<sup>80</sup>.

The biofilm structure gives the opportunity to single-cell microorganism to take part on a multicellular lifestyle group which is must well equipped and prepared. It allows increased resistance to either antibiotics, microbicidal agents, host immune responses (innate and adaptive) or other adverse conditions presented in the environment<sup>79,82,83</sup>. This is due to the fact that sessile bacteria presents different phenotypes regarding growth, gene expression and protein production which confers higher resistance<sup>84</sup>. In fact, the biofilms is believed to be 100-1000 folds less susceptible than equivalent planktonic bacteria in terms of Minimum Inhibitory Concentration (MIC) and Minimum Bactericidal Concentration (MBC)<sup>83,85</sup>. Biofilm infection is, therefore, in contrast to acute planktonic infection, usually associated to chronic infections<sup>86</sup> and there are 6 principal factors that confer to this structures its incredible resistance: (1) biofilm matrix as diffusion barrier against antibiotics penetration; (2) microenvironments inside biofilm (lack of nutrient lead to reduced antimicrobial activity which diminish their susceptibility to antimicrobials); (3) bacterial differentiation into persistent cells (dormancy state/antimicrobial tolerance); (4) chemical interaction between antimicrobials and biofilm components; (5) induced resistant factors – high mutation frequency (horizontal gene transmission and heterogeneity); and (6) programmed apoptosis (population is able to growth faster after adverse conditions due to cell death content release)<sup>83,85,86</sup>.

From the strategies applied against pathogenic biofilm, unquestionably the most desired one, is to simply prevent its formation by rapidly eradicating the bacteria in the planktonic state before the possibility of biofilm development occurrence. At this stage, planktonic bacteria is still vulnerable to host defence mechanisms and antimicrobial agents since it is not under the biofilm environment protection. The difficulty here is to detect initial biofilm formation which reveals to be very tricky once little inflammation is observed from a clinical perspective. Therefore, the use and creation of implant devices/materials where antimicrobials are implemented and *in situ* released from the very beginning seems to be



the most convenient strategies targeting and killing planktonic bacteria avoiding sessile bacteria establishment<sup>87</sup>

Antibiotics, for instance, have been used as prophylactic drugs by being directly incorporated within materials. Hendriks et al, have developed gentamicin modified bone cement for total hip arthroplasty fixation where is proposed the delivering of the antibiotic both at the time of surgery and in the years to come to fight infection. Also utilizing metal ions, Ewald et al, have developed a silver-doped calcium phosphate cement where the  $\text{Ag}^{2+}$  ions release was investigated for their antimicrobial properties. The silver ions revealed a controlled release over time with excellent antimicrobial activity both against *S. epidermidis* and *S. aureus*<sup>88</sup> These are examples of approaches that provide a controlled release of the antimicrobial agent given by a gradual degradation of the material preventing an antimicrobial infection right at the time of surgery and in the years after. Planktonic bacteria are therefore attacked from the very first beginning precluding biofilm development.

## 7. Antimicrobial systems: contact and leaching

Over the years, some strategies have been designed in order to avoid implant-related infections. These strategies are based on different approaches in the creation of antimicrobial materials. Such approaches may be based on contact and leaching systems and they both represent mechanisms that act only locally, avoiding systemic administration of antimicrobial substances.

In general, the approaches utilized to fight against implant-related infection can be categorized in: (i) biomaterials design to inhibit microbial adhesion to its surface; (ii) biomaterials with covalently linked antimicrobial agents; and (iii) biomaterials with physically arrested antimicrobial agents.<sup>66</sup>

In the first case (i), anti-adhesive surfaces are able to significantly reduce the amount of adherent microorganism and it is clear the benefit of this by diminishing the chance of contamination of a biomaterial. For instance, an anti-adhesive surface can be accomplished by functionalization of the surface with covalent linkage of poly(ethylene glycol) (PEG). In fact, PEG molecules represent one of the most effective systems in decreasing bioadhesion as demonstrated by its ability to reduce, by between two and four orders of magnitude, the adherence of *Pseudomonas sp.*<sup>89</sup> However, it is important to denote that, besides the anti-adhesive properties of the surface, the microorganisms that enter in contact with it are not killed. Therefore, despite the advantage of non-adherence, microorganisms are still able to survive and proliferate in case of contamination. Furthermore, besides the good anti-adherent properties of some materials, in reality it is practically impossible to form a complete non-adherent surface. This happens given thermodynamic reasons and

consequently, *in vivo*, the surface of a material is promptly covered by plasma and connective proteins.<sup>90</sup> Hence, different and better strategies can be designed to prevent implant-related infections, instead of anti-adherent surfaces, by the modification/functionalization of materials with antimicrobial components such as antibiotics and/or metals.

In the second case (ii), the goal is the creation of a non-leaching contact killing antimicrobial material. The surface of these materials should have the ability to kill microorganisms in contact without occurring significant leaching of the antimicrobial agents into the surrounding environment. In the design of these contact systems, it is possible to promote, upon direct microbial contact, a selective transference of the antimicrobial agent to the microorganism through a “hand-off” mechanism where engagement and cell membrane penetration occurs. Thus, antimicrobial contact systems can, theoretically, afford extended efficacy and activity without releasing possible toxic components to the involving areas.<sup>91</sup> However, in these materials where antimicrobial substances are covalently and permanently bound to the surface, a phenomenon of accumulation of killed microorganisms occurs. This process can significantly decrease the antimicrobial activity of the surface over time as more and more killed microorganisms gather onto the surface covering the antimicrobial coating.<sup>66</sup> Therefore, other approaches should be developed and applied in order to overcome the observed diminished antimicrobial efficacy of these contact systems over time.

The third case (iii), offers the possibility of physically immobilizing the antimicrobial agents in the material. These represent leaching systems which allow for a gradual release of antimicrobial agents over time from the material to the involving areas. This mechanism is, therefore, meant for a local delivery of antimicrobial components which is believed to be sufficient to provide enough concentration to eradicate microbes.<sup>92</sup> Nonetheless, these systems have also some concerns that are related with the necessary amount of antimicrobial agent (e.g. antibiotics and metal ions) to be incorporated in the material. It is known that it is possible to verify a gradual decrease in the level of antimicrobial agents released with time.<sup>66</sup> This aspect can cause the formation of an under inhibitory concentration of antimicrobial compounds that, besides being insufficient to kill the microbes, provides a good environment for the development of microbial resistance. For that, it is crucial to have in consideration the quantity of time that the material is going to serve its purpose within the patient’s body, to understand the amount of antimicrobial agents to be incorporated in the material together with the problem of resistant pathogens development<sup>90</sup>. Within the leaching systems there is also the possibility of designing biodegradable biomaterials that release antimicrobial compounds, *in situ*, upon its degradation, *in vivo*. Metal cations like silver and strontium, for instance, have been used

as antimicrobial agents by incorporation in the formulation of biodegradable calcium phosphate materials<sup>93</sup>. Additionally, it was also demonstrated that higher amount of strontium substitution, for instance, was related with increased degradation profiles. Thus, this gives the possibility to manipulate, as needed, the degradation kinetics in order to develop the most efficient leaching system.<sup>94</sup> One important aspect in the use of metal ions as antimicrobial agents is that the antimicrobial activity of silver, for instance, has been attributed to its oxidized form ( $\text{Ag}^+$ ) which is only present upon its release from the implant material.<sup>11</sup> Thus, similarly to silver, strontium ions in antimicrobial materials would have to be implemented in a leaching system in order to release the strontium cations ( $\text{Sr}^{2+}$ ) to the surrounding environment.

## 8. Metal ions as antimicrobial agents and its incorporation in biomaterials

The use of metals and metalloids as antimicrobial have been, unquestionably, one of most important application in medicine<sup>95</sup>. Table. 2 enumerates the metal and metalloids that had been or are still being used as antimicrobial agents in medicine.

From the listed elements below (Table 2.), Ag, Cu, Zn and Sr, have already been described in the **section 3.2.1., Table 1** as possible cationic substitutes on the HAp structure. Therefore, the substitution of calcium by antimicrobial ions in the calcium phosphate structure suggests an exciting approach to the development of new modified antimicrobial ceramic materials. One example are calcium phosphate cements that have been doped with silver and upon degradation the cations are released to the surrounding areas with antimicrobial activity both against *S. aureus* and *S. epidermidis*<sup>88,93</sup>. Similarly, strontium-doped HAp nanoparticles have been created with the same purpose and results showed significant effect over *S. aureus*, *E. coli* and *Lactobacillus*<sup>94</sup>.

Also, from the elements present in Table 2, Sr and Cu catch our attention as they have been presented in **section 3.1.1.** as potential ionic cross-linking agents employed in the obtainment of alginate hydrogels. Here too arises the possibility of creating alginate hydrogel rich in antimicrobial ions. For instance, Madzovska-Malagurski et al, have development Cu-alginate hydrogels in the form of microbeads utilizing a gelling solution of  $\text{Cu}^{2+}$  for antimicrobial purposes. Both against *S. aureus* and *E. coli* the microbeads have revealed instant bactericidal activity<sup>35</sup>. Also using  $\text{Cu}^{2+}$  ions, Grace et al, have developed copper alginate-cotton cellulose (CACC) fibres which proved to kill in an effective manner the challenged bacteria *E. coli* upon copper ion release<sup>96</sup>. Using a different metal ion such as zinc, nano zinc oxide-sodium alginate cellulose fibres were created by Varaprasad et al, which showed excellent antimicrobial properties over *E. coli*<sup>97</sup>.

**Table 2.** Metal and metalloids used as antimicrobials (elements presented by their chemical symbol).

<b>Antimicrobial elements</b> (chemical symbol)	<b>Ag</b> <sup>93</sup>	<b>As</b> <sup>95</sup>	<b>Au</b> <sup>98</sup>	<b>Bi</b> <sup>99</sup>	<b>Ce</b> <sup>100</sup>	<b>Cu</b> <sup>35</sup>	<b>Ga</b> <sup>101</sup>	<b>Hg</b> <sup>102</sup>
	<b>Pb</b> <sup>95</sup>	<b>Pd</b> <sup>98</sup>	<b>Sb</b> <sup>95</sup>	<b>Sn</b> <sup>103</sup>	<b>Sr</b> <sup>94</sup>	<b>Te</b> <sup>104</sup>	<b>Tl</b> <sup>95</sup>	<b>Zn</b> <sup>105</sup>

Concerning the discussed metal ions, Strontium emerges as the most polyvalent given its possibility to be both introduced in the structure of calcium phosphate materials and in the production of alginate hydrogels.

## 9. The potential of Strontium

### 9.1. Strontium incorporation and distribution in bone

Animal tissues have in their composition several trace minerals and strontium is one of them (0.00044% of body mass).<sup>18</sup> Strontium is predominantly present in bone tissues given its great affinity to them. Thus, strontium accumulates almost exclusively in the bone. The incorporation of this element occurs by two distinct mechanisms: ionic substitution and surface exchange.<sup>106</sup> Besides strontium preference in accumulating in bone, its concentration in this tissue is actually always very low. Indeed, even in animals administered with high doses during extended period of times, the quantity of strontium is significantly smaller than the one of calcium. This is coherent with the theoretical value that determines, in maximum, that only one out of ten atoms of calcium can be substituted by one of strontium.<sup>107</sup>

Researches have defined that the uptake of strontium comprehends two different phases based on its dynamics: one that occurs initially and relatively rapid; and another that happens in a slow manner. The first one is dependent on osteoblastic activity and then, when saturated, is mediated by ionic exchange of  $\text{Ca}^{2+}$  or by linkage with preosteoid proteins. The second one corresponds to the integration of strontium ions into the crystal lattices of the bones.<sup>108</sup> This two phase concept is generally recognised being the rapid phase related with the uptake into newly formed bone and the slow long-term ion exchange related with old bone. Accordingly, studies made in cynomolgus monkeys demonstrated that strontium was heterogeneously distributed within bone. Both newly formed compact and cancellous bone presented, respectively, around three and 2.5-folds more strontium than in old one.<sup>106</sup> There are a diversity of factors that influence the strontium incorporation into the bone. Experiments conducted in animals have identified five: dose, plasma strontium level, gender, duration of treatment and skeletal site.<sup>106,109</sup>

### 9.2. Effects of strontium in modified biomaterials

It is well established that the  $\text{Ca}^{2+}$  ions in the structure of hydroxyapatite can be substituted by other compatible metal ions. These substitutions allow for several improvements of the material providing the possibility to modulate its properties and bioactivity.<sup>1</sup> Thus, the use of strontium and the alteration of its concentration in the material structure can be manipulated in order to influence the final mechanical strength, degradation profiles and cell-material interactions.<sup>44</sup> This ionic substitution can also bring some alterations in the structure of the material, as the crystal morphology, crystallinity, and lattice parameters as well as in the solubility and in the thermal stability of hydroxyapatite<sup>40</sup>. The ionic radius of strontium (113 pm) is significantly larger than that of calcium (99 pm), and, consequently, its incorporation in the structure of hydroxyapatite induces variations in the crystalline unit cells. At low amounts of substitution, strontium induces distortions in the crystal's shape, whilst high substitution increases the mean dimensions and the crystallinity of the crystals.<sup>110,111</sup>

Our group has previously developed a hybrid polymer-ceramic injectable system where Sr-rich microspheres are embedded in an alginate matrix that reticulates, *in situ*, by the presence of strontium. Thus, the loading forces acting over the alginate matrix are supported and dispersed through the microspheres rigid structure. In fact, the created microspheres revealed similar friability, but twice the hardness when compared to the pure HA microspheres. These mechanical properties are important aspects since no damages should occur to the microspheres in the processes of their handling and extrusion by injection. Furthermore, the spherical shape (without sharp edges) of the HAp microparticles allows for a good injection ability without separation of the two phases (vehicle and microspheres) as well as for a good spatial accommodation in the body site. Accordingly, an appropriate temporary scaffold is created allowing cells to migrate through, ensuring bone tissue ingrowth. This hybrid system was design to have two different strontium release kinetics: one initial and faster from the strontium prevenient from the degradation of the alginate matrix; and a second and slower originated from the degradation of the HAp microspheres.<sup>112</sup>

The strontium incorporation in calcium phosphate cements has also been reported to influence the porous structure of the material.<sup>14</sup> Such alteration can be advantageous once the specific surface area of the cement is significantly increased creating more available sites, for instance, for antibiotic adsorption. Therefore, if it is aimed to load the biomaterial with antibiotics or any other agents, increased pore size induced by strontium may be implemented in order to improve the loading capacity. This way, for instance, a higher and more effective local drug delivery may be accomplished.<sup>14</sup> In another study, in

contrary, the higher incorporation of strontium in biphasic calcium phosphate granules demonstrated less porosity and higher percentage of HAp leading to a lower degradation rate and subsequently a possible extended drug release *in vivo*.<sup>113</sup> However, it has been demonstrated that the doping of BCP with strontium provokes a decrease in hardness and in the elastic modulus when compared to pure BCP.<sup>41</sup> Modulating the porosity of the material and, therefore, its degradation profile it is possible to create systems with an initial burst of loaded agents (accommodated in the porous lattices) followed by a continuous long-term release of strontium ions upon material dissolution.<sup>114</sup> In fact, increasing amounts of strontium substitution has been related with higher solubility of HAp ceramics consequence of structure destabilization, once the ionic radius of calcium is considerably smaller than that of strontium.<sup>110</sup> For instance, structurally, the addition of strontium showed to induce an increase in the grain size of strontium doped HAp and TCP when compared to the respective pure material. In the case of Sr-TCP the bigger grain size observed was related with a decrease in osteoclast resorption ability. Actually, it had been reported before that an increase osteoclast-like-cellular resorption activity is observed in HAp when grain size is decreased. Therefore, incorporation of strontium in HAp and TCP may be used to decrease osteoclast activity since it is proposed that osteoclast cells do not readily resorb bigger grains.<sup>115</sup> Thus, strontium incorporation induces alterations in the structure and physico-chemical properties of the materials changing their biological performance.<sup>110</sup> Additionally, the incorporation of strontium has also been used to increment radio-opacity of the material. For instance, a strontium-containing calcium phosphate cement have been proved to be three times more radio opaque than cortical bone, which represents a noteworthy advantage as radio-opacity is a requirement, for instance, for spinal surgery.<sup>116</sup>

The interest in the substitution of  $\text{Ca}^{2+}$  ions for  $\text{Sr}^{2+}$  does not rely only on the modification of calcium phosphate materials *per se*, but also in the knowledge that strontium has beneficial effects over bone metabolism and in the fight against microbial infection, as it will be further discussed in the next sections.

### 9.3. Strontium activity in bone regeneration

Strontium acts in two different ways at the same time once it promotes bone formation while inhibiting bone resorption.<sup>117</sup> For instance, several studies, both *in vitro* and *in vivo*, have revealed that Sr-substituted HAp stimulates osteoblast proliferation and inhibits osteoclastogenesis in both osteopenic and normal cells.<sup>18</sup>

There are several mechanisms involved in the activity of strontium in bone formation and resorption inhibition. The mechanism of action of strontium consists in its ability to

displace  $\text{Ca}^{2+}$  ions in osteoblastic calcium-mediated processes; for instance, strontium revealed to increase bone formation by activating the calcium sensing receptor (CaSR).<sup>44</sup> It has been described that the strontium osteoblast stimulator concentration is in the range of 25 ppm.<sup>118</sup> Studies have been made to prove the influence of strontium in osteoblast cell differentiation. For instance, ALP activity of hFOB cells, a key enzyme expressed during osteoblast differentiation, revealed to be moderate in HAp coatings and significantly up-regulated in Sr-HAp, both after 5 and 11 days culture. Strontium, acts also over osteoclast activity and it has been reported to inhibit it at concentrations around 85 ppm.<sup>119</sup> Strontium acts too by the CaSR to induce apoptosis in osteoclasts in a process similar to that of the calcium.<sup>120</sup> CaSR are fundamental regulators of the bone cell metabolism and they control multiple processes such as recruitment, differentiation and survival of osteoclasts and osteoblasts. This is done by CaSR-mediated activation of intracellular signalling pathways.<sup>121</sup> Thus, strontium activity over this receptor represents a useful weapon to fight against problems associated with unbalance between bone formation and resorption such as osteoporosis. Additionally, strontium has also been reported to activate the Wnt/ $\beta$ -catenin signalling, a signalling pathway that is strongly present in embryonic development and largely contributes to bone development and homeostasis. Wnt/ $\beta$ -catenin strontium-induced activation has shown to contribute to ECM accumulation and to the osteogenic differentiation of mesenchymal stem cells (MSCs) into preosteoblasts and osteoblasts.<sup>122</sup> Another mechanism by which strontium acts as inhibitor of bone resorption is related with the receptor activator of nuclear factor  $\kappa$ -B ligand (RANKL) and osteoprotegerin (OPG). This process starts with the receptor activator of nuclear  $\kappa$ B ligand (RANKL), a stimulator of osteoclast differentiation produced by osteoblast that acts by binding and activating the RANK in the cell-surface of precursors and mature osteoclasts.<sup>123</sup> This signalling activation step results in the expression of genes involved in the promotion of osteoclast survival and differentiation leading to osteoclastogenesis and bone resorption.<sup>124</sup> Another intervenient, the osteoprotegerin (OPG), which is also produced by osteoblasts, acts as an inhibitor of this osteoclast activation process. OPG functions as a soluble competitor interacting with RANKL and preventing this last one to activate RANK, impeding osteoclastogenesis and consequently bone resorption.<sup>125</sup> It's by increasing the production of OPG that strontium performs its inhibition activity. Thus, the triad OPG/RANK/RANKL represents a critical signalling mechanism in the regulation of osteoclast activity since abnormalities in this system have been associated with skeletal diseases related with excessive osteoclastogenesis and bone resorption.<sup>123</sup> Here, strontium may embody an important approach in the regulation of the molecular OPG/RANKL ratio for a diminished osteoclast activation.<sup>44</sup> In *in vitro* studies, strontium showed also to be effective in inhibiting the formation of a podosome belt that defines the sealing zone, a process that is crucial in

osteoclast bone resorption. In the control test, without addition of strontium ranelate, osteoclasts revealed a typical sealing zone formation, whereas cells with 0.1 and 6 mM of strontium ranelate showed sealing zone disruption <sup>117</sup>.

Nevertheless, the strontium ability to interfere with osteoclast size and number has been reported to be dependent on free ion concentration. Thus, Rousselle et al. have demonstrated that  $\text{Sr}^{2+}$  up to 10 ppm in the culture media does not affect osteoclast activity. It is important to have this value in consideration in the design of new biomaterials in order to be able to deliver a therapeutic amount of  $\text{Sr}^{2+}$ . <sup>126</sup> Besides the importance of delivering a sufficient amount of strontium to the bone, it is also of great relevance to guarantee this release since the early stages of healing. Our group, for instance, has accomplished this with the development of the already discussed hybrid system with two strontium release kinetics which potentiate the effectiveness of strontium in bone remodelling. <sup>112</sup> This hybrid system has already proved its value by showing promising results, *in vivo*, in two different animal models (rat and sheep) where bone formation was successfully induced without occurrence of a fibrous interface (unpublished results). In addition to the mentioned activities of strontium in bone regeneration, one preliminary but promising study has revealed that strontium, in Sr-doped HAp ceramic, has significantly decreased the production of TNF- $\alpha$ , a pro-inflammatory cytokine. It has already been discussed, in previous sections, how excessive inflammation may impair bone healing, thus this finding could be of great importance in the creation and design of new Sr-doped calcium phosphate materials. Therefore, it would be possible to both modulate inflammation and osteogenic properties of the biomaterial. <sup>1</sup>

#### 9.4. Strontium cytotoxicity

As a bone seeking element, strontium may have different effects over bone metabolism. These effects are directly connected with the dose at which strontium is present in the tissue. Hence, as already mentioned before, strontium has incredible beneficial effects on bone formation and remodelling. <sup>117</sup> However, its positive effects are only appreciated when administered at low doses. According to the literature, a low dose of strontium is considered to be  $\leq 4$  mmol Sr/kg/day. In agreement with that, several *in vivo* studies in normal rats and mice have revealed that, for instance, doses of 1.6, 1.9, 2.4 and 3.51 mmol/kg/day, induce bone mass augmentation at diverse skeletal sites without secondary effects over bone mineralization. Contrary, high doses of strontium have been related to provoke bone abnormalities such as defective bone mineralization, induced rickets and alterations of the mineral profile. <sup>127</sup> Studies have been conducted in normal rats in order to assess the effect of high doses of strontium and after administration of doses



superior to 8 mg/kg/day changes were observed in the mineralization characterized by decreased mineral density of bone and decreased size of bone apatite crystals.<sup>128</sup>

*In vitro* studies conducted on fibroblastic cells have been done in order to evaluate the cytotoxic effect of strontium substituted HAp and several percentages of incorporation were used, namely, pure HAp, 1% Sr-HAp, 5% Sr-HAp, 10% Sr-HAp and pure (100%) Sr-HAp (materials fabricated to the shape of 10x10x1 mm and then soaked for 48h to prepare extract solutions of the materials for cell incubation). MTT assays didn't show any signs of cytotoxicity for all Sr concentrations. However, it was noticeable a decrease in the relative growth rate (RGR) of the cells with the increase of strontium concentration. In agreement, also flow cytometry analysis to the cell cycle revealed that augmentation in Sr concentration was correlated with a decrease in the cell proliferative ability.<sup>129</sup> Thus, strontium materials appear to demonstrate good biocompatibility especially for 1% and 5% Sr concentration.<sup>130</sup> Additionally, another *in vitro* study has been made with osteoblast cells seeded on strontium-doped calcium polyphosphate (SCPP) scaffolds with several strontium concentrations (0%, 0.5%, 1%, 5%, 10%, 20% till 100%). MTT and ALP analysis were conducted to assess cell proliferation and differentiation and no cytotoxic effect were found in osteoblast cells. However, and concordant with previous results, SCPP containing low doses of strontium demonstrated higher osteoblast cell proliferation and differentiation being the 1% strontium the optimal concentration, given the MTT and ALP activity assay<sup>131</sup>.

### 9.5. Strategies using strontium as antimicrobial

Dopants such as metal ions have been used to alter the biomaterial structure in order to manipulate its final mechanical strength, degradation profiles and cell-material interactions. The concentration of these dopants and its combinations with others are determinant parameters in the establishment of the final material properties.<sup>44</sup> As already discussed before, the potential of strontium in bone regeneration in the treatment of bone defects and diseases such as osteoporosis is unquestionable.<sup>18</sup> However, other factors such as post-operative infection may be equally important to the very ability of the material itself to promote bone growth. This is understandable given the collateral damage that can be observed upon infection by a pathogen with its produced toxins that lead to an inflammatory reaction that significantly impair bone healing and regeneration.<sup>58,61</sup> This section of the document is aimed to address the use of strontium as an antimicrobial agent both alone and incorporated in calcium phosphate ceramic materials in order to fight against implant-related infection.

Few studies have been made in order to assess the antimicrobial effect of strontium substituted/enriched biomaterials. Lin et al, have studied the antimicrobial activity of strontium in half and totally substituted hydroxyapatite nanoparticles over *E. coli* (gram negative bacteria; Gram -), *S. aureus* (gram positive bacteria; Gram +) and *Lactobacillus* (Gram + bacteria). Bacterial inhibition zone tests and antibacterial ratio of inhibitors determined by Shake Flask method were made to assess the antimicrobial activity. It was demonstrated that the antibacterial properties were improved when  $\text{Ca}^{2+}$  was half or totally substituted by  $\text{Sr}^{2+}$ . Both pure HAp and Sr-half substituted HAp nanoparticles showed inhibition zones no greater than 7 mm (defined limit of significant inhibition) and antimicrobial properties at concentration of 0.1 g/mL (10 g powder in 100 mL sterilized and distilled water) only when in dynamic contact with the microorganisms (pure HAp with lower antimicrobial activity). In contrary, Sr-total substituted HAp revealed inhibitions zones approximately three-fold higher and antimicrobial activity independently from static or dynamic contact with bacteria for the same powder concentration (0.1 g/mL). It was also highlighted the potential of the Sr-half and total substituted nanoparticles over *Lactobacillus* in the fight against dental caries. The higher antimicrobial activity was correlated with the higher content on strontium of the material since it induces a higher rate of HAp dissolution releasing more  $\text{Sr}^{2+}$  ions. Thus, higher amounts of  $\text{Sr}^{2+}$  ions are released as we go from half to totally substituted hydroxyapatite. The higher solubility allows, therefore, for a much more efficient leaching system where the antimicrobial ions are released in higher amounts to the surroundings.<sup>94</sup> Also Ravi et al. have conducted an experiment where the antibacterial properties of strontium substituted calcium deficient hydroxyapatite (CDHA) nanoparticles (5% and 10% substitution) were assessed at powder concentrations of 0.1 mg/mL against *S. aureus* and *E. coli* for 24h incubation. Here in this study, authors were also able to prove that the bacterial colonies significantly decrease according to the density of strontium substitution. Thus, the 10% substitution showed the higher antibacterial activity followed by the 5% and the pure CDHA nanoparticles. These nanoparticles demonstrated, respectively, a maximum of microbial reduction of 56%, 25% and 10% against *E. coli* and 35%, 13% and 12% against *S. aureus*. These results are in agreement with the already discussed effect of the increased ion release from higher strontium substituted materials.<sup>18</sup> Contrary to these results, Kumar et al., developed CDHA nanoparticles with 2.5%, 5% and 7.5% strontium substitution that showed weak activity on *S. aureus* (MIC of 200 mg/mL and MBC of 300 mg/mL) and no effect on *E. coli* for concentrations up to 300 mg/mL.<sup>114</sup> The concentrations of powder used were significantly higher than that used by Ravi et al., thus the bad results obtained were not expected. Since powder dispersion was ensured and incubation times were the same, the explanation may be connected with the efficiency in  $\text{Sr}^{2+}$  ion elution. Like Lin et al and Ravi et al., Gopi et al. have also assessed the antimicrobial activity of ion

substituted hydroxyapatite nanoparticles. In this case, despite of the fact that the aim of the work was to develop a co-substituted HAp by  $\text{Sr}^{2+}$  and  $\text{Ce}^{3+}$ , it was also evaluated the potential of strontium substitution alone in what respects to its antimicrobial properties. Disc diffusion method was conducted to determine the inhibition zone against *E. coli* and *S. aureus*. The Ca/Sr-HAp nanoparticles have then revealed inhibition zones of 8 mm and 9 mm against *E. Coli* and 7 mm and 8 mm against *S. aureus* for 100  $\mu\text{L}$  and 125  $\mu\text{L}$  (volume containing nanoparticles as synthesized), respectively. Against both bacteria, the Ca/Sr-HAp nanoparticles revealed antimicrobial activity (inhibition zones greater than 7 mm as described by Lin et al) showing a slightly greater effect against the Gram - *E. coli*.<sup>132</sup> All the discussed studies have clearly shown that strontium modified hydroxyapatite nanoparticles can act both against Gram + and Gram - bacteria. Nevertheless, it was also in concordant that the effects over Gram + bacteria were noticeably smaller than those on Gram -. This can be explained by the differences in cell wall composition as Gram + bacteria possess a much thicker peptidoglycan cell wall which may significantly preclude the  $\text{Sr}^{2+}$  ion penetration in the bacterial membrane and ultimately, cytoplasm.<sup>133</sup> With different application, but also with interesting results, strontium titanate ferrite metal oxide (STF) nanoparticles have been developed and proved to be efficient in microorganism elimination. In this experiment, these nanoparticles, at powder concentration of 1 g/L, were tested against *E. coli* and all the bacteria were killed after only 15 minutes incubation. Antibacterial properties were correlated with the positive surface charge, high pH environment, nano-size and  $\text{Sr}^{2+}$  release, which has been found in concentrations of 49.3 mg/L after overnight resting of 1 g/L of STF nanoparticles in distilled water.<sup>134</sup>

Similarly to Gopi et al., strontium and cerium were also chosen to co-substitute hydroxyapatite, but in this case in order to obtain a composite material of S-PEEK/Sr,Ce-HAp to be used as coating. Nonetheless, also in this study the antimicrobial activity of strontium was evaluated alone by disc diffusion method against *E. coli* and *S. aureus*. S-PEEK/Sr-HAp composite showed inhibition zones of 8 mm against *E. coli* and 5 mm against *S. aureus* after 14 days incubation for a volume of 125  $\mu\text{L}$  of composite sample.<sup>135</sup> Contrary to these results, a work with the goal to improve the antimicrobial and biological properties of silver substituted hydroxyapatite coatings by co-incorporation of strontium in the material did not show positive antimicrobial action. The action of strontium alone was addressed by disc diffusion method and the inhibition zones were null for the Sr-HAp both against *E. coli* and *S. aureus* after 24h incubation. Thus, the contribution of strontium in this work was only attributed regarding its osteogenic abilities. The bad results may be related with a non-efficient release of strontium from the coating as the assessed amount of  $\text{Sr}^{2+}$  ion release for the 24h period was only of 50  $\mu\text{g/L}$ , which is manifestly lesser than the quantities reported by Zang et al. that had good antimicrobial activity.<sup>136</sup> The antibacterial properties of

strontium have also been tested against *P. aeruginosa* (Gram -) by assessing the viable and adherent bacteria (Live/Dead Backlight kit) on the surface of Sr doped (1 wt.% SrO) plasma sprayed HAp-coatings on pure titanium substrates. This study showed that after 24h of culture, the Sr-HAp samples demonstrated no significant antibacterial effect on this microorganism as low quantities of dead bacteria and high amount of live ones were found on sample's surface.<sup>44</sup> This study did not address the Sr<sup>2+</sup> ion release from the coatings and therefore the obtained results are only respected to the live or dead bacteria adherent to the surface. Thus, conclusions can only be taken considering an antimicrobial contact system and as it was discussed in a previous section, the antimicrobial activity of strontium is potentially closely related with its ion oxidized form Sr<sup>2+</sup>, only concordant with a leaching system. Therefore, further analysis should be taken in this particular system in order to determine the reason for the week results obtained, which may be related with the degradation profile of the coatings and consequently with the released amount of Sr<sup>2+</sup>. In this same category of materials, strontium doped apatite deposited onto titanium have also been evaluated for its antibacterial properties against *S. aureus*. Contrary to the results of Fielding et al, direct contact of these modified surfaces (with approximately 9±1 ppm of strontium) with bacteria revealed to produce a significant reduction in the numbers of bacteria as 49% kill was observed both before and after 30 days incubation. However, low levels of bacterial kill, no greater than 26%, were detected from incubation of ions eluted from the surface for 30 days. This was concordant with the only 10% ion release observed over this period of time. Thus, given the low release rate, the concentration of eluted ions was most probably under the minimum inhibitory concentration (MIC) of *S. aureus* what clarifies the observed week antimicrobial activity. In this study it was described that the low ion release explains the maintenance of the antibacterial activity of the direct contact of the coatings as high levels of strontium were still present (90%).<sup>137</sup> However, these last results and conclusions go against the premise that only leaching systems are suitable for antimicrobial activity of strontium. Nevertheless, there are some studies that have reported a different mechanism by which metal ions may induce antimicrobial activity. In fact, it was described that in metal ion substituted HAp an interaction phenomenon between redox couples like Ag<sup>0</sup>/Ag<sup>+</sup> or Cu<sup>0</sup>/Cu<sup>2+</sup> and O<sub>2</sub> result in the formation of superoxide anions (O<sub>2</sub><sup>-</sup>). Therefore, interaction of redox couple Sr<sup>0</sup>/Sr<sup>2+</sup> with O<sub>2</sub> may explain the observed antimicrobial activity given the low strontium ion elution.<sup>138</sup>

Different class of materials have also been subjected to strontium incorporation to assess increased antimicrobial activity. Indeed strontium in glass ionomer cements (GIC) for dental applications were used against *S. mutans* and *A. viscosus*, both Gram + bacteria, as these species are known to invade dental cavity floor under restorations. Against both bacteria the presence of strontium in the cement revealed increased inhibition zones. For

instance, against *S. mutans* and *A. viscosus*, GICs with different Sr:Ca molar ratio revealed inhibition zones of, respectively, 2.3 mm and 1.2 mm for 1.5:3.5, and 2.5 mm and 0.7 mm for 3:2, while the control demonstrated only 0.1 mm and non-detectable inhibition. In addition, only the cements containing strontium showed significant antibacterial contribution against *A. viscosus* in this study. It is also important to refer that all the GICs formulations had fluoride on its constitution, which raises the question if the antimicrobial effect is solely due to strontium activity or to a synergetic effect with fluoride. The analysis conducted in this experiment did not evaluate the strontium release from the material. Nevertheless, the observed antimicrobial activity can only be attributed to strontium (and possible synergetic fluoride) elution as inhibition zone tests evaluate the effects of diffusion of a microbicidal agent.<sup>139</sup> Also for dental application, the leaching of strontium ions was evaluated in resin modified glass ionomer cements (RMGIC). Several bacterial strains were tested (supra-gingival plaque strains: *S. mutans*, *S. sorbinus*, *S. salivarius*, *A. naeslundii*, *A. odontolyticus*, *A. viscosus*, *L. caesi*, *L. acidophilus*; and sub-gingival plaque strains: *P. gingivalis*, *P. intermedia*, and *A. actinomycetemcomitans*) using growth inhibition method and strontium (as strontium chloride hexahydrate) concentrations of 0.19, 0.37, 0.74 and 1.11 mol/L. Only for the highest strontium concentration it was observed a reduction of one log in bacterial concentration, whereas no significant alteration was noticeable for the other concentrations.<sup>140</sup> These results are contrary to those previous from Guida et al., which revealed significant inhibition against *S. mutans* and *A. viscosus*. The reason for the observed differences may be related with the presence of fluoride in the GICs developed by Guida et al. Thus, this study conducted by Dabsie et al., by assessing the strontium antibacterial activity alone, ended up to corroborate the synergistic effect of strontium and fluoride at least against *S. mutans* and *A. viscosus*. Despite this possibility, previous experiments conducted by Eisenberg et al., have equally shown low activity of strontium (up to 100 mg/L) alone against *S. mutans* and *A. viscosus*; however they also evaluated the synergistic effect of strontium and fluoride which they concluded to be inexistent. Therefore, it was proposed that instead of antimicrobial activity, strontium, in combination with fluoride, enhance enamel remineralisation and decrease demineralization explaining the less occurrence of caries.<sup>141</sup> Nevertheless, more recent studies have also evaluated the antimicrobial activity of strontium alone (strontium chloride hexahydrate concentrations: 0.25, 0.5, 1, 2 and 4 mM) and of strontium-substituted bioactive glasses with increasing strontium concentration (Sr substitutions: 1.95 mol% - 5Sr; 19.50 mol% - 50Sr; and 39.00 mol% - 100Sr). The challenged bacteria were *A. actinomycetemcomitans* and *P. gingivalis* and the results were obtained as percentage of inhibition of bacterial growth. In opposite to the reported inefficacy, by Dabsie et al., of strontium chloride to induce bacterial inhibition against *S. mutans* and *A. viscosus*, in this experiment strontium alone was able to significantly reduce

bacterial growth. *A. actinomycetemcomitans* and *P. gingivalis* were thus, inhibited in 30% and 45%, respectively, after 6h incubation. The motive for this may rely in the fact that these two bacteria are Gram - and, therefore, have a much thinner protective cell wall. Also incubation of bacteria with glass particulate material showed an increased growth inhibition with the increase in strontium substitution and in glass particle concentration, thus, demonstrating the direct relation between higher strontium concentration and higher antimicrobial activity.<sup>142</sup> In another study, an injectable strontium-releasing bone cement was developed based on bioactive glasses (BGs) and PAA with strontium percentages of 2.5%, 10% and 50 %. These materials showed reduced cell counts against *S. aureus* and *S. faecalis* (Gram + bacteria) by several orders of magnitude. For instance, even small strontium substitution (2.5%) originated *S. faecalis* inhibition by 0.5-1 orders of magnitude comparing with the strontium-free cement. The developed cements originated strontium concentration between 0.16 mmol/L (14 ppm) and 2.5 mmol/L (219 ppm) and it was observed that strontium concentration in the culture medium above 0.16 mmol/L didn't result in further bactericidal activity.<sup>118</sup> This is an important aspect in the development of new strontium materials with both antimicrobial and osteogenic activity. Thus, the design of new leaching systems cannot be restricted only to the antimicrobial strontium concentration (for instance in this case 14 ppm) as it must not be forgotten that the strontium effective concentration in bone regeneration, as it was previously described in the above sections, has been reported to be at least in the range of 85 ppm for both combined induced inhibition of osteoclast and stimulation of osteoblast.

Strontium formate dehydrate crystals have also been reported to have some antimicrobial activity both against bacterial (Gram +: *B. subtilis* and *S. aureus*; and Gram -: *P. aeruginosa* and *E. coli*) and fungal (*A. niger*, *F. solani*, *C. lunata* and *C. albicans*) pathogens. In its work, Greena et al., were able to demonstrate by well diffusion method that the strontium crystals provoked inhibition zones of 11 mm, 12 mm, 8 mm and 9 mm respectively for *B. subtilis*, *S. aureus*, *P. aeruginosa* and *E. coli* after 24h incubation. Challenging the fungi microorganism it was obtained inhibition zones of 7 mm, 9 mm, 6 mm and 13 mm, respectively against *A. niger*, *F. solani*, *C. lunata* and *C. albicans*. Interestingly, it is noticeable a slightly better antimicrobial activity over Gram + bacteria rather than over Gram - bacteria known to be less resistant. Against fungal pathogen the *C. albicans* revealed to be the most affected microorganism by the strontium crystals.<sup>143</sup>

The potential of strontium alone and incorporated in materials for antimicrobial applications is still far from being completely understood. It was proved that the use of strontium has in fact antimicrobial properties, nevertheless, it has not been well defined yet the exact amounts of strontium and its concentration needed in order to produce replicable and effective antimicrobial activity over the different microorganism (Gram + bacterium,

Gram - bacterium, fungi). This is probably due to the fact that the mechanism by which strontium mediates its antimicrobial activity is, so far, not fully understood. Thus, further investigations are still necessary in this area to turn feasible the controlled design and creation of new strontium enriched biomaterials to fight against microbial infection.

### 9.6. Strontium antimicrobial mechanism of action

There are very few studies about strontium as an antimicrobial agent and even less are about its antimicrobial mechanism of action. Therefore, till the necessary assessment of its antimicrobial properties, the only available source of information relies in analogies with other already used metallic ions for the same purpose. For instance, silver is by far the most studied and used cation in the fight against microbial infection and its properties have been known and utilized since ancient times.<sup>144</sup> Silver, in its oxidized form,  $\text{Ag}^+$ , reacts and interferes with the microbial cell membranes causing its disruption and making them non-functional. Additionally,  $\text{Ag}^+$  also interferes with critical metabolic proteins and enzymes. All these processes compromise cell integrity and functionality which leads to microbial dead. Besides these actions,  $\text{Ag}^+$  cations have the ability to substitute other metal ions such as  $\text{Ca}^{2+}$  and  $\text{Zn}^{2+}$  that are crucial in bacterial survival. Thus, silver may act by diverse mechanisms and have been shown to be effective against a relative broad number of pathogens encountered in implants like *E. coli*, *S. aureus*, *S. epidermidis* and *P. aeruginosa*.<sup>11</sup> Similarly, strontium in its oxidized state is also a cation ( $\text{Sr}^{2+}$ ). Thus, we may extrapolate the antimicrobial action of silver to strontium. For instance, such as reported for silver, strontium has also the ability to displace other metal ions such as  $\text{Ca}^{2+}$  as discussed before. This way, strontium may also have some lethal effects over fundamental bacterial processes where metal ions are involved. Furthermore, antimicrobial potential of strontium may also be connected with interference with membrane stability and fundamental proteins and enzymes. The ability of  $\text{Ag}^+$  to interfere with membrane and cellular components is highly connected with its tendency to strongly complex with electron donor groups. Such groups are composed of oxygen, nitrogen and sulphur which correspond, respectively, to hydroxyls, amines, phosphates and thiols that are abundant in microbial cells.<sup>145</sup> For instance,  $\text{Ag}^+$  ions as well as other heavy metals such as  $\text{Cu}^{2+}$  ions are known to readily interact with SH groups which allow them to rapidly penetrate the membrane. By doing this, these metal ions can now interfere with membrane functions as well as interact with other internal SH groups inhibiting the function of several enzymes.<sup>146</sup> Furthermore, silver ions have been reported to interact with the respiratory chain impairing an efficient electron passage and consequently a correct pumping of protons through membrane. This leads to the impossibility of maintenance of the vital proton gradient. Additionally, this deregulation

caused in respiration also promotes the formation of superoxide and hydroxyl radicals that provokes severe cell damage. <sup>147</sup>

Although, the necessary studies in the assessment of the antimicrobial mechanism of action of strontium have not been made yet, there are several studies that demonstrate the antimicrobial activity of different heavy metal ions. Thus, all the mentioned mechanism are possible ways by which strontium may exert its antimicrobial action. Figure 5 schematically represents the mechanisms by which metal ions induce their bactericidal action.

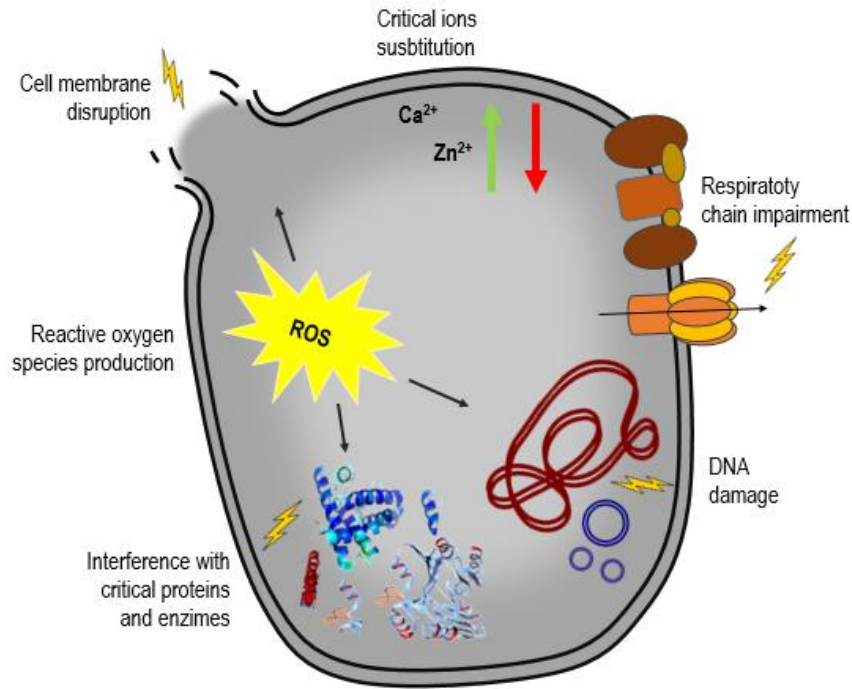


**Figure 5** – Scheme of the potential strontium antimicrobial mechanisms of action <sup>148</sup>.



# Chapter 3

## Materials and Methods

### 3.1. Strontium chloride solutions

#### 3.1.1. Preparation of the strontium chloride solutions.

A stock strontium chloride solution of 16,384 g/L, in ddH<sub>2</sub>O, was prepared and stored at 4°C until use. From serial dilutions of the stock solution was obtained a sequence of decreasing concentrations ranging from 16384 µg/mL to 32 µg/mL that were then used to test the bacteria. These solutions were prepared with twice the concentration of the final concentration used to test the bacteria since the same volume of strontium chloride solution and bacterial inoculum are added. Therefore, the working test concentrations ranged from 8192 µg/mL to 16 µg/mL.

### 3.2. Ca- and Sr-rich alginate discs

#### 3.2.1. Ca- and Sr-rich alginate discs production

Ultrapure LVG Alginate (Pronova FMC Biopolymers, G content ≥60%, MW 131±13 kDa) sterilization was carried out by preparing a 0.5% ultrapure alginate solution manageable to be filtered through a 0.22 µm mesh filter. After filtration, the ultrapure alginate solution was frozen at -20°C and afterwards lyophilized for 72 hr. The lyophilized ultrapure alginate was stored at -20 °C to lessen the risk of rehydration of the material until used. To produce the Ca- and Sr-rich alginate discs, 4% w/v alginate solution was prepared by mixing the ultrapure lyophilized alginate with deionised water, ddH<sub>2</sub>O. The solution was left shaking overnight (o/n) at room temperature to ensure complete solubilisation of the alginate. Having the 4% ultrapure alginate solution, a Ca- or Sr-mediated gelation process is conducted by adding CaCO<sub>3</sub> or SrCO<sub>3</sub>, respectively, to obtain the Ca- or Sr-rich alginate hydrogel. Given the very low solubility of the CaCO<sub>3</sub> or SrCO<sub>3</sub>, the final mixture needed to be acidified which was done by subsequently adding D-(+)-Gluconic acid δ-lactone (GDL) to the solution. This final step allows for a lowering of the pH allowing a more efficient solubilisation of the carbonate salts making the Ca<sup>2+</sup> or Sr<sup>2+</sup> ions gradually more available for the alginate reticulation. Upon the addition of the GDL, the alginate solution must be rapidly transferred to cylindrical templates (4 mm x 3 mm) that will give rise to the disc-like shape where the alginate (3.5% wt) remains until complete gelation. A schematic

representation of the production procedure of the Ca- or Sr- rich alginate discs is illustrated in Figure 6.

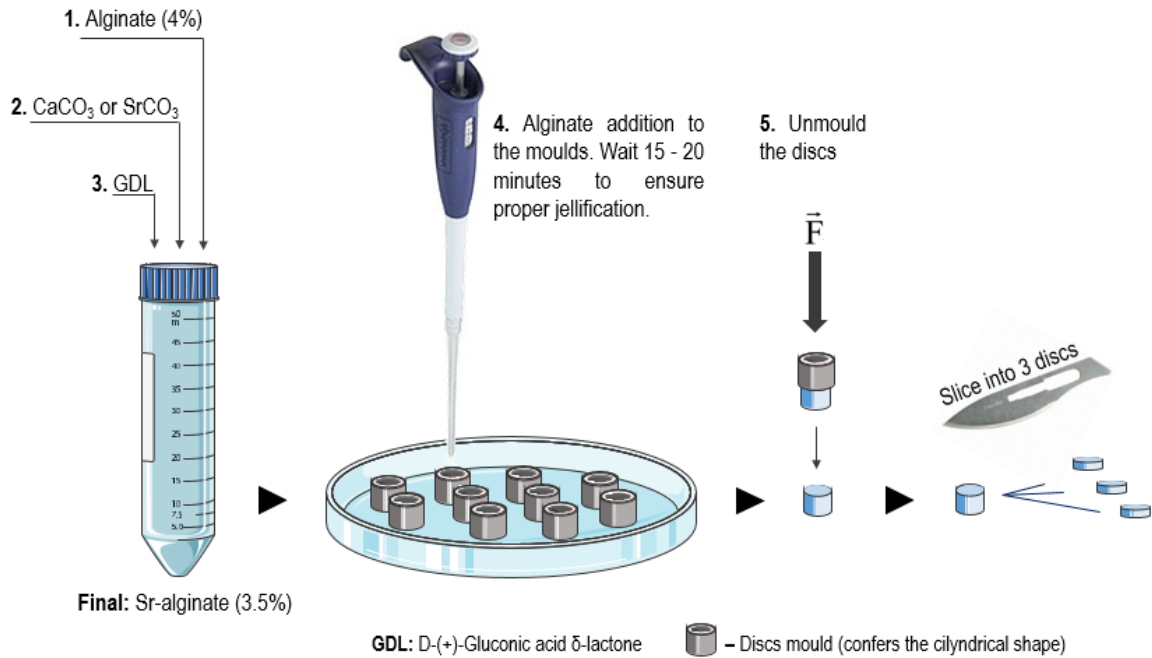


**Figure 6**– Schematic representation of the production of the Ca- and Sr-alginate discs.

### 3.2.2. Preparation of Ca- and Sr-rich alginate discs' extracts

Discs prepared as described above were used to obtain extracts both in PBS or TSB medium. 6 well plates were used to immerse 25 discs, per well, in 5 mL of the respective medium correspondent to a ratio of 1 disc to 200  $\mu\text{L}$  of medium. The plates were then conveniently placed into sealed containers creating a saturated environment in order to avoid well content/volume evaporation. Incubation was carried out at 37°C and extracts were recovered at time-points 1h, 24h, 48h, 72h and 7 days. Immediately after recovery, extracts were frozen and stored at -20°C, until use, for evaluation of Ca and Sr release and antimicrobial properties assessment. A schematic representation of the discs extracts obtainment is given in Figure 7.



**Figure 7** – Schematic representation of the discs extracts preparation.

### 3.2.3. Ca and Sr release from the Ca- and Sr-rich alginate discs

Inductive coupled plasma - atomic emission spectroscopy (ICP-AES) analysis as performed with the obtained extracts in order to assess the amount of  $\text{Sr}^{2+}$  and  $\text{Ca}^{2+}$  ions released at each respective time point. (1h, 24h, 48h, 72h and 7 days extracts in TSB). For the analysis, extracts were diluted with the same medium as they were prepared. After ICP analysis, a calcium and strontium release curve was constructed

## **3.3. Ca- and Sr-rich microspheres**

### 3.3.1. Ca- and Sr-rich microspheres preparation

Microspheres were produced applying the droplet extrusion method combined with ionotropic gelation in the presence of  $\text{Ca}^{2+}$  or  $\text{Sr}^{2+}$ . The used method followed the protocol already optimized by Ribeiro et al in previous works<sup>149</sup>. A homogenous paste was prepared dispersing the ceramic powders: nanometric HAp (nHAp) (Fluidinova), micrometric HAp ( $\mu\text{HAp}$ ) (Plasma Biotal) and Strontium tri-phosphate (SrTriP) (Sigma Aldrich); in a 3% (w/v) sodium alginate solution (FMC Biopolymers) with a ceramic-to-polymer ratio of 0.25. The obtained paste was extruded drop-wise into a  $\text{CaCl}_2$  or  $\text{SrCl}_2$  crosslinking solution prepared at a concentration of 0.1 M using a syringe pump (Cole Parmer® 74900 series). Upon extrusion, spherical-shaped particles are immediately formed given the rapid establishment of Ca or Sr mediated connections between the polyguluronate chains present on the polymer backbone. Microspheres size was controlled by manipulating the extrusion flow rate which was set to 40 mL/h and by applying a coaxial air stream (also important in directing the microspheres straight to the gelation solution). Microspheres were left in the gelation solution for at least 30 minutes in order to ensure complete reticulation of the polymer all the way through the inner parts of the particles. Completed the reticulation period, microspheres were rinsed 3 times with deionised water  $dd\text{H}_2\text{O}$  (10-fold more water than the weight of microspheres was used) and then dried o/n in an incubator at 37°C. At last, microspheres were recovered and sintered at 1200°C ( $\mu\text{HAp}$ ,  $\mu\text{SrHAp}$  and SrTriP) and 800°C (nHAp and nSrHAp). Exceptionally, the  $\mu\text{HAp}$  and  $\mu\text{SrHAp}$  microspheres were rinsed again in deionised water  $dd\text{H}_2\text{O}$  (10-fold more water than the weight of microspheres was used) in order to remove soluble additional compounds possibly formed. A schematic representation of the microspheres production setup is provided in Figure 8.

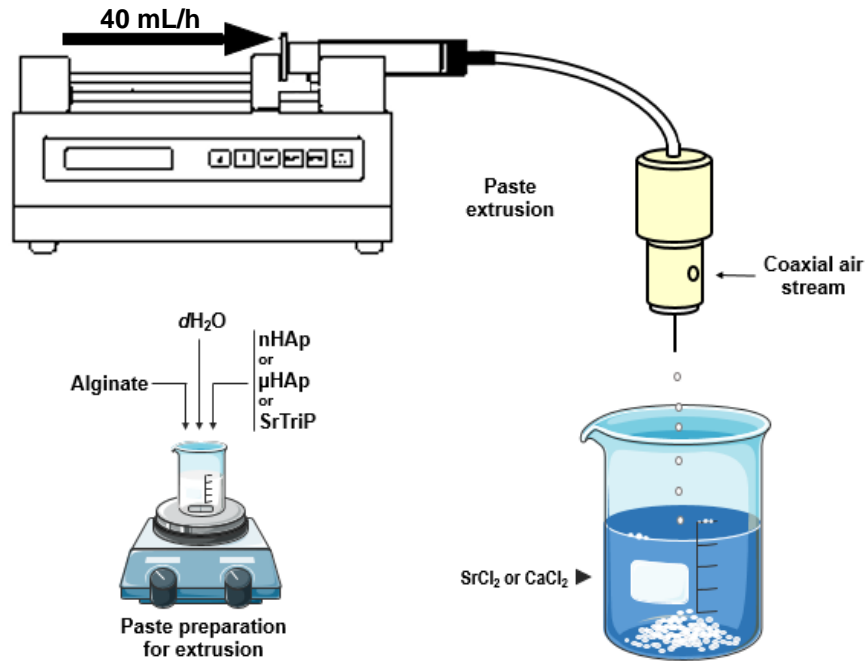


**Figure 8** – Schematic representation of the droplet extrusion method setup. Paste preparation and paste extrusion.

### 3.3.2. Ca- and Sr-rich microsphere characterization

nHAp, nSrHAp,  $\mu$ HAp,  $\mu$ SrHAp and SrTriP microspheres were first sorted into different size categories by sieving them through sieves with several mesh granulometries ranging from 560, 500, 450 to 250  $\mu\text{m}$ . The microspheres within the size of interest (350-450  $\mu\text{m}$ ) were recovered and subjected to further analysis. Morphological and physico-chemical characterization of the microspheres was determined using Scanning Electron Microscopy and Energy Dispersive Spectroscopy (SEM-EDS), Fourier Transform Infrared Spectroscopy (FTIR) and Zeta Potential (ZP) analysis.

#### 3.3.2.1. SEM/EDS analysis

The SEM/EDS analysis were conducted on a high resolution (Schottky) Environmental Scanning Electron Microscope with X-ray Microanalysis and Electron Backscattered Diffraction analysis: Quanta 400 FEG ESEM/EDAX Genesis X4M. For examination, samples were coated with an Au/Pd thin film by cathodic pulverisation (sputtering) using the SPI Module Sputter Coater equipment.

#### 3.3.2.2. FTIR analysis

Concerning FTIR analysis, microspheres and powders were left o/n to completely dry in a vacuum incubator at 60  $^{\circ}\text{C}$ . Powders and microspheres reduced to powder were analysed as KBr pellet using a spectrophotometer (Spectrometer frontier,

Perkin Elmer FT-IR). Pellets were prepared with 2 mg of the tested material mixed with 200 mg of KBr and with the help of a hydraulic press (Graseby specac) to produce 8 t of pressure under vacuum. All the samples were run at a spectral resolution of  $4\text{ cm}^{-1}$  and hundred scans were accumulated in order to obtain a high signal-to-noise level.

### 3.3.2.3. Zeta Potential analysis

Zeta potential analysis of the microspheres was determined from streaming potential measurements with an Electro Kinetic Analyser (EKA, Anton Paar GmbH) using a special cylindrical cell with a powder insert for granular samples. The electrolyte utilized was 1mM KCl and the pH ranged between 5.5 and 6.8 during measurements.

### 3.3.3. Preparation of Ca- and Sr-rich microsphere and powders extract

Microspheres and powders were used to obtain extracts in Tryptic Soy Broth (TSB, Sigma Aldrich) medium. 12 well plates were used to immerse the microspheres and powders in a ratio of 0.2 g/mL on the respective medium. Microspheres and powders were autoclaved for sterilization. The plates were then conveniently placed into sealed containers creating a saturated environment in order to avoid well content/volume evaporation. Incubation was carried out at  $37^{\circ}\text{C}$  and 150 rpm and extracts were recovered at the time-points 72h, 10 days and 21 days. Immediately after recovery, extracts were frozen and stored at  $-20^{\circ}\text{C}$  until use.

### 3.3.4. Ca and Sr release from the microspheres and powders

From the obtained extracts inductive coupled plasma - atomic emission spectroscopy (ICP-AES) analysis (Horiba Jobin-Yvon, Ultima spectrometer, generator RF of 40,68 MHz) were performed in order to assess the amount of  $\text{Sr}^{2+}$  and  $\text{Ca}^{2+}$  ions released at each respective time point. Therefore, 72 hr, 10 days and 21 days extracts were diluted with the same medium as they were prepared and subjected to the ICP-AES analysis. Afterwards, a calcium and strontium release curve over time was constructed.

## **3.4. Antimicrobial assessment**

### 3.4.1. Bacterial strains and growth conditions

The bacteria chosen in this work were *S. aureus* obtained from American Type Culture Collection (ATCC 49350) and *S. epidermidis* obtained from American Type Culture Collection (ATCC 35984). Prior to use, bacteria stored at  $-80^{\circ}\text{C} \pm 2^{\circ}\text{C}$  in cryovial tubes were

sub-cultured in Tryptic Soy Agar (TSA) (Merck) plates at 37°C during 24 hours before testing. Subsequently, a 2 or 3 colonies of *S. aureus* or *S. epidermidis* were re-suspended in 50 mL conical centrifuge tubes containing 5 mL of Tryptic Soy Broth (TSB) (Sigma Aldrich) or Mueller-Hinton Broth (MHB) (Sigma Aldrich) and incubated overnight (period comprehended between 16 to 18 hours) at 37°C and 150 rpm in an orbital shaker oven (Orbital IKA KS 4000 ic control). The aforementioned conditions of temperature and agitation were maintained for all experiments performed on this work.

#### 3.4.2. Minimum inhibitory concentration (MIC) and minimum bactericidal concentration (MBC)

The MIC of the strontium chloride solutions, discs extracts and microspheres and powders extracts was determined by microdilution broth method according to Wiegand et al. <sup>150</sup>. Overnight cell culture of *S. aureus* or *S. epidermidis* in the exponential phase of growth was adjusted by OD ( $\lambda=600\text{nm}$ ) to an initial inoculum concentration of  $2 \times 10^5$  (for all  $\text{SrCl}_2$  solution assay and all *S. epidermidis* experiments),  $2 \times 10^6$  (for Ca- and Sr-rich alginate discs; and microspheres and powders assays – *S. aureus* experiments) CFUs/mL (in fresh TSB or MHB) using a spectrophotometer.

##### 3.4.2.1. $\text{SrCl}_2$ solutions

A volume of 100  $\mu\text{L}$  of the prepared bacterial suspension (initial inoculum) was added to a round bottom sterile 96-well microtiter plate together with 100  $\mu\text{L}$  of a range of different concentrations of strontium chloride solutions (8192  $\mu\text{g/mL}$  to 16  $\mu\text{g/mL}$ ). All tests were performed with five replicates except for the blank controls of each condition where two replicates were used.

##### 3.4.2.2. Ca- and Sr-rich alginate discs extracts

The recovered 48 hr and 72 hr discs extracts were serially diluted with fresh PSB or TSB obtaining a range of solutions with different extract concentrations (non-diluted (ND),  $\frac{1}{2}$ [ND] (D1),  $\frac{1}{2}$ [D1] (D2),  $\frac{1}{2}$ [D2] (D3), ...).

For the PBS extracts (*S. epidermidis* experiments) a volume of 100  $\mu\text{L}$  of each prepared dilutions of the discs extracts was added to a round bottom sterile 96-well plate microtiter plate. Afterwards, 100  $\mu\text{L}$  of the cell suspension (initial inoculum:  $2 \times 10^5$  CFUs/mL) was added to each testing well.

Concerning TSB extracts (*S. aureus* experiments) a volume of 200  $\mu\text{L}$  of each the prepared dilutions of the discs extracts was added to a round bottom sterile 96-

well microtiter plate. Afterwards, 10  $\mu\text{L}$  of cell suspension (initial inoculum:  $2 \times 10^6$  CFUs/mL) was added to each testing well.

All tests were performed with five replicates except for the blank controls of each condition where two replicates were used.

#### 3.4.2.3. Microspheres and powders extracts

Performed as stated in sub-section 3.4.2.2. (concerning TSB extracts). Minor alterations should be mentioned: 3 days and 21 days extracts were used and serially diluted. All tests were performed with three replicates except for the blank controls of each condition with one well only.

Wells containing only cell suspension in TSB or MHB were used as negative control (normal bacterial growth) and wells only containing PBS, TSB or MHB and PBS, TSB or MHB together with  $\text{SrCl}_2$  solution, alginate discs extracts or microspheres and powders extracts as blanks to assess if the medium or the  $\text{SrCl}_2$  solution or the extracts were contaminated. The microtiter plates were afterwards incubated at  $37^\circ\text{C}$  between 18 to 22 hours. MIC was obtained by visual observation and it was recorded as the lowest concentration tested in which there was no visible bacterial growth in the wells bottom. MIC assessment was also aided by metabolic activity quantification by AlamarBlue assay, as described next.

#### 3.4.2.4. Metabolic activity quantification by AlamarBlue Assay (ABA)

Metabolic activity quantification of the wells content was performed by AlamarBlue (AB) assay. For the staining procedure 50  $\mu\text{L}$  of the content of each well together with another 50  $\mu\text{L}$  of fresh TSB or MHB were added to 96-well polystyrene black plate reader. Next, 20% of the AB indicator solution was added to each well and plates were incubated for 15 minutes in darkness at room temperature (RT). Fluorescence was measured at  $\lambda_{\text{excitation}} = 530$  nm and  $\lambda_{\text{emission}} = 590$  nm. All tests were performed with five replicates except for the blank controls of each condition with two replicates only. The results were also analysed as percentage of metabolic activity reduction when bacteria was exposed to different solution concentrations/extracts dilutions. The percentage of metabolic activity reduction was determined following the Eq. 1, as described by Monte et al.<sup>151</sup> :

$$\%MAR = \frac{FLC - FLW}{FLC} \times 100 \quad (\text{Eq.1})$$

where %MAR represents the percentage of Metabolic Activity Reduction,  $FL_C$  is the fluorescence intensity of not exposed bacteria and  $FL_W$  is the fluorescence intensity for bacteria exposed to a certain testing solution/concentration.

Subsequently to MIC determination, the content of the wells corresponding to the concentration/dilutions equal and above the MIC was added to plate count agar (TSA) plates using the drop method. Three 10  $\mu$ L drops were added for each dilution (ND, - 2, - 4, - 6 and - 8) to the TSA plates. After 24h incubation at 37°C the plates were visually analysed for bacterial growth by counting the observed colony forming unit (CFU). The MBC was recorded as the lowest concentration tested which totally inhibited the growth of *S. aureus* or *S. epidermidis*. All tests were performed with three replicates. CFUs/mL were calculated according to Eq.2:

$$CFUs/mL = CFU \times \left(\frac{1}{10^x}\right) \times 100 \quad (\text{Eq.2})$$

where, CFU represents the counted colony forming units and x (0, - 2, - 4, - 6 and - 8) is the dilution where CFUs was counted. Log percentages of kill were also calculated after CFUs/mL calculation according to Eq.3:

$$\%PK = \frac{L_C - L_E}{L_C} \times 100 \quad (\text{Eq.3})$$

where %LPK represents the Percentage of Kill,  $L_C$  is the logarithm of the CFUs/mL of not exposed bacteria and  $L_E$  is the logarithm of the CFUs/mL of bacteria exposed to a certain solution/concentration.

### 3.4.3. Direct exposure of microspheres and powders

The produced microspheres ( $\mu$ HAp,  $\mu$ SrHAp, n HAp, nSrHAp and SrTriP) and used powders (pSrTriP and pSrCO<sub>3</sub>) were evaluated for its antimicrobial properties by direct contact with the *S. aureus*. Overnight cell culture of *S. aureus* in the exponential phase of growth was adjusted by OD ( $\lambda=600\text{nm}$ ) to an initial inoculum concentration of  $1 \times 10^5$  CFUs/mL (in fresh TSB) using a spectrophotometer. Microspheres and powders were weighted, 40, 60 and 80 mg of each, in eppendorfs, sterilized and dispensed to each well of 48-well plates following by the addition of 750  $\mu$ L of the prepared initial inoculum ( $1 \times 10^5$  CFUs/mL). Wells containing only cell suspension in TSB (750  $\mu$ L) were used as negative control (normal bacterial growth) and wells only containing TSB and TSB together with the microspheres or powders as blanks to assess if the medium or the microspheres or powders were contaminated. The plates were afterwards incubated at 37°C for 24 hr at 150 rpm. All tests



were performed with three replicates except for the blank controls of each condition where only one well was used.

Subsequently, the content of the wells (supernatant) were added to plate count agar (TSA) plates using the drop method. 10  $\mu$ L were retrieved from each well and serially diluted (non-diluted (ND),  $10^{-2}$ ,  $10^{-4}$ ,  $10^{-6}$  and  $10^{-8}$ ) in order to be able to proceed CFU count. Three 10  $\mu$ L drops were added for each dilution to the TSA plates (as there are five dilutions the TSA plates were divided in five quadrants). After 24h incubation at 37°C the plates were visually analysed for bacterial growth by counting the observed colony forming unit (CFU). The MBC of the extracts and its dilutions was recorded as the lowest mass of microspheres or powders tested which totally inhibited the growth of *S. aureus*. All tests were performed with three replicates.

### 3.5. Statistical analysis

For statistically analysis the potentialities of Graphpad Prism 6 program were used. D' Agostino-Pearson omnibus normality test followed by one-way analysis of variance were used. When confirmed a Gaussian distribution, Friedman test was applied and when not the non-parametric Kruskal-Wallis test was used. Data are expressed as the mean standard deviation (SD) and *P* values of <0.05 were considered significant.



# Chapter 4

## Results and discussion

### 4.1. Bactericidal activity of SrCl<sub>2</sub> solutions

The injectable system under investigation in this work relies on the benefits of strontium release from the material to the involving areas. The main interest of this work focus on the evaluation of the ability of the strontium ions to inhibit bacterial colonization and infection. Therefore, as a primordial investigation, it is of the most importance to evaluate its potential alone on the eradication of both pathogenic bacteria *S. epidermidis* and *S. aureus*, in vitro. Accordingly, several strontium chloride solutions in different concentrations were prepared from a stock solution by serial dilutions. Bacteria were challenged against SrCl<sub>2</sub> solution and after exposure, MIC was visually analysed and afterwards confirmed by the metabolic activity assessment recurring to AlamarBlue assay. Concerning *S. epidermidis* grown on TSB, MIC was visually defined at 1024 µg/mL and then confirmed by the sharp decrease in the bacterial metabolic activity observed also for the same concentration (Figure 9.A1). Still, regarding the metabolic activity evaluation of strontium chloride solution, the percentage of metabolic activity inactivation are summarised in Table 3 showing that, concentrations of 1024 µg/mL reduced the metabolic activity by 78%, 2048 µg/mL reduced 96% and 4096 µg/mL 100% (the other concentrations revealed reduced effect on the bacteria). MBC was then determined by assessing the culturability of the bacteria exposed to SrCl<sub>2</sub> solution in concentrations equal and above the MIC. Colony forming units (CFUs) were visually counted and a MBC was firstly found at the concentration of 2048 µg/mL (data not shown). However, in order to better define the bactericidal concentration, the range of concentrations evaluated was narrowed. The results suggest that the MBC of SrCl<sub>2</sub> exposed to *S. epidermidis* on TSB medium was 1536 µg/mL (Figure 9. A2). SrCl<sub>2</sub> solution at 1024 and 1280 µg/mL concentrations were able to kill 16% and 65% of the bacteria, respectively, (Table 3), showing that the bactericidal effect is concentration dependent.

With respect to *S. epidermidis* cultivated in MHB medium, MIC was not found as no significant inhibition of the bacterial growth was observed for all of the concentrations tested (Table 4). Moreover, metabolic activity assay did not show good bacterial inactivation when exposed to the SrCl<sub>2</sub> solutions as concentrations of 2048 µg/mL only presented a metabolic activity reduction of 14%, not significant from the control (Table 3 and Figure 9. B1).

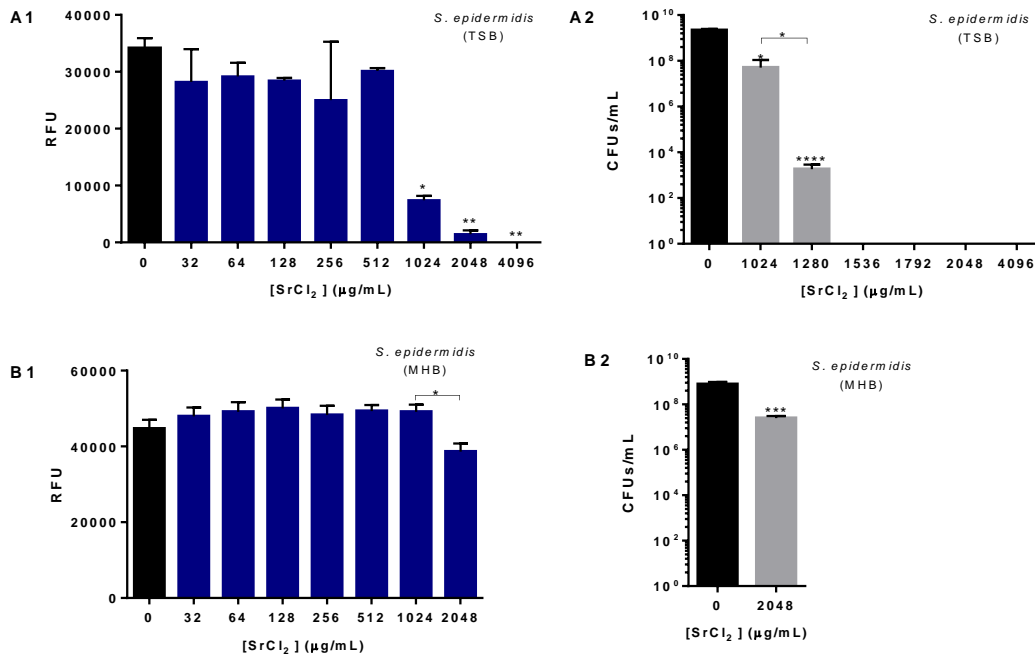


**Figure 9 – Strontium chloride solution against *S. epidermidis* grown on TSB (A) and MHB (B).** A1 and B1 – Metabolic activity evaluation. Relative fluorescence units (RFU) are presented as a function of SrCl<sub>2</sub> concentration. A2, A3 and B2 – Bacteria culturability. CFUs count is presented as a function of SrCl<sub>2</sub> concentration. *S. epidermidis* represents the negative control (no treatment). Mean values ± standard deviation are illustrated. Bars marked with \* are statistically different from the control and bars marked with (\*) and brackets are statistically different between them ( $P < 0.05$ ).

No MBC was observed (Figure 9 A2 and Table 4) on the range of concentrations tested and, besides statistically significant, only a slight decrease on the *S. epidermidis* culturability was observed when exposed to the highest concentration of 2048 μg/mL in MHB (17% of bacterial death) (Figure 9 B2 and Table 3).

As said, and as summarised in Table 3, there is a disparity on the potential of strontium to inhibit the bacterial growth, metabolic activity and to promote cell killing depending on the culture medium for bacterial growth which, must be further analysed and discussed.

*S. aureus* was challenged against the same range of strontium chloride solutions concentrations using the same approach. Once more, the degree of bacterial inhibition was concentration dependent. Furthermore, *S. aureus* revealed higher susceptibility when exposed to lower SrCl<sub>2</sub> concentrations than *S. epidermidis*. Thus, MIC was observed for a concentration as low as 512 μg/mL (Figure 10 A1) (in opposition to *S. epidermidis* MIC of 1024 μg/mL) (Table 4). In agreement with the previous data, the metabolic activity assessment results (Figure 10. A1) revealed to be very significant as a sharp increase in

the bacterial metabolic inactivation of 51% at 512  $\mu\text{g/mL}$  concentration and roughly total metabolic inactivation for the subsequent higher concentrations (Table 3). In order to assess the concentration of strontium in solution required to completely eradicate the culturability of *S. aureus*, bacteria was plated on solid medium after exposure to different concentrations and colony forming units (CFUs) visually analysed. The MBC was observed at the concentration of 1792  $\mu\text{g/mL}$  (Figure 10. A2 and Table 4). Nevertheless, lower concentrations of 1024, 1280 and 1536  $\mu\text{g/mL}$  were also able to significantly kill 47%, 70% and 76% of bacteria, respectively (Table 3). Besides the lower MIC obtained, *S. aureus* showed to be less susceptible to complete killing (higher MBC) when compared to *S. epidermidis*, in terms of culturability on solid medium. Regarding the results shown in Figure 10 A2, it is important to refer that for the concentrations 1024, 1280, 1536  $\mu\text{g/mL}$  there was not a consistent behaviour of the bacteria (in four independent experiments) as within the three replicates of the culturability assay, two showed to completely eliminate

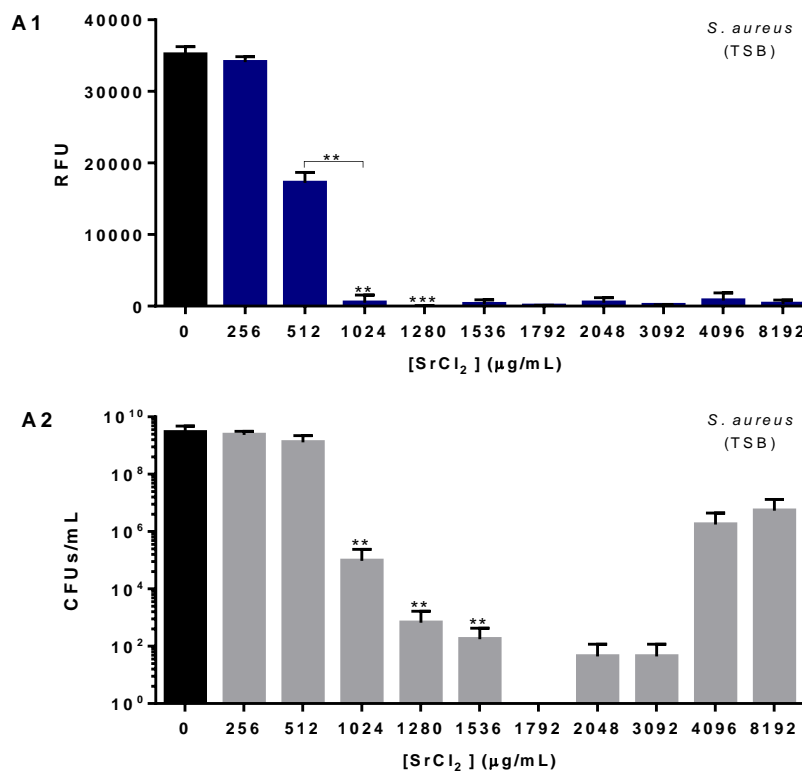


**Figure 10 – Strontium chloride solutions against *S. aureus* grown on TSB.** A1 – Metabolic activity evaluation. Relative fluorescence units (RFU) are presented as a function of SrCl<sub>2</sub> concentration. A2 – Bacteria culturability. CFUs count is presented as a function of SrCl<sub>2</sub> concentration. *S. aureus* represents the negative control (no treatment). Mean values  $\pm$  standard deviation are illustrated. Bars marked with \* are statistically different from the control and bars marked with (\*) and brackets are statistically different between them ( $P < 0.05$ ).

*S. aureus* whereas one presented colonies formation. Only for the 1792 µg/mL concentration there was consistency between the three replicates being therefore defined as the MBC. Moreover, and surprisingly, also within the four independent experiments it was possible to identify that for the higher concentrations (2048 to 8192 µg/mL) *S. aureus* was cultivable again. This may be described as an Eagle-type effect (paradoxical zone phenomenon) which could be connected to a reverse effect of bactericidal activity with increasing SrCl<sub>2</sub> concentrations. This phenomenon has been described *in vitro* for increasing concentrations of penicillin against *S. aureus*, for instance<sup>152</sup>. Thus, further research should be done to completely understand the *S. aureus* behaviour to SrCl<sub>2</sub> solutions. Despite the uncertainties, it is possible to conclude that, if there is not a MBC at 1792 µg/mL, there is at least a bactericidal concentration.

**Table 3** – Percentages of metabolic activity inhibition and percentage of death for *S. epidermidis* and *S. aureus* after exposure to several SrCl<sub>2</sub> solution concentrations.

Bacteria	Metabolic inactivation (%)			Percentage of death (%)		
	<i>S. epidermidis</i>		<i>S. aureus</i>	<i>S. epidermidis</i>		<i>S. aureus</i>
	TSB	MHB	TSB	TSB	MHB	TSB
SrCl <sub>2</sub> concentrations (µg/mL)	256	9	0	-	-	1
	512	10	0	-	-	4
	1024	78	0	16	-	47
	1280	95	0	65	-	70
	1536	95	0	100	-	76
	1792	99	6	100	-	100
	2048	96	14	99	17	83
	3092	-	-	100	-	83
	4096	100	-	98	-	34
	8192	-	-	99	-	29

**Table 4** – MIC and MBC values for *S. epidermidis* and *S. aureus* after exposure to SrCl<sub>2</sub> solutions.

Medium	<i>S. epidermidis</i>		<i>S. aureus</i>
	TSB	MHB	TSB
<b>MIC</b> (µg/mL)	1024 (566)	> 2048 (1132)	512 (283)
<b>MBC</b> (µg/mL)	1536 (849)	> 2048 (1132)	1792 (990) *

\* Despite this MBC being achieved, *S. aureus* was not susceptible to higher SrCl<sub>2</sub> concentrations.

Values in parenthesis correspond to Sr concentration only. M[SrCl<sub>2</sub>]=158.53 g/mol; M[Sr]=87.62 g/mol; SrCl<sub>2</sub> ⇌ Sr<sup>2+</sup> + 2Cl<sup>-</sup>.

Analysing the results, it is possible to suggest that the MHB medium may interfere with the bactericidal potential of  $\text{SrCl}_2$  solutions on *S. epidermidis*. For instance, the composition of MHB medium may interact with the strontium ions and, consequently, disabling the mechanisms of action by which strontium ions provoke their antibacterial activity. However, according to the medium composition none of its constituents would relate to metal chelation. Though, ion complexation/chelation may explain the obtained results by requesting the strontium ions from solution and significantly reducing its activity concerning the mechanisms of action associated to strontium on the bacterial cells presented in Figure 4. Thus, cell membrane disruption, production of ROS, DNA damage, protein inactivation and essential ions substitutions could not be achieved in strontium chelated form.

Regarding experiments using TSB medium against both bacterial strains, as summarised in Table 4, even though *S. aureus* needs lower amounts of  $\text{SrCl}_2$  to be inhibited than *S. epidermidis*, it requires higher concentrations to be killed, suggesting that *S. epidermidis* is more susceptible and *S. aureus* more resistant to strontium. This idea is, thus, sustained by the higher MBC found for *S. aureus* as well as by the knowledge that this bacteria presents, based on epidemiologic studies, higher incidence of persistent infections than *S. epidermidis*<sup>153</sup>.

So far, just a couple of works have assessed the antimicrobial properties of strontium chloride alone against bacteria. As previously discussed in **Chapter 2, section 9.5**, Dabsie et al, have evaluated several strontium chloride concentrations against a diversity of bacteria found in mouth. The work revealed that no significant effect was observed up to concentrations of 295950  $\mu\text{g/mL}$  showing only one log reduction correspondent to approximately 10% bacterial death. Despite the fact that different bacterial strains were tested, the concentrations used were incredibly higher (~100 fold) than the ones utilized in the present work. Also, strontium chloride hexahydrate was used by Dabsie et al whereas at this work strontium chloride anhydrous is used. Nevertheless, ignoring all the protocol divergences, the results obtained here are very distinct comparing to the ones from Dabsie et al as strontium chloride managed to completely eradicate both *S. epidermidis* and *S. aureus* in concentrations much smaller than the ones reported. Another work, by Liu et al, has used  $\text{SrCl}_2$  concentration in the range of the ones described in our work. They exposed *P. gingivalis* and *A. actinomycetemcomitans* to concentrations ranging from 66.7 to 1066.7  $\mu\text{g/mL}$  for 2, 4 and 6 hours. After the 6 h incubation the higher concentration revealed a metabolic activity reduction of 45% and 30% for *P. gingivalis* and *A. actinomycetemcomitans*, respectively. Since the bacterial strains tested by Liu et al, and the ones under study in this work are different it is difficult to compare the results. Nevertheless, it is possible to conclude that strontium chloride alone has antimicrobial

activity and that can be used both against Gram - (*P. gingivalis* and *A. actinomycetemcomitans*) and Gram + bacteria (*S. epidermidis* and *S. aureus*).



## 4.2. Characterization and antimicrobial activity of the injectable hybrid system

After assessing the effectiveness of strontium alone over the *S. epidermidis* and *S. aureus*, it is important to understand if the injectable hybrid system itself is capable to deliver a sufficient amount of strontium ions to eradicate bacteria. Therefore, the system was sub-divided into two parts: alginate discs (vehicle) and microspheres and each evaluated separately regarding their antimicrobial properties.

### 4.2.1. Characterization of the Ca- and Sr-rich alginate discs extracts

In order to address alginate discs bactericidal activity, extracts of Sr-rich discs (and Ca-rich discs as control) were prepared to be used against *S. epidermidis* and *S. aureus*. 1 hr, 24 hr, 48 hr, 72 hr and 7 days extracts were obtained and subjected to ICP-AES analysis to determinate the amount of strontium and calcium that the discs managed to release. The chosen time points are tightly connected to an approach that comprehends the inhibition of infection right at the first hours/stages after surgery. This is the moment where the risk of bacterial infection and colonization are increased, however it is also the moment when bacteria is most vulnerable and easier to eliminate since biofilm is not fully developed, yet<sup>79,82,83,87</sup>. The concentrations ( $\mu\text{g/mL}$ ) of calcium and strontium ions present at the different time-point extracts for each type of disc are presented in Figure 9.

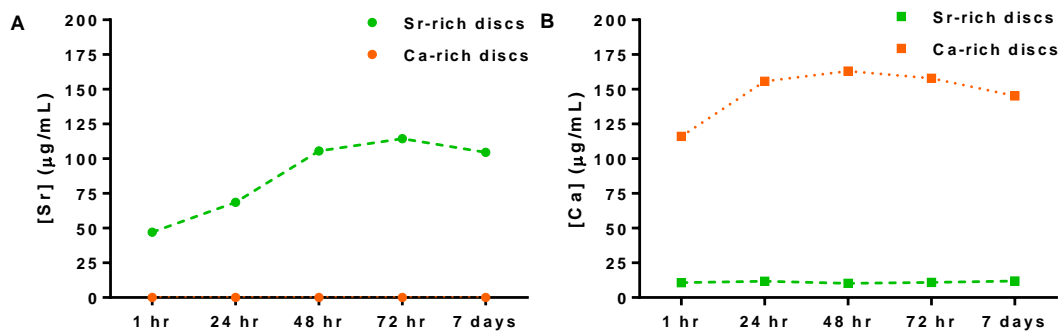


**Figure 11 –Strontium and calcium release from the alginate discs over time.** 1 hr, 24 hr, 48 hr, 72 hr and 7 days discs extracts (in TSB) were quantified regarding Sr (A) and Ca (B) composition ( $\mu\text{g/mL}$ ) by ICP-AES.

Analysis of strontium composition of extracts (Figure 11 A) showed that no strontium was released from the Ca-rich discs ([Sr]  $\mu\text{g/mL}$ : 1 hr – 0.07; 24 hr – 0.03; 48 hr – 0.01; 72 hr – 0.00; 7 days – 0.04), as expected, and no differences were observable comparing to the amounts released from the control (control: TSB only) ([Sr]  $\mu\text{g/mL}$ : 0.03, data not shown). On the other hand, also in terms of Sr release, the extracts of the Sr-rich alginate

discs revealed to delivery substantial amounts of strontium ([Sr]  $\mu\text{g/mL}$ : 1 hr – 47.10; 24 hr – 68.55; 48 hr – 105.60; 72 hr – 114.36; 7 days – 104.62, the main released achieved after 72 hr). In what concerns calcium release (Figure 11 B) from the discs, the Ca-rich discs were able, as expected, to deliver high quantities of the ion ([Ca]  $\mu\text{g/mL}$ : 1 hr – 111.70; 24 hr – 151.32; 48 hr – 158.64; 72 hr – 153.46; 7 days – 140.82) comparing to the amounts measured in the control ([Ca]  $\mu\text{g/mL}$ : 4.46). Despite in very low amounts, the Sr-rich discs also released some calcium, mainly in the first hours ([Ca]  $\mu\text{g/mL}$ : 1 hr – 10.79). Furthermore, it was also proved that the rich alginate discs are reliable to work as a leaching system as there is a gradual release of the strontium and calcium ions over time. Nonetheless, one of the critical aspects in a leaching system is if that delivery of Sr ions is in sufficient amount to effectively inhibit growth or eliminate bacteria. According to the MIC and MBC determined for the  $\text{SrCl}_2$  solutions both for *S. aureus* and *S. epidermidis*, the strontium ion concentration found in the discs extracts is still far from the desirable. The necessary concentrations of Sr to reach the MIC were 283 and 566  $\mu\text{g/mL}$  and the MBC were 990 and 849  $\mu\text{g/mL}$  for *S. aureus* and *S. epidermidis*, respectively. Concerning the strontium concentrations measured from the Sr-rich alginate discs extracts, none of the time-points achieved the concentrations of neither the MBC nor the MIC, as the maximum concentration registered was 114.36  $\mu\text{g/mL}$ . Therefore, *a priori*, it is expected that the Sr-rich extracts will not be able to both completely eradicate bacteria or inhibit bacterial growth in great extent. However, it should be considered that the highest amount of strontium (114  $\mu\text{g/mL}$ ) released is substantially smaller than the amount of strontium theoretically present in the discs itself (2415  $\mu\text{g/mL}$ ), and that, if fully release, would be superior to superior to the MBC for both *S. aureus* and *S. epidermidis*.

#### 4.2.2. Bactericidal activity of the Ca- and Sr-rich alginate discs extracts

As first attempt of testing the antimicrobial properties of the discs extracts, *S. epidermidis* cultured on TSB was subjected to 48 hr extracts of Sr-rich alginate discs obtained in PBS. After challenging the bacteria with the extracts (and its dilutions) metabolic activity evaluation revealed that D2, D1 and ND extracts managed to significantly induce 41%, 53% and 80% of bacterial inactivation, respectively (Figure 12. A1 and Table 5). Nevertheless, MIC was not possible to be visually determined as well as MBC was not achieved after culturability of *S. epidermidis* in solid medium (Figure 12.A2). Effectively, despite statistically significant, it was only possible to observe 13.5% of bacterial kill when bacteria was exposed to ND extracts (Table 5).

As already verified in the antimicrobial assays with  $\text{SrCl}_2$  solution, experiments where MHB medium was used significantly impaired the strontium effect over bacteria.

Accordingly, from the metabolic activity assessment by AlamarBlue, very limited bacterial inactivation is observed. Only for the non-diluted (ND) extract 23% inactivation was observed, despite not statistically different from control (Figure 12. B1). It was not possible either, to visually define a MIC and the culturability assessment of *S. epidermidis* in solid medium after exposure to extracts did not result also in a MBC (Figure 12 B2 and Table 5). Only 4.5% of cell kill was achieved with statistical significance. Therefore, the use of MHB medium for bacteria growth in the evaluation of the antimicrobial properties of strontium was abandoned.

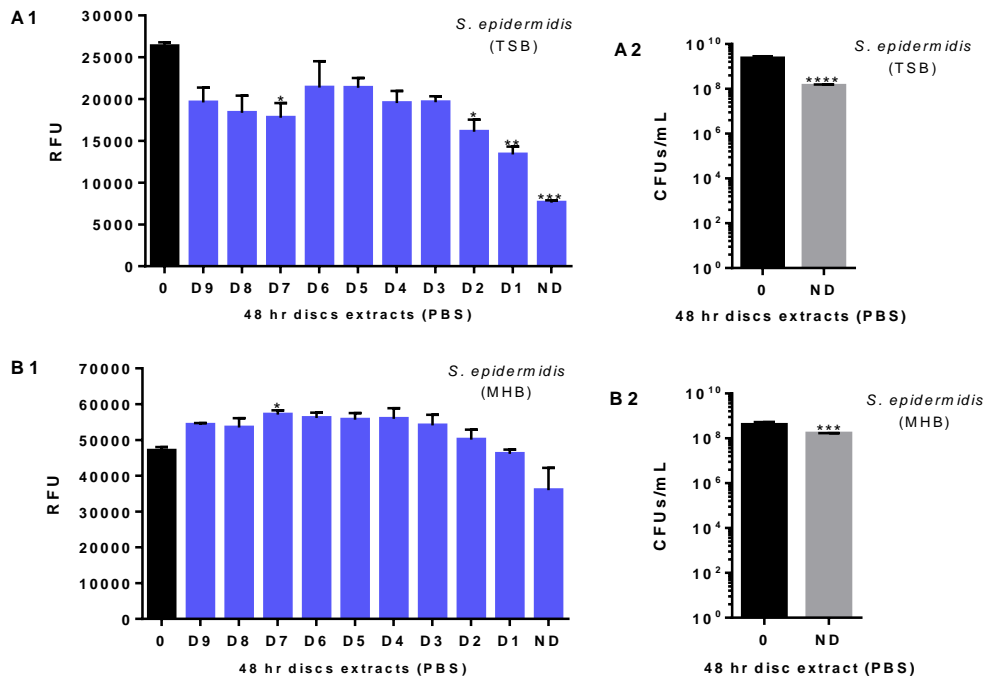


**Figure 12 – Antimicrobial activity of Sr-rich discs extracts (in PBS) towards *S. epidermidis* grown on TSB (A) and MHB (B).** A1 and B1 – Metabolic activity evaluation. Relative fluorescence units (RFU) are presented as a function of extracts dilutions. A2 and B2 – Bacteria culturability. CFUs count is presented as a function of SrCl<sub>2</sub> concentration. *S. epidermidis* represents the negative control (no treatment). Mean values ± standard deviation are illustrated. Bars marked with \* are statistically different from the control ( $P < 0.05$ ).

The amount of strontium released from the discs in PBS has not been quantified due to time restrictions, but assuming a release profile similar to the one in TSB medium, and taking into account the dilution made upon incubation with *S. epidermidis*, around 52 µg/mL of strontium would be expected to have contacted the bacteria in ND extracts. As such, PBS as extraction media was altered to TSB in order to be able to use the ND extracts directly without further dilution upon addition of the bacteria with medium (extracts in TSB allow addition of small volumes of bacteria without compromising access to nutrients). Also,

since the effect of the extracts against *S. epidermidis* was low, the extracts time was extended and besides the 48 hr time-point, 72 hr extracts were also prepared and tested.

With all protocol modifications, *S. aureus* was thus grown on TSB and exposed to both 48 hr and 72 hr Sr- and Ca-rich discs extracts obtained in TSB. Regarding the 48 hr extracts, the metabolic activity assay did not show relevant bacterial inactivation as D1 and ND extract, despite statistically significant, were only able of an activation reduction of 18% and 15%, respectively (Figure 13 A1 and Table 5) and visually it was not possible to find a MIC. Culturability of the *S. aureus* after exposure to the extracts did not result in MBC as D1 and ND extracts, despite significant, were only able to induce 2.5% and 2.9% of death, respectively (Figure 13. A2 and Table 5). The 72 hr extracts, similar results were obtained with low inactivation of *S. aureus* (Figure 13. B1 and Table 5) and MIC not visually found. Culturability of the bacteria did not show MBC, despite ND extracts being able to kill 15.4% of the bacteria (Figure 13 B2 and Table 5).

After the evaluation of the antimicrobial activity of the tested alginate disc extracts it is important to determine if the observed effect was due to the strontium ion release and or

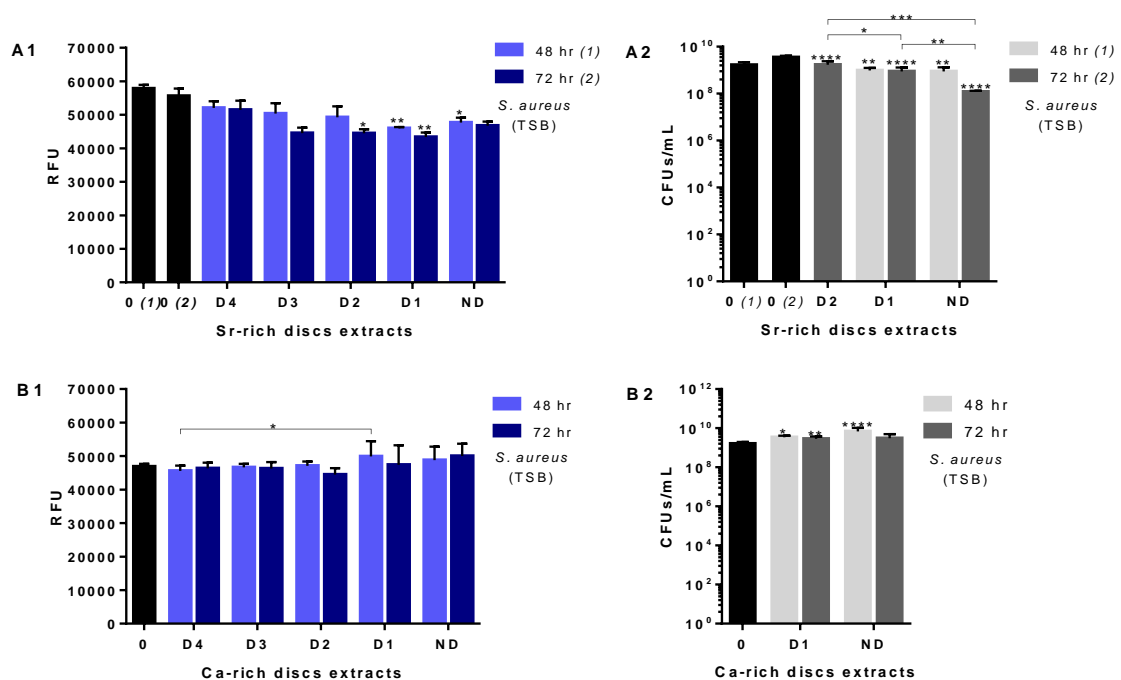


**Figure 13 – Antimicrobial activity of the Ca- and Sr-rich alginate discs extracts (in TSB) towards *S. aureus*.** Sr-rich (A) and Ca-rich (B) discs, *S. aureus* grown on TSB. A1 and B1 – Metabolic activity evaluation. Relative fluorescence units (RFU) are presented as a function of extracts dilutions. A2 and B2 – Bacteria culturability. CFUs count is presented as a function of the discs extracts. *S. aureus* represents the negative control (no treatment). Mean values  $\pm$  standard deviation are illustrated. Bars marked with \* are statistically different from the control and bars marked with (\*) and brackets are statistically different between them ( $P < 0.05$ ).

to other factor present in the alginate discs or its extracts. Therefore, control Ca-rich alginate discs were produce and 48 hr and 72 hr extracts prepared in order to challenge *S. aureus*. This experiment revealed that the Ca-rich alginate discs extracts were not able to induce any kind of bactericidal activity as shown in Figure 13 B and Table 5. Metabolic activity by AlamarBlue assay showed 0% bacterial inactivation for both the 48 hr and 72 hr extracts and CFU counting showed no MBC for all the ND extracts.

Analysing the summarized results in Table 5, despite not very relevant, the 72 hr extracts showed slightly higher bactericidal activity when compared to the 48 hr extracts. Therefore, there is the evidence that the antimicrobial activity of the extracts is dependent on extract time. Also, it was proved that Ca-rich alginate disc extracts didn't induce any effect on *S. aureus*. Thus it is conceivable to suggest that the antimicrobial activity observed on *S. epidermidis* and *S. aureus*, despite small, is given to the strontium ion release from the discs to the surrounding environments. Therefore, the antimicrobial activity of the Sr-rich alginate discs are strontium concentration dependent, as already discussed<sup>18,94</sup>, which is, as proved here, dependent on the extracts time. This perspective is concordant with a gradual degradation of the alginate discs which allows for a continuous release over time of the strontium ions present within its structure. This degradation has been described as alginate dissolution process given by the release of the divalent cross-linking ions,  $\text{Sr}^{2+}$ , into the surrounding media. This release is possible owing to exchange reactions of the strontium ions with the existing monovalent cations in the media, such as  $\text{Na}^+$ <sup>112</sup>.

Moreover, the attained results are in agreement with the previous predictions made after addressing the concentration of strontium present in the discs extracts. Accordingly, no MIC or MBC was achieved by exposing *S. aureus* to both 48 hr and 72 hr extracts and therefore, overall antimicrobial properties of the discs extracts revealed to be insufficient on their own (containing 105.6  $\mu\text{g}/\text{mL}$  and 114.36  $\mu\text{g}/\text{mL}$  of strontium, respectively). The reason for the low antimicrobial activity may rely in the extent of ion released as alginate degradation is considered to be slow and poorly regulated<sup>154</sup>. Hence, in an *in vivo* perspective, alginate is not naturally enzymatically degraded in mammals (as they lack the alginate enzyme) as well as cells do not naturally adhere to alginate. To compensate this drawbacks, alginate MW and composition may be manipulated in order to ensure controlled degradation *in vivo*<sup>154</sup>.

**Table 5** – Percentages of metabolic activity inhibition and percentages of death for *S. epidermidis* and *S. aureus* after exposure to 48 hr and 72 hr Sr-rich and Ca-rich alginate discs extracts and its dilutions.

		<i>S. epidermidis</i>				<i>S. aureus</i>									
Bacteria	Metabolic inactivation (%)	Percentage of death (%)				Metabolic inactivation (%)				Percentage of death (%)					
Alginate disc	Sr-rich	Sr-rich				Sr-rich		Ca-rich		Sr-rich		Ca-rich			
Extract time	48 hr	48 hr				48h	72h	48h	72h	48h	72h	48h	72h		
Medium	TSB	MHB	TSB	MHB	TSB	TSB	TSB	TSB	TSB	TSB	TSB	TSB			
<b>Extracts' dilutions</b>	<b>D9</b>	25	0	-	-	-	-					-	-	-	-
	<b>D8</b>	30	0	-	-	-	-					-	-	-	-
	<b>D7</b>	33	0	-	-	-	-					-	-	-	-
	<b>D6</b>	17	0	-	-	-	-					-	-	-	-
	<b>D5</b>	17	0	-	-	-	-					-	-	-	-
	<b>D4</b>	26	0				7	8	3	1	-	-	-	-	-
	<b>D3</b>	26	0				10	21	1	1	-	-	-	-	-
	<b>D2</b>	41	0				12	21	0	5	-	3	-	-	-
	<b>D1</b>	53	1				18	23	0	0	2.5	6	0	0	0
	<b>ND</b>	80	23	13.5	4.5	15	16	0	0	2.9	15.4	0	0	0	0

### 4.2.3. Characterization of the Ca- and Sr-doped microspheres and powders and its extracts

As described before, the different components of the injectable system were divided in order to separately evaluate their antimicrobial properties. Thus, after characterizing and assessing the antimicrobial properties of the discs extracts, the microspheres  $\mu$ SrHAp, nSrHAp and SrTriP are now in this section, along with the respective control microspheres prepared without strontium, namely  $\mu$ HAp and nHAp, to be evaluated against *S. aureus*. Powders of pSrTriP and pSrCO<sub>3</sub> were also characterized and analysed their bactericidal properties in order to open perspectives of use as future materials.

After production, microspheres were firstly sorted within a size range by sieving, and microspheres with diameters between 350 and 450  $\mu$ m selected and used throughout this work.

A qualitative analysis of size, morphology and porosity (qualitative) of each type of microspheres was also assessed by SEM (Figure 14). Regarding  $\mu$ HAp,  $\mu$ SrHAp and SrTriP microspheres, good sphericity was achieved with average diameters of approximately 398.1  $\mu$ m, 408.3  $\mu$ m and 414.2  $\mu$ m, respectively, for each type of microsphere. Size and shape was, therefore, consistent between these three microsphere formulations (Figure 14 A1, B1 and E1). However, the  $\mu$ HAp and  $\mu$ SrHAp formulations in this work revealed smaller microsphere diameters when compared to previous works that reported an average size of 555  $\mu$ m<sup>112</sup>. Surface morphology of each  $\mu$ HAp,  $\mu$ SrHAp and SrTriP microspheres and between them was also very homogeneous, however the microspheres formulated with micrometric HAp ( $\mu$ HAp and  $\mu$ SrHAp) showed a tighter microstructure (Figure 14 A6 and B6) relatively to the strontium phosphate formulation microspheres (SrTriP) which revealed a more open one (Figure 14 E6). Therefore, a qualitative analysis of the SEM micrographs, suggest that the SrTriP microspheres presents a more porosity structure than the  $\mu$ HAp and  $\mu$ SrHAp. For the three, it is clear the existence of a porous network of interconnected cavities. This microarchitecture was achieved after the sintering of the polymeric alginate phase leaving the fused ceramic phase of HAp and strontium phosphate<sup>112</sup>, respectively. Also, the incorporation of strontium in the micrometric HAp microspheres formulation did not show to induce any type of structural alteration in the microstructure. This is important as it has been reported that high incorporation of strontium in HAp induces alteration on its structure as the Sr diameter (113 pm) is higher than the one of Ca (99 pm)<sup>110,111</sup>. Concerning nHAp and nSrHAp particles, low sphericity was attained as particles revealed an aspect ratio ( $d/D$ , were  $d$  is the smaller diameter and  $D$  is the largest) of 0.624 ( $d = 437.4 \mu\text{m}$ ;  $D = 701.2 \mu\text{m}$ ) and 0.729 ( $d = 430.4 \mu\text{m}$ ;  $D = 591.3 \mu\text{m}$ ), respectively, far from the one of a perfect sphere (1) (Appendix 1). The evidence is that this phenomenon of low

sphericity seems to be directly connected to the formulations where nanometric HAp is used. Concordantly, at the time of the production of this type of microspheres, it was noticed that extrusion of the paste was much impaired, probably by quick drying of the drops on the

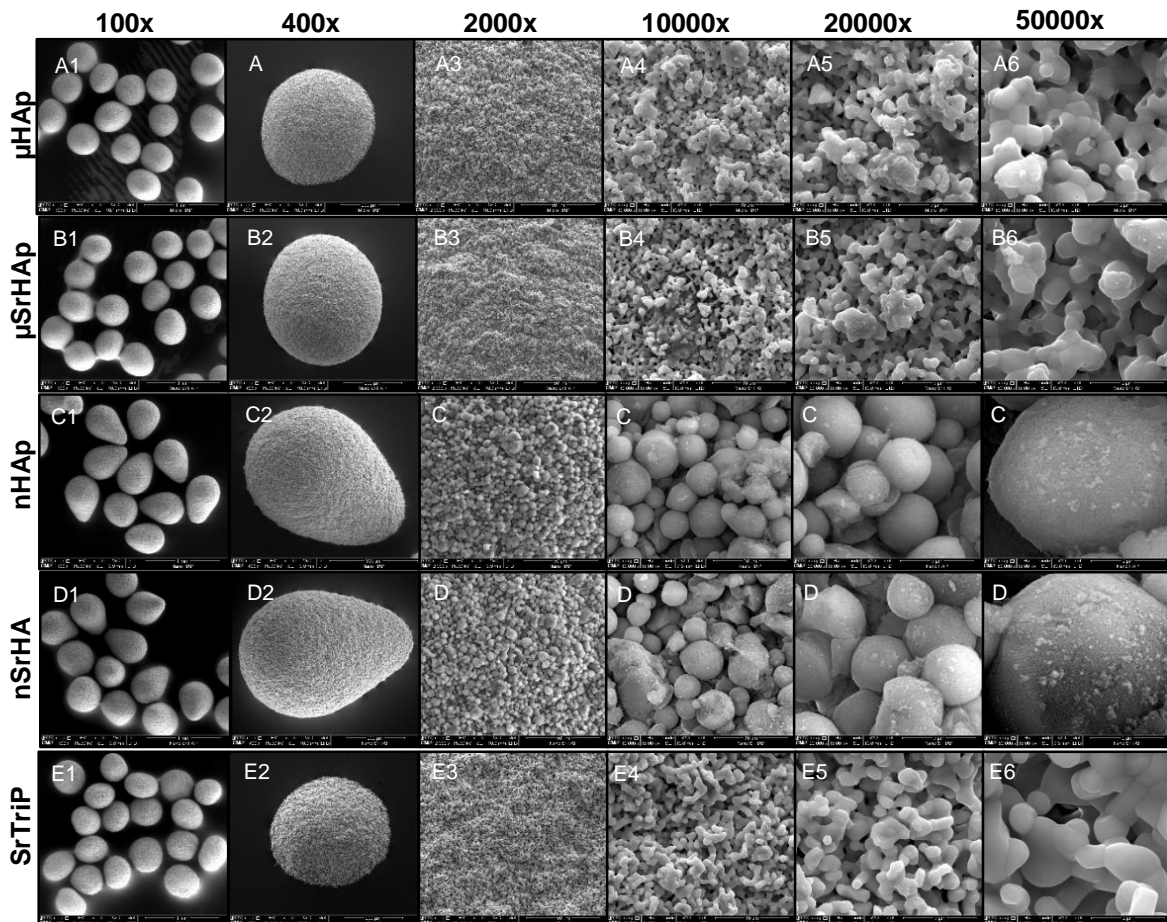


**Figure 14** – SEM micrographs of the  $\mu$ HAp (A),  $\mu$ SrHAp (B), nHAp (C), nSrHAp (D) and SrTriP (E) microspheres. Increasing magnification is presented from left to right (1. 100x; 2. 400x; 3. 2000x; 4. 10000x; 5. 20000x and 6. 50000x) revealing the porous microarchitecture of the microspheres.

needles edge. This led to a delay of the drops fall which causes the stretch of the drop giving rise to the tear-like shape. Nonetheless, despite not being completely spherical, there was homogeneity in terms of size and shape for these two types of microspheres (Figure 14 C1 and D1). Surface morphology was also consistent between the nHAp and nSrHAp formulations with no differences found on the microstructure of the microspheres upon incorporation of strontium. Nevertheless, it showed to be very different from the surface morphology found for the  $\mu$ HAp,  $\mu$ SrHAp and SrTriP. Microspheres prepared with nanometric HAp appear with much less porosity where an angled maze topography gives rise to a more tight/compact and smoother surface where round forms prevail (Figure 14 C and D). For these microspheres, the sintering was done at lower temperatures in order not to promote the fusion of the nanometric HAp (otherwise micrometric HAp would be formed). Therefore, this microspheres are arranged in a hierarchical manner as they are constituted



by large and compact round structures which in turn are composed by the nanometric (few tens of nanometers) HAp grains (Figure 15).

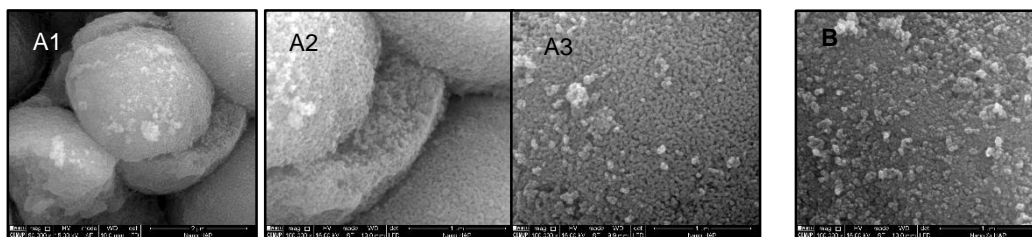


**Figure 15** – SEM micrographs of nHAp (A) and nSrHAp (B) microspheres. **A1** and **A2** with increasing magnifications (left to right, 50000x, 100000x and 100000x, respectively) revealing the interior of the microspheres and the nanometric grain and **B** the nanometric grain (100000x).

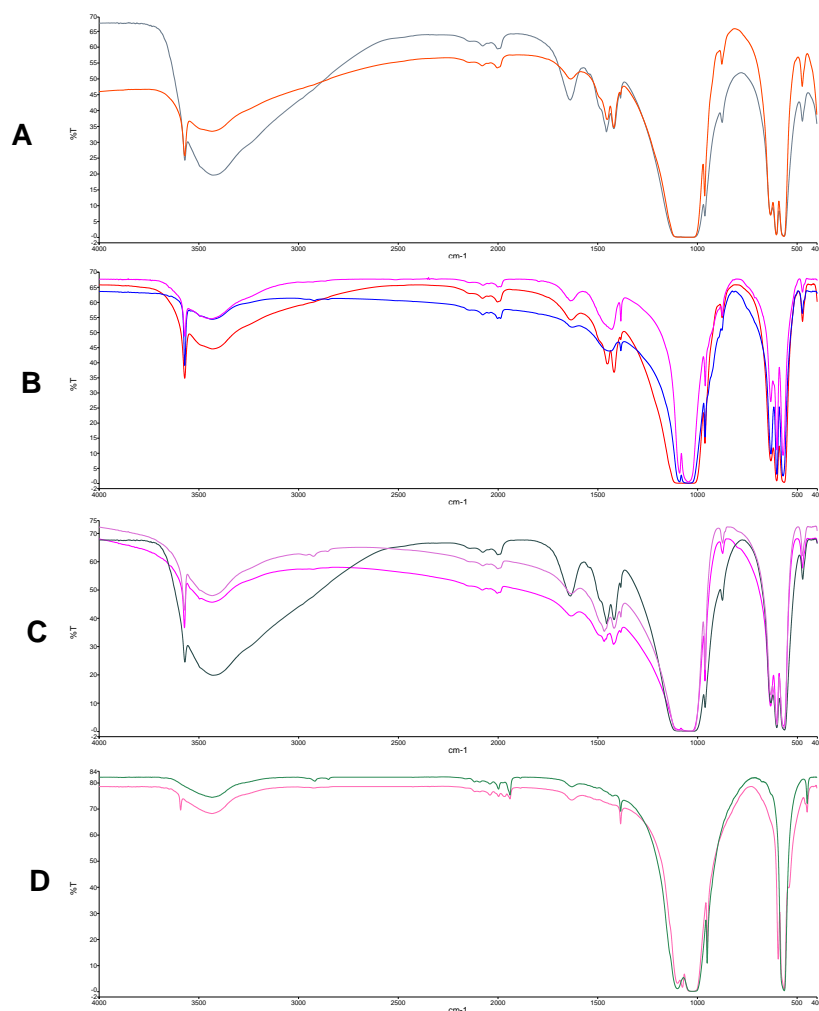
In Figure 15 A3 and B, it is possible to see the nanometric grains of HAp both for nHAp and nSrHAp, respective. Additionally, in Figure 15 A, a cracked microsphere exposes its interior where it is possible to notice that the microstructure observed at the surface is maintained through the inner parts. Data is not provided for the interior of the  $\mu$ HAp,  $\mu$ SrHAp and SrTriP microspheres, however it is conceivable to suggest that the porous network visible at the surface is also sustained into the interior of the microspheres. The porosity and the interconnection between cavities within the microspheres microstructure may prove to be essential in the success of the antimicrobial leaching system. So that, the strontium ions present in the innermost regions can leach from the microsphere to the surrounding areas to exert their antimicrobial action. Accordingly, higher specific surface area in contact with the environment fluids, for instance, should improve the capacity of the system to release the ions and increase the effect on bacteria <sup>155</sup>.

EDS analysis performed to all the microspheres revealed that the  $\mu$ SrHAp, nSrHAp and SrTriP, incorporated 4.3% wt (1.2% At), 7.4% wt (2.1% At) and 65.4% wt (29.3% At) of Sr, respectively. The Sr incorporation of  $\mu$ SrHAp microspheres is in agreement with a previously reported work where 4% wt (1.2% At) incorporation is described <sup>112</sup>. According to these results, and concerning the antimicrobial activity of the Sr-doped microspheres it is expectable that SrTriP will perform better followed by the nSrHAp and at last the  $\mu$ SrHAp. Regarding the  $\mu$ HAp and nHAp no significant Sr was detected and no other contamination were detected for all the analysed microspheres (Appendix 1).

Zeta potential was another parameter evaluated on the produced microspheres. As shown in Table 6, all the microspheres showed to be negatively charged at physiological pH (pH ~6, during measurement). Only the  $\mu$ SrHAp microspheres showed to have a slightly more negative zeta potential comparing to the  $\mu$ HAp and to the other microspheres. This difference has already been reported for the same type of microspheres by Neves et al <sup>112</sup>.

**Table 6** – Zeta potential (ZP) analysis of the produced microspheres.

	$\mu$ HAp	$\mu$ SrHAp	nHAp	nSrHAp	SrTriP
<b>Zeta Potential</b>	-13,72	-19.20	-11.63	-11.13	- 12.82
(mV $\pm$ SD)	$\pm$ 0.19	$\pm$ 1.33	$\pm$ 0.51	$\pm$ 0.22	$\pm$ 0.16



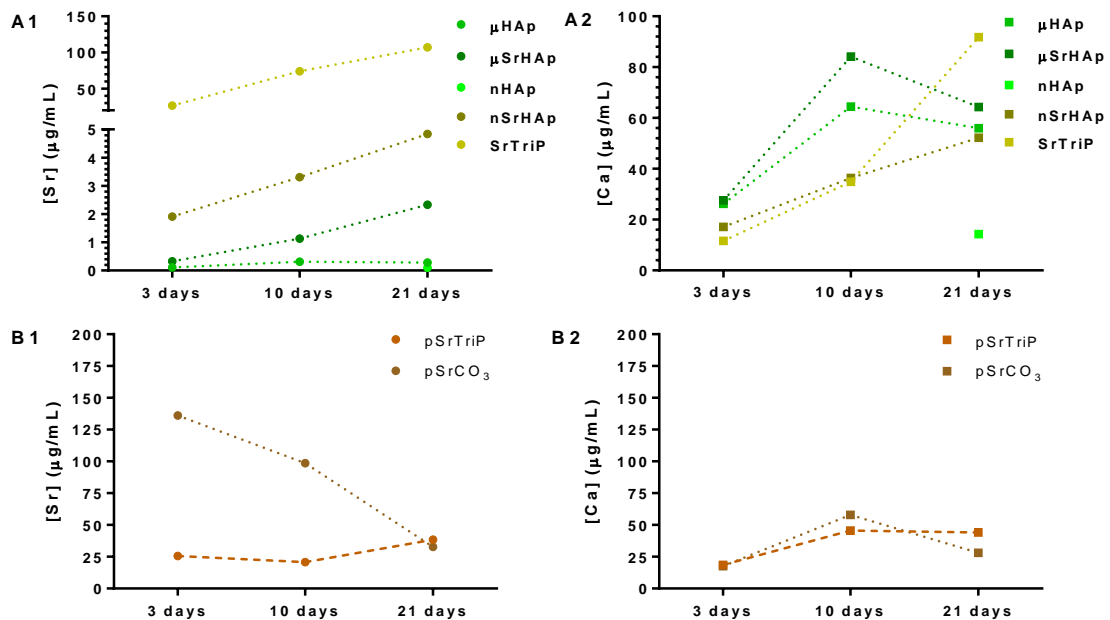
**Figure 16** – FTIR-ATR spectra (%Transmittance as function of wavelength,  $\text{cm}^{-1}$ , is plotted). **A** – nanometric (blue line) and micrometric (red line) HAp powders; **B** – micrometric HAp powders (red line),  $\mu$ HAp microspheres (dark blue line) and  $\mu$ SrHAp microspheres (pink line); **C** – nanometric HAp powders (black line), nHAp microspheres (pink line) and nSrHAp microspheres (purple line); **D** – strontium phosphate powders (green line) and SrTriP microspheres (pink line).

Figure 16 A shows the overlay of FTIR spectrum of nano and micro hydroxyapatite powders used in the preparation of the microspheres. Both spectrum are similar and characterized by OH stretching ( $3572 \text{ cm}^{-1}$ ) and vibrational ( $632 \text{ cm}^{-1}$ ) bands and  $\text{PO}_4$  ( $\nu_3 \sim 1090 \text{ cm}^{-1}$  and  $1041 \text{ cm}^{-1}$ ,  $\nu_1$   $963 \text{ cm}^{-1}$ ,  $\nu_4$   $602$  and  $571 \text{ cm}^{-1}$ ,  $\nu_2$   $473 \text{ cm}^{-1}$ ) bands. The bands corresponding to the  $\nu_3$  vibration of C-O between  $1410$  and  $1470 \text{ cm}^{-1}$  and the  $\nu_2$  vibrations between  $850$  and  $890 \text{ cm}^{-1}$ , characteristic of the carbonate group are

observed in the FTIR spectrum of both hydroxyapatite powders, indicating that we are in the presence of carbonated hydroxyapatites. Nevertheless, the carbonate bands are more intense in the nano hydroxyapatite powder. The broad bands at 3452 and 1631  $\text{cm}^{-1}$  are due to the presence of lattice water in the powders. Those bands are also much more intense in the nanohydroxyapatite powder. In what concerns the Ca-HAp microspheres, after sintering, the FTIR spectra are very similar to the one of the powders except for the nano hydroxyapatite where a significant reduction of the water bands is observed (Figure 16 B and C). When Sr is present in the  $\mu\text{HAp}$  microspheres, a decrease in the OH stretching band, which appears in hydroxyapatite as a narrow peak at 3572  $\text{cm}^{-1}$  is observed, indicating that changes are occurring in the Hap structure. This observation suggests that Sr is incorporated in the  $\mu\text{HAp}$  lattice, being the same phenomena not so evident in the nSrHAp microspheres. In what concerns the SrTriP microspheres, its spectrum is very similar to the one of the strontium phosphate powder indicating that during sintering of the particles, no degradation occurs (Figure 16 D).

In order to address microspheres and powders bactericidal activity, extracts of  $\mu\text{HAp}$ ,  $\mu\text{SrHAp}$ , nHAp, nSrHAp and SrTriP microspheres and powders were prepared to be used against *S. aureus*. 3 days, 10 days and 21 days extracts were obtained and subjected to ICP-AES analysis to determinate the amount of strontium and calcium that the microspheres and powder were able to release. Here, longer time-points than the discs extracts were chosen since ceramic materials have slower degradation kinetics than alginate. Thus, in the hybrid system context, the microspheres, are intended to promote its antimicrobial activity in a perspective of a long time prevention of bacterial infection after surgery. This approach tries to accomplish a gradual release of strontium to the surrounding tissues/areas maintaining an ion concentration that is able to impair microbial proliferation. The concentration ( $\mu\text{g/mL}$ ) of calcium and strontium ions present at the different time-point extracts for each type of microsphere and powders are presented in Figure 17. In what concerns strontium concentration release from microspheres, (Figure 17 A1) the SrTriP microspheres were the most effective leaching system ([Sr]  $\mu\text{g/mL}$ : 3 days – 26.54; 10 days – 73.97; 21 days – 107.12). From the SrTriP to the remaining microspheres there was a substantial gap in the ability of the microspheres to release strontium. nSrHAp, which were the second microspheres with better strontium release kinetics, only managed to release one-twentieth ([Sr]  $\mu\text{g/mL}$ : 3 days – 1.91; 10 days – 3.31; 21 days – 4.84) of the amount accomplished by the SrTriP microspheres. At last the, the  $\mu\text{SrHAp}$  microspheres were the worst of the Sr-doped microspheres releasing the ion ([Sr]  $\mu\text{g/mL}$ : 3 days – 0.33; 10 days – 1.13; 21 days – 2.33). These results are concordant with previously discussed EDS analysis results where the SrTriP microspheres revealed a strontium content approximately 9 and 15 folds higher than nSrHAp and  $\mu\text{SrHAp}$ , respectively. Thus, it is clear the direct relation

between the amount of strontium incorporation on microspheres and their ability to effectively release high concentration of the ion. The higher the incorporation, the higher the delivered amount of strontium. Therefore, it is expected higher antimicrobial activity for the SrTriP microspheres followed by the nSrHAp, as it has been reported that higher amounts of strontium release induce higher bactericidal activity<sup>18,94</sup>. For the  $\mu$ HAp and nHAp no relevant concentrations of strontium were found (Figure 17 A1). Ca release evaluation showed that Ca was very present in all the microspheres extracts except for nHAp which showed low release even after 21 days (Figure 17 A2). The presence of calcium in all the prepared microspheres is obvious as calcium phosphate ceramic materials are being used. Regarding the 21 days extracts, it was noticed considerable loss of well volume by evaporation despite measurements against this effect having been taken. Therefore, the results presented for the concentrations of ions for this time point may be significantly biased from the real ones. This deviation is clear, for instance, in the decrease of calcium concentration for the  $\mu$ HAp and  $\mu$ SrHAp microspheres from the 10 to the 21 days. Thus, with the loss of volume the extracts would saturate faster hindering the solubilisation of more strontium and calcium to the media. Nevertheless it is clear the tendency that the ion concentration of the extracts is time dependent.



**Figure 17 – Strontium and calcium release from the microspheres (A) and powders (B) over time.** 3 days, 10 days and 21 days microspheres and powder extracts were quantified in Sr (1) and Ca (2) composition ( $\mu\text{g}/\text{mL}$ ) by ICP-AES. (For the nHAp only the 21 days' time-point was done given to material restriction).

Powder extracts, namely pSrTriP and pSrCO<sub>3</sub>, were also prepared in order to investigate the potential of new ceramics in the fight against bacterial infection (Figure 17 B). The extracts of pSrTriP powder showed higher strontium release ([Sr] µg/mL: 3days – 25.51; 10 days – 20.82 and 21 days – 38.37) than all the microspheres except for the SrTriP. The pSrCO<sub>3</sub> reveals an inconsistent profile of strontium release as the 3 days extracts show higher concentration of strontium than the 10 days which also shows higher concentration than the 21 days extracts ([Sr] µg/mL: 3 days – 136.01; 10 days – 98.63 and 21 days – 32.69). This unreliable results may be caused, as described for the microspheres extracts, by the drying of the wells observed at the time of the extracts recovery. Also, working with the powders revealed to be very difficult as it is almost impossible to ensure good particle dispersion since they promptly deposited forming a compact pellet on the wells-bottom. Thus, new extracts having this issues in consideration should be prepared in order to accurately determine the concentration of strontium present in the 21 days extracts of both the microspheres and powders. To our knowledge, there are no works on the literature, addressing the strontium release from Sr-doped microspheres. There is instead works were different materials and strategies are used. For instance, strontium release for antimicrobial purpose has been evaluated in silver substituted HAp coating with co-incorporation of strontium, but revealed a release of only 0.05 µg/mL of Sr ions after 24h<sup>136</sup>. Those amount are significantly lower than the amounts released by our microspheres. On the other hand, strontium ferrite metal oxide (STF) has been described as able to release amounts of Sr, (49.3 µg/mL) which are in the range of the ones accomplished by our SrTriP microspheres<sup>134</sup>. In another work, bioactive glass (BGs) with strontium were able to release between 14 and 219 µg/mL of strontium ion. These values are also in the same range of what our SrTriP microspheres are able to release<sup>118</sup>. However, comparison between such different materials with completely different properties is very difficult.

#### 4.2.4. Bactericidal activity of the Ca- and Sr-doped microspheres and powders and its extracts

After the extracts preparation and recovery they were used to evaluate their bactericidal activity, *in vitro*. *S. aureus* was challenged both against the 72 hr and the 21 days extracts. Respecting the exposure to the 72 hr extracts, *S. aureus* was not significantly inhibited or killed by either the ND extracts of µHAp or of µSrHAp. Therefore, no MIC or MBC were detected as no metabolic activity reduction and bacterial death was observed for both these materials extracts (Figure 18 A1, A2 and Table 7). The nHAp and nSrHAp extracts were able to induce significant metabolic activity inactivation of 69% and 89%, respectively. Despite the fact that, no MIC was visually detectable for both the materials,

the nSrHAp showed (by visual inspection) higher inhibition of bacterial growth (Appendix 2). Despite not achieving MBC or MIC, both the materials were capable of provoking bacterial death, 21% and 19%, respectively. These results are not in agreement neither with the previous discussed percentage of incorporation of strontium in the microspheres neither with the concentration of strontium found in the extracts. In fact, the  $\mu$ SrHAp microspheres revealed higher values in both cases and here presents a similar bactericidal activity compared with the  $\mu$ HAp. Thus, the differences found in the amounts of strontium that the  $\mu$ SrHAp is able to release is probably not sufficient to induce higher activity compared to  $\mu$ HAp microspheres. Concerning the SrTriP microspheres, by visual inspection, it was already possible to find a MIC for the ND extracts (Appendix 2). Accordingly, the metabolic activity of the bacteria was totally inhibited (100%) for the ND extracts while for the rest of the dilutions no significant reduction was observed compared to control (Figure 18 A1 and Table 7). However, after culturability on solid medium and CFUs count, the ND extracts of

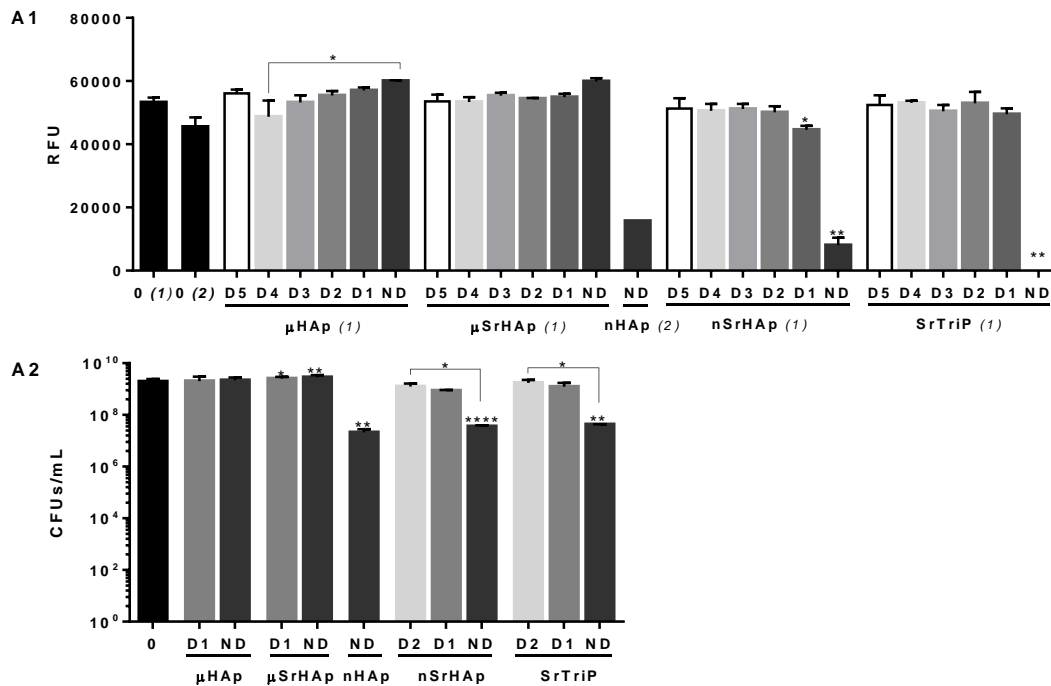


**Figure 18 – Antimicrobial evaluation of 72 hr microspheres extracts towards *S. aureus*.** **A1** – Metabolic activity evaluation. Relative fluorescence units (RFU) are presented as a function of extracts dilutions. **A2** – Bacteria culturability. CFUs count is presented as a function of the extracts dilutions. *S. aureus* represents the negative control (no treatment). Mean values  $\pm$  standard deviation are illustrated. Bars marked with (\*) are statistically different from the control and bars marked with (\*) and brackets are statistically different between them ( $P < 0.05$ ). No statistical analysis is presented for nHAp extracts as only one sample was used, given to material restrictions.

the SrTriP microspheres showed only to be able to induce 23% of cell death (Table 7). Thus, no MBC was found. Nevertheless, a MIC was obtained for the ND extracts which. Were already described to have a strontium concentration of 26.54  $\mu\text{g/mL}$ , significantly below the MIC (283  $\mu\text{g/mL}$  of Sr) determined using  $\text{SrCl}_2$  solutions. Therefore, more experiments should be done in order to confirm these results and to understand why such a high activity of the ND extracts of SrTriP microspheres was noticed.

With respect to the 21 days extracts, since evaporation from the wells was observed

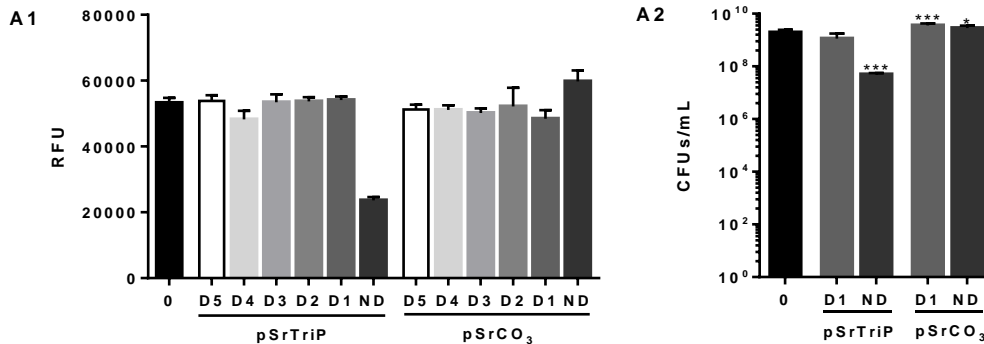


**Figure 19 – Bactericidal evaluation of the powders extracts.** 72 hr extracts against *S. aureus*. **A1** – Metabolic activity evaluation. Relative fluorescence units (RFU) are presented as a function of extracts dilutions. **A2** – Bacteria culturability. CFUs count is presented as a function of the extracts dilutions. *S. aureus* represents the negative control (no treatment). Mean values  $\pm$  standard deviation are illustrated. Bars marked with \* are statistically different from the control ( $P < 0.05$ ).

and unexpected results were attained in Sr release experiment and given the observed uncertainty associated to the extracts viability for both microspheres and powders, the results for this time-point were chosen not to be presented in the core dissertation and may be found in the Appendix 3.

The antimicrobial activity of the powders was also tested, *in vitro*, and none of the 72 hr powders extract were able to achieve either MIC or MBC by challenging *S. aureus*. However, the pSrTriP extracts were capable of inducing a bacteria metabolic activity inactivation of 58% (Figure 19 A1 and Table 7). Concordantly, the pSrTriP ND extracts demonstrated better bactericidal activity (17%) than the pSrCO<sub>3</sub> (Figure 18 A2 and Table 7). The incoherence present between the concentration of strontium analysed in the extracts and their respective bactericidal activity may be connected, once more, with the difficulties found on working with the ceramics as powders and therefore more investigation should be made on this matter as already discussed.

Besides the evaluation of the antimicrobial properties of the microspheres and powders as extracts, experimental work was also done by culturing the bacteria directly together with the testing material, *in vitro*. Thus, in order to address microspheres and powders bactericidal activity, direct exposure for 6 hr and 24 hr of increasing amounts (40, 60 and 80 mg) of each testing material was performed.

**Table 7** - Percentages of metabolic activity inhibition and percentages of death for *S. aureus* after exposure to 72 hr extracts of the microspheres and powders.

Material		$\mu$ HAp	$\mu$ SrHAp	nHAp	nSrHAp	SrTriP	pSrTriP	pSrCO <sub>3</sub>
Extract time		72 hr						
<b>Metabolic inactivation (%)</b>								
Extracts dilutions	D5	0	0	-	4	2	0	4
	D4	4	0	-	5	1	10	4
	D3	0	0	-	4	6	0	6
	D2	0	0	-	6	1	0	9
	D1	0	0	-	17	7	0	10
	ND	0	0	69	89	100	58	0
<b>Percentage of death (%)</b>								
Extracts dilutions	D2	-	-	-	2	1	-	-
	D1	0	0	-	4	2	3	0
	ND	0	0	21	19	23 *	17	0

\* from the three replicates of the ND SrTriP extracts, two did not show any CFUs formed, thus, the value presented only respect to the other (one) replicate

After 6 hr exposure,  $\mu$ HAp and  $\mu$ SrHAp microspheres did not induce bacteria inactivation (AlamarBlue assay) comparing to the control (Figure 20 A1 and Table 8). Concordantly, no inhibitory or bactericidal concentration was determined for these two types of microspheres as 0% and 3% of bacterial death was achieved by the  $\mu$ HAp and  $\mu$ SrHAp microspheres, respectively. In fact, throughout the experimental work elaborated it has been consistent that the antimicrobial properties of these two types of microspheres is very limited. On the other hand, nHAp, nSrHAp and SrTriP showed significant antimicrobial properties. nHAp microspheres managed to reduce the bacterial metabolic activity in 50%, 84% and 92%, respectively for the 40, 60 and 80 mg (Figure 20 A1 and Table 8). Nevertheless, concerning culturability of the bacteria after exposure, CFUs count indicated only 10%, 18% and 19% bacterial death, respectively (Figure 20 A2 and Table 8). Despite being low, the observed bactericidal activity was not expected as these microspheres have no content in strontium. A possible intrinsic antimicrobial activity of the nHAp microspheres which should be further investigated in the future. With respect to nSrHAp and SrTriP microspheres, they did show very significant bactericidal activity. Both were able to



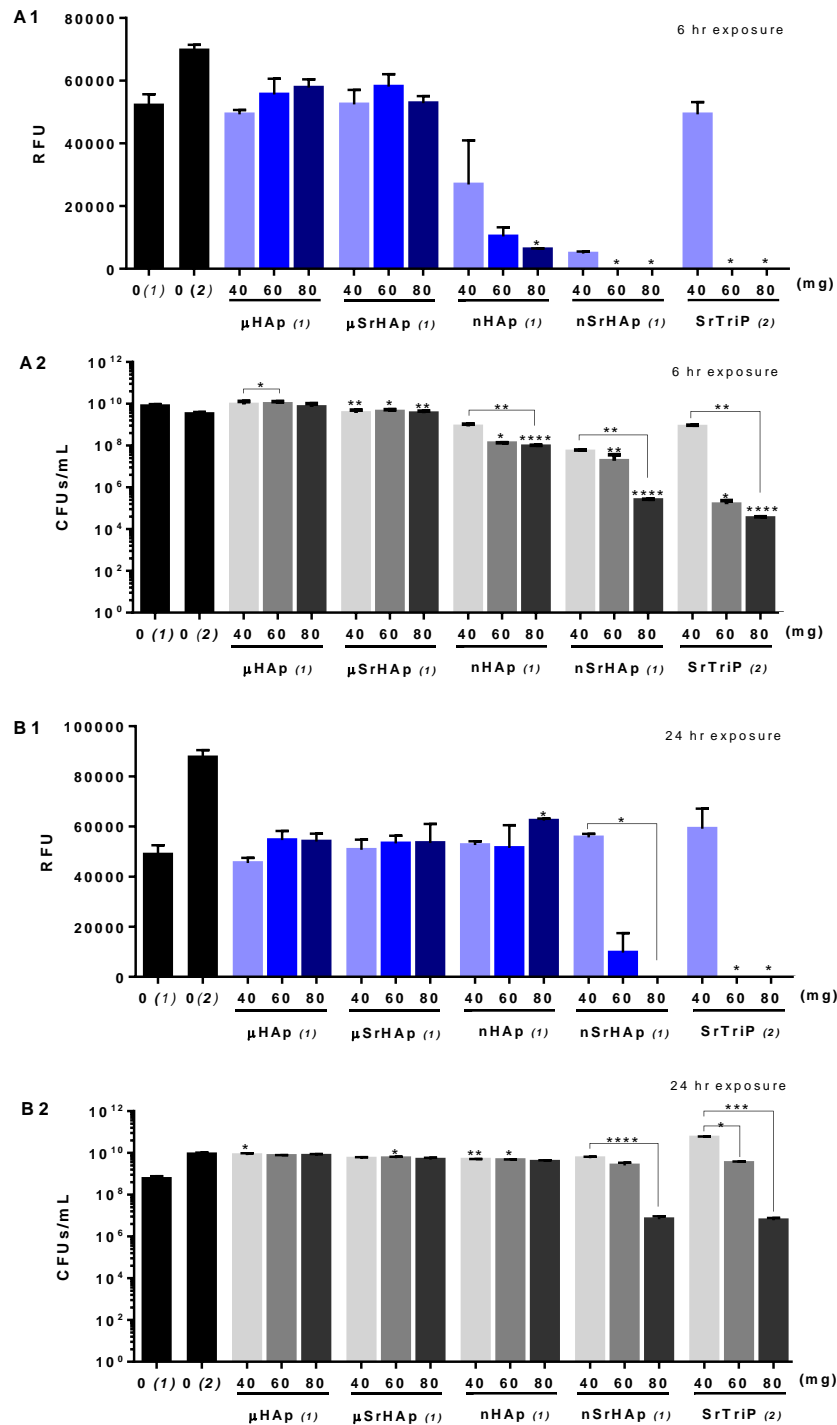


**Figure 20 - Bactericidal evaluation of the direct exposure of microspheres to *S. aureus*.** 6h (A) and 24h (B) exposure against *S. aureus*. **A1** and **B1** – Metabolic activity evaluation. Relative fluorescence units (RFU) are presented as a function of the masses of powders used. **A2** and **B2** – Bacteria culturability. CFUs count is presented as a function of the masses of microspheres used. *S. aureus* represents the negative control (no treatment). Mean values  $\pm$  standard deviation are illustrated. Bars marked with (\*) are statistically different from the control and bars marked with (\*) and brackets are statistically different between them ( $P < 0.05$ ).

completely inhibit metabolic activity of the *S. aureus* when 60 or 80 mg of microspheres were used (Figure 20 A1 and Table 8). Indeed, for instance, for the SrTriP microspheres, by visual inspection, medium turbidity was significantly reduced by the microspheres exposure revealing a significant inhibition of bacterial growth (Appendix 4). Culturability of the bacteria after exposure also demonstrated the bactericidal activity of both microspheres by killing, respectively, 26% and 45% (for the nSrHAp) and 45% and 52% (for the SrTriP) of bacteria (Figure 20 A2 and Table 8). Despite the massive discrepancy found in the amount of strontium incorporated between these two formulations of microspheres (nSrHAp: 7.4% wt (2.1% At) vs SrTriP: 65.4% wt (29.3% At) and in the concentration of ions release (Figure 15 A1), in the *in vitro* antimicrobial tests, these differences are not noticed. These results, together with the limited, but consistent, antimicrobial activity demonstrated by the nHAp microspheres suggest that the microspheres formulated with nanometric HAp have itself bactericidal activity. This conclusion may respond to the similar antimicrobial activity observed for the nSrHAp and the SrTriP microspheres. Therefore, the lack of strontium ion incorporated in nSrHAp microspheres is compensated by the antimicrobial activity provided by the nHAp itself. The reason why nHAp present bactericidal effect over *S. aureus* is not comprehended by this study, thus more work should be done to fully evaluate the extent of the action of nHAp against bacteria.

Regarding the 24 hr exposure of the microspheres to *S. aureus*, similar results were obtained for the metabolic activity assay. No activity inhibition was again observed for both the  $\mu$ HAp and  $\mu$ SrHAp microspheres, whereas the nSrHAp induced bacterial inactivation of 83% and 100% and the SrTriP of 100% and 100%, respectively for the 60 and 80 mg. Only the nHAp showed more preeminent differences with 0% inactivation of the bacteria (Figure 20 B1 and Table 8). Culturability of the bacteria showed that, in general, the bactericidal activity of the microspheres was weakened and no bactericidal concentration of microspheres was found. The nSrHAp and SrTriP microspheres maintained some bactericidal activity, but substantially impaired as only 3%, 29% and 4%, 32% of cell death was observed after the 24 hr exposure (Figure 20 B2 and Table 8). Thus, the microspheres seem to lose their antimicrobial potential from the 6 hr to 24 hr exposure. This phenomenon may be given to bacteria adaptation, strontium complexation/chelation impeding the free and more reactive state of the ion, or other aspects which are yet not comprehended )<sup>83,85,86</sup>. Also the fact that we were probably working with sub-inhibitory concentration may allowed for the perpetuation of bacterial proliferation, which may reach a point where the strontium ion concentration was simply not enough to face all the bacteria.

As described above, powders (pSrTriP and pSrCO<sub>3</sub>) were also used in *in vitro* tests to evaluate their antimicrobial properties against *S.aureus*. After the 6 hr exposure, pSrTriP showed to reduce (despite not statistically significant) the metabolic activity in 8%, 36% and

47% and after the 24 hr, 30%, 20% and 13%, respectively for the 40, 60 and 80 mg (Figure 21 A1 and B1 and Table 8). For the 6 hr exposure the results followed a consistent concentration-effect dependency, however, for the 24 hr higher concentrations of the powders induced less metabolic activity inactivation. This contradiction may be connected to the already discussed difficulty on working with powders, *in vitro*. In fact, it has already been reported that the antimicrobial activity of Sr-HAP nanoparticle (powder) was only present when particles were in dynamic contact with bacteria <sup>94</sup>. Therefore, the uneven dispersion of the powders may respond to the contradictory results observed. Regarding

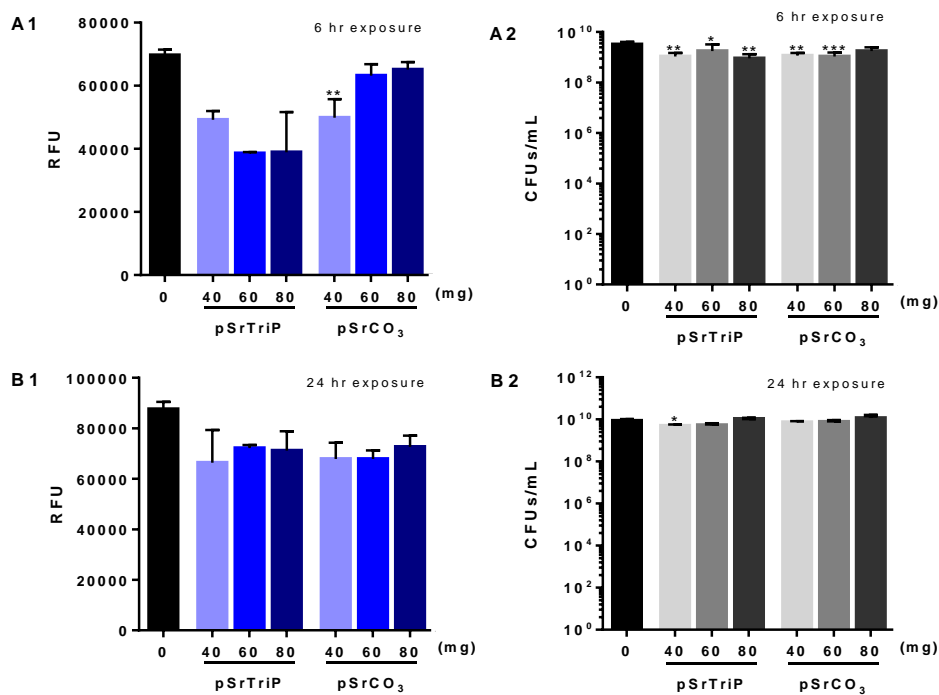


**Figure 21 - Bactericidal evaluation of the direct exposure of powders to *S. aureus*.** 6h (A) and 24h (B) exposure against *S. aureus*. **A1** and **B1** – Metabolic activity evaluation. Relative fluorescence units (RFU) are presented as a function of the masses of powders used. **A2** and **B2** – Bacteria culturability. CFUs count is presented as a function of the masses of microspheres used. *S. aureus* represents the negative control (no treatment). Mean values  $\pm$  standard deviation are illustrated. Bars marked with (\*) are statistically different from the control ( $P < 0.05$ ).

the culturability of the bacteria after exposure to pSrTriP, the CFUs count revealed very limited ability to kill bacteria, both after 6 hr and 24 hr, respectively for 40, 60 or 80 mg of microspheres (Figure 21 A2 and B2 and Table 8). The antimicrobial activity assessment of the pSrCO<sub>3</sub> showed also limited ability to induce bacterial inactivation (Figure 21 A1 and B1 and Table 8). Again contradictory bactericidal activity is observed. Regarding culturability in solid medium, CFUs counting demonstrated that after the 6 hr exposure only 4%, 5% and 3% bacterial kill was detected for the 40, 60 and 80 mg, respectively, and 0% of death after

the 24h exposure for all the powders concentrations (Figure 21 A2 and B2 and Table 8). In general, no substantial bactericidal activity was noticeable for any of the powders and concentrations used. Also, no significant differences between the powders or its concentrations used were evident.

Regarding the antimicrobial properties of Sr- rich microspheres and the used powders, no works to our knowledge have been done addressing this matter. However, there are some systems developed where strontium is used as antimicrobial agent against bacteria. Several Sr-substituted calcium deficient hydroxyapatite nanoparticles and Sr incorporated bone cements, for instance, have been created and demonstrated to show antimicrobial properties against a diversity of microorganisms, (*S. aureus*, *Lactobacillus*, *E. coli*, *S.mutans*, *A. viscosus*) from Gram + to Gram - <sup>94,113,132,139</sup>. However, in all the literature and here in this work, the working concentrations of strontium that the materials were able to release were all sub-inhibitory (meaning, no complete eradication of bacteria was achieved). Therefore, the use of strontium in an implant biomaterial should mostly address preventive strategies, or as a complement for current antibiotic treatment.

**Table 8-** Percentages of metabolic activity inhibition and percentages of death for *S.aureus* after direct exposure of 6 hr and 24 hr to the microspheres and powders

Material	μHAp		μSrHAp		nHAp		nSrHAp		SrTriP		pSrTriP		pSrCO <sub>3</sub>		
	6	24	6	24	6	24	6	24	6	24	6	24	6	24	
<b>Metabolic inactivation (%)</b>															
	40	6	7	0	0	50	0	95	0	30	33	8	30	22	28
mass (mg)	60	0	0	0	0	84	0	100	83	100	100	36	20	15	19
	80	0	0	0	0	92	0	100	100	100	100	47	13	11	18
<b>Percentage of death (%)</b>															
	40	0	0	3	0	10	0	23	0	6	0	5	2	4	0
mass (mg)	60	0	0	3	0	18	0	26	3	45	4	6	2	5	0
	80	0	0	3	0	19	1	45	29	52	32	5	0	3	0

# Chapter 5

## Concluding remarks and future research perspectives

### 5.1. General conclusions

The Strontium-rich Injectable Hybrid System (IHS) developed by our research group was successfully addressed regarding its potential antimicrobial properties against the main opportunistic pathogenic bacterial strains *S. aureus* and *S. epidermidis* in bone surgery associated nosocomial infections.

It is important to emphasize that the antimicrobial potential of Strontium alone was assessed, for the first time to our knowledge, against both *S. aureus* and *S. epidermidis* in the present work. MIC and MBC were determined, for both bacteria. Respectively, *S. aureus* presented 512 µg/mL and 1792 µg/mL while, *S. epidermidis* 1024 µg/mL and 1536 µg/mL. *S. aureus* revealed less susceptibility to killing than *S. epidermidis* when exposed to Strontium. The use of Müller Hinton Broth (MHB) medium was observed to severely impair the bactericidal activity of strontium. Therefore, the use of Tryptic Soy Broth (TSB) medium, which was used in this thesis, is suggested for testing the antimicrobial properties of strontium.

The bactericidal properties of Sr-rich alginate component were investigated using Sr-alginate discs extracts. Elementary analysis of the extracts in terms of Sr and Ca contents revealed that strontium was successfully released from the discs with an increase in a time dependent faction. The extracts were able to significantly reduce the cells metabolic activity against *S. epidermidis*. However, its bactericidal potential was limited. Concerning *S. aureus*, the discs extracts revealed low metabolic inactivation, as well as little ability to induce bacterial death. Generally, discs proved to have limited antimicrobial activity in both bacteria tested. Therefore, it is suggested that, by manipulating the alginate degradation rate, higher amounts of strontium in the medium could be induced.

The Sr-doped microspheres were successfully produced and its characterization showed that Sr incorporation in the microspheres structure was achieved. Elementary analysis of the microspheres extracts in terms of Sr and Ca contents also revealed an increase in strontium concentration in a time dependent manner. It is to highlight that, from the tested microspheres, nHAp, nSrHAp and SrTriP were the particles with the highest antimicrobial activity and, therefore, with the highest potential to be incorporated in an antimicrobial leaching system. Despite no MIC or MBC determination, microspheres were

able to significantly reduce the cells metabolic activity, as well as to reduce bacterial culturability on solid medium, specially nSrHAp and SrTriP, highlighting the strontium antimicrobial activity. The  $\mu$ HAp,  $\mu$ SrHAp and nHAp microspheres demonstrated the lowest antimicrobial activity. The pSrTriP and pSrCO<sub>3</sub> powders also presented limited antimicrobial activity. Overall, the direct exposure of the microspheres and powders to *S. aureus* revealed better antimicrobial performance than exposure to both microsphere and discs extracts.

Based on the overall results, the Sr-rich alginate together with nSrHAp or SrTriP microspheres represent the combination with the highest potential for the development of new implant biomaterial aiming bone regeneration and the prevention of bacterial infection. Besides being an alternative strategy for its use alone, it can also be used as a complement to current treatments, such as antibiotics, which causes numerous costs to the patients and to the National Health Services and in some cases ineffectively. This can diminish antibiotic doses administrated to patients and therefore, enabling a less toxic and invasive approach.

## 5.2. Future research perspectives

Based on the experimental work and literature review performed, there are several interesting aspects which were worth of further investigation as they would provide remarkable information about the mechanisms underlying and that were not fully understood. However, time constraints made it impossible to perform.

The weakened effect of strontium in the presence of MHB medium should be further analysed in order to understand why this phenomenon occurs.

Alginate discs revealed limited antimicrobial activity compared with the microspheres, though, for instance, similar amounts of strontium were found in both SrTriP extracts and the discs extracts. Investigation should be made to understand this phenomenon.

Direct exposure of the nHAp microspheres also showed an unexpected antimicrobial activity. This together with the similar antimicrobial activity verified for the nSrHAp and SrTriP given the enormous difference in Sr composition, also points to an intrinsic antimicrobial activity for the microspheres formulated with nanometric HAp.

Experiments assessing the effect of strontium on cell surface hydrophobicity and motility, important features on the bacteria initial adhesion to a surface, colony spreading and biofilm formation are important aspect to be evaluated concerning prevention of bacterial infection.

In order to understand the strontium bactericidal mechanism of action Live/Dead microscopy could be used to evaluate the possible impairment of the cells membrane integrity, for instance.

*In vivo* experiments would be of great clinical interest as it would be possible to better evaluate the behaviour of the IHS in an organism, in the presence of the host defence mechanisms and to assess its cytotoxicity and leaching kinetics.

Regarding the potential of the system to be used as complement to current treatments, the assessment of the potential dual combination with a currently used antibiotic in bone infections would be of great interest.





## References

1. Renaudin, G., Laquerrière, P., Filinchuk, Y., Jallot, E. & Nedelec, J. M. Structural characterization of sol–gel derived Sr-substituted calcium phosphates with anti-osteoporotic and anti-inflammatory properties. *J. Mater. Chem.* **18**, 3593 (2008).
2. Rodan, G. a & Martin, T. J. Therapeutic approaches to bone diseases. *Science* **289**, 1508–1514 (2000).
3. Harvey, N., Dennison, E. & Cooper, C. Osteoporosis: impact on health and economics. *Nat. Rev. Rheumatol.* **6**, 99–105 (2010).
4. Hernlund, E. *et al.* Osteoporosis in the European Union: medical management, epidemiology and economic burden. *Arch. Osteoporos.* **8**, 136 (2013).
5. Paderni, S., Terzi, S. & Amendola, L. Major bone defect treatment with an osteoconductive bone substitute. *Chir. Organi Mov.* **93**, 89–96 (2009).
6. Burg, K. J., Porter, S. & Kellam, J. F. Biomaterial developments for bone tissue engineering. *Biomaterials* **21**, 2347–2359 (2000).
7. Rizzo, M. & Moran, S. L. Vascularized bone grafts and their applications in the treatment of carpal pathology. *Semin. Plast. Surg.* **22**, 213–227 (2008).
8. Uskoković, V. & Uskoković, D. P. Nanosized hydroxyapatite and other calcium phosphates: Chemistry of formation and application as drug and gene delivery agents. *J. Biomed. Mater. Res. - Part B Appl. Biomater.* **96 B**, 152–191 (2011).
9. Pesce, V. *et al.* Surgical approach to bone healing in osteoporosis. *Clin. Cases Miner. Bone Metab.* **6**, 131–135 (2009).
10. Beaubien, B. C. de. Antibiotic delivery system for treating an infected synovial joint during re-implantation of an orthopedic prosthesis. (2014).
11. Hetrick, E. M. & Schoenfisch, M. H. Reducing implant-related infections: active release strategies. *Chem. Soc. Rev.* **35**, 780–789 (2006).
12. Gilbert, P., Collier, P. J. & Brown, M. R. Influence of growth rate on susceptibility to antimicrobial agents: biofilms, cell cycle, dormancy, and stringent response. *Antimicrob. Agents Chemother.* **34**, 1865–1868 (1990).
13. Schierholz, J. M. & Beuth, J. Implant infections: A haven for opportunistic bacteria. *J. Hosp. Infect.* **49**, 87–93 (2001).
14. Alkhraisat, M. H. *et al.* Loading and release of doxycycline hyclate from strontium-substituted calcium phosphate cement. *Acta Biomater.* **6**, 1522–1528 (2010).
15. Drury, J. L. & Mooney, D. J. Hydrogels for tissue engineering: Scaffold design variables and applications. *Biomaterials* **24**, 4337–4351 (2003).
16. Shorr E, C. A. The usefulness of strontium as an adjuvant to calcium in the remineralization of the skeleton in man. *Bull. Hosp. Joint Dis.* **13**, 59–66 (1952).

17. Skoryna, S. C. Effects of oral supplementation with stable strontium. *Can Med Assoc J* **125**, 703–712 (1981).
18. Ravi, N. D., Balu, R. & Sampath Kumar, T. S. Strontium-substituted calcium deficient hydroxyapatite nanoparticles: Synthesis, characterization, and antibacterial properties. *J. Am. Ceram. Soc.* **95**, 2700–2708 (2012).
19. Medzhitov, R. Inflammation 2010: New Adventures of an Old Flame. *Cell* **140**, 771–776 (2010).
20. Stevens, M. M. Biomaterials for bone tissue engineering. *Mater. Today* **11**, 18–25 (2008).
21. Olszta, M. J. *et al.* Bone structure and formation: A new perspective. *Mater. Sci. Eng. R-Reports* **58**, 77–116 (2007).
22. Currey, J. D. Role of collagen and other organics in the mechanical properties of bone. *Osteoporos. Int.* **14 Suppl 5**, S29–S36 (2003).
23. Rho, J. Y., Kuhn-Spearing, L. & Zioupos, P. Mechanical properties and the hierarchical structure of bone. *Med. Eng. Phys.* **20**, 92–102 (1998).
24. Meurice, E. *et al.* New antibacterial microporous CaP materials loaded with phages for prophylactic treatment in bone surgery. *J. Mater. Sci. Mater. Med.* **23**, 2445–52 (2012).
25. Viguier-Carrin, S., Garnero, P. & Delmas, P. D. The role of collagen in bone strength. *Osteoporos. Int.* **17**, 319–336 (2006).
26. Sun, J. & Tan, H. Alginate-based biomaterials for regenerative medicine applications. *Materials* **6**, 1285–1309 (2013).
27. Narayanan, R. P., Melman, G., Letourneau, N. J., Mendelson, N. L. & Melman, A. Photodegradable iron(III) cross-linked alginate gels. *Biomacromolecules* **13**, 2465–2471 (2012).
28. Li, J., Illeperuma, W. R. K., Suo, Z. & Vlassak, J. J. Hybrid hydrogels with extremely high stiffness and toughness. *ACS Macro Lett.* **3**, 520–523 (2014).
29. Kuo, C. K. & Ma, P. X. Ionically crosslinked alginate hydrogels as scaffolds for tissue engineering: Part 1. Structure, gelation rate and mechanical properties. *Biomaterials* **22**, 511–521 (2001).
30. Chemical Structure. (2009). at [http://images.google.de/imgres?imgurl=http://www.kimica-alginate.com/img/fig\\_chemical\\_structure.jpg&imgrefurl=http://www.kimica-alginate.com/alginate/chemical\\_structure.html&h=230&w=660&tbnid=lb7pKx51\\_C-fzM:&docid=LpzyF6vqgHX2FM&ei=o](http://images.google.de/imgres?imgurl=http://www.kimica-alginate.com/img/fig_chemical_structure.jpg&imgrefurl=http://www.kimica-alginate.com/alginate/chemical_structure.html&h=230&w=660&tbnid=lb7pKx51_C-fzM:&docid=LpzyF6vqgHX2FM&ei=o)
31. Ahmed, E. M. Hydrogel: Preparation, characterization, and applications: A review. *Journal of Advanced Research* **6**, 105–121 (2015).

32. Tan, H. & Marra, K. G. Injectable, biodegradable hydrogels for tissue engineering applications. *Materials (Basel)*. **3**, 1746–1767 (2010).
33. Lee, K. Y. & Mooney, D. J. Alginate: Properties and biomedical applications. *Prog. Polym. Sci.* **37**, 106–126 (2012).
34. Balakrishnan, B. & Jayakrishnan, A. Self-cross-linking biopolymers as injectable in situ forming biodegradable scaffolds. *Biomaterials* **26**, 3941–3951 (2005).
35. Madzovska-Malagurski, I., Vukasinovic-Sekulic, M., Kostic, D. & Levic, S. Towards antimicrobial yet bioactive Cu-alginate hydrogels. *Biomed. Mater.* **11**, 035015 (2016).
36. Paredes Juárez, G. A., Spasojevic, M., Faas, M. M. & de Vos, P. Immunological and technical considerations in application of alginate-based microencapsulation systems. *Front. Bioeng. Biotechnol.* **2**, 26 (2014).
37. Crow, B. B. & Nelson, K. D. Release of bovine serum albumin from a hydrogel-cored biodegradable polymer fiber. *Biopolymers* **81**, 419–427 (2006).
38. Šupová, M. Substituted hydroxyapatites for biomedical applications: A review. *Ceram. Int.* **41**, 9203–9231 (2015).
39. Dorozhkin, S. V. Calcium orthophosphates in nature, biology and medicine. *Materials* **2**, 399–498 (2009).
40. Best, S. M., Porter, a. E., Thian, E. S. & Huang, J. Bioceramics: Past, present and for the future. *J. Eur. Ceram. Soc.* **28**, 1319–1327 (2008).
41. Kanchana, P. & Sekar, C. Influence of strontium on the synthesis and surface properties of biphasic calcium phosphate (BCP) bioceramics. *J. Appl. Biomater. Biomech.* **8**, 153–158 (2010).
42. Bohner, M. Calcium orthophosphates in medicine: From ceramics to calcium phosphate cements. *Int. J. Care Inj.* **31**, 37–47 (2000).
43. Lindner, T. *et al.* Fractures of the hip and osteoporosis: the role of bone substitutes. *J. Bone Joint Surg. Br.* **91**, 294–303 (2009).
44. Fielding, G. a., Roy, M., Bandyopadhyay, A. & Bose, S. Antibacterial and biological characteristics of silver containing and strontium doped plasma sprayed hydroxyapatite coatings. *Acta Biomater.* **8**, 3144–3152 (2012).
45. Landi, E., Tampieri, A., Celotti, G. & Sprio, S. Densification behaviour and mechanisms of synthetic hydroxyapatites. *J. Eur. Ceram. Soc.* **20**, 2377–2387 (2000).
46. Kannan, S., Rebelo, A., Lemos, A. F., Barba, A. & Ferreira, J. M. F. Synthesis and mechanical behaviour of chlorapatite and chlorapatite/??-TCP composites. *J. Eur. Ceram. Soc.* **27**, 2287–2294 (2007).
47. Kim, S. J., Bang, H. G., Song, J. H. & Park, S. Y. Effect of fluoride additive on the mechanical properties of hydroxyapatite/alumina composites. *Ceram. Int.* **35**, 1647–

- 1650 (2009).
48. Rodríguez-Valencia, C. *et al.* Novel selenium-doped hydroxyapatite coatings for biomedical applications. *J. Biomed. Mater. Res. - Part A* **101 A**, 853–861 (2013).
  49. Wang, Y. *et al.* Dual functional selenium-substituted hydroxyapatite. *Interface Focus* **2**, 378–386 (2012).
  50. Zamani, A., Omrani, G. R. & Nasab, M. M. Lithium's effect on bone mineral density. *Bone* **44**, 331–334 (2009).
  51. Kannan, S., Ventura, J. M. G., Lemos, A. F., Barba, A. & Ferreira, J. M. F. Effect of sodium addition on the preparation of hydroxyapatites and biphasic ceramics. *Ceram. Int.* **34**, 7–13 (2008).
  52. Weissmueller, N. T., Schiffter, H. A., Pollard, A. J. & Cuneyt Tas, A. Molten salt synthesis of potassium-containing hydroxyapatite microparticles used as protein substrate. *Mater. Lett.* **128**, 421–424 (2014).
  53. Heidenau, F. *et al.* A novel antibacterial titania coating: Metal ion toxicity and in vitro surface colonization. *J. Mater. Sci. Mater. Med.* **16**, 883–888 (2005).
  54. Albrektsson, T. & Johansson, C. Osteoinduction, osteoconduction and osseointegration. *Eur. Spine J.* **10**, 96–101 (2001).
  55. Kurashina, K., Kurita, H., Wu, Q., Ohtsuka, a. & Kobayashi, H. Ectopic osteogenesis with biphasic ceramics of hydroxyapatite and tricalcium phosphate in rabbits. *Biomaterials* **23**, 407–412 (2002).
  56. Alsberg, E., Anderson, K. W., Albeirutti, A., Franceschi, R. T. & Mooney, D. J. Cell-interactive Alginate Hydrogels for Bone Tissue Engineering. *J. Dent. Res.* **80**, 2025–2029 (2001).
  57. Trippel, S. B., Coutts, R. D., Einhorn, T. A., Mundy, G. R. & Rosenfeld, R. G. Growth factors as therapeutic agents. *J. Bone Jt. Surg.* **78-A**, 1272–1286 (1996).
  58. Signore, A. About inflammation and infection. *EJNMMI Res.* **3**, 8 (2013).
  59. Anderson, J. M. Chapter 4 Mechanisms of inflammation and infection with implanted devices. *Cardiovasc. Pathol.* **2**, 33–41 (1993).
  60. Serhan, C. N. *et al.* Resolution of inflammation: state of the art, definitions and terms. *FASEB J.* **21**, 325–32 (2007).
  61. Medzhitov, R. Origin and physiological roles of inflammation. *Nature* **454**, 428–435 (2008).
  62. Dunkelberger, J. R. & Song, W. Complement and its role in innate and adaptive immune responses. *Cell Res.* **20**, 34–50 (2010).
  63. Gristina, a G. Biomaterial-centered infection: microbial adhesion versus tissue integration. *Science* **237**, 1588–1595 (1987).
  64. Malone, D. L., Genuit, T., Tracy, J. K., Gannon, C. & Napolitano, L. M. Surgical site

- infections: reanalysis of risk factors. *J. Surg. Res.* **103**, 89–95 (2002).
65. Cheadle, W. G. Risk factors for surgical site infection. *Surg. Infect. (Larchmt)*. **7 Suppl 1**, S7–11 (2006).
66. Ferreira, L. & Zumbuehl, a. Non-leaching surfaces capable of killing microorganisms on contact. *J. Mater. Chem.* **19**, 7796 (2009).
67. Darley, E. S. R. & MacGowan, A. P. Antibiotic treatment of Gram-positive bone and joint infections. *Journal of Antimicrobial Chemotherapy* **53**, 928–935 (2004).
68. Costerton, J. W., Montanaro, L. & Arciola, C. R. Biofilm in implant infections: its production and regulation. *Int. J. Artif. Organs* **28**, 1062–8 (2005).
69. Brown, L., Wolf, J. M., Prados-Rosales, R. & Casadevall, A. Through the wall: extracellular vesicles in Gram-positive bacteria, mycobacteria and fungi. *Nat. Rev. Microbiol.* **13**, 620–30 (2015).
70. Namvar, A. E. *et al.* Clinical characteristics of Staphylococcus epidermidis: a systematic review. *GMS Hyg. Infect. Control* **9**, Doc23 (2014).
71. Foster, T. J. Immune evasion by staphylococci. *Nat.Rev.Microbiol.* **3**, 948–958 (2005).
72. Polgreen, P. M. & Herwaldt, L. a. Staphylococcus aureus Colonization and Nosocomial Infections: Implications for Prevention. *Curr. Infect. Dis. Rep.* **6**, 435–441 (2004).
73. Lowy, F. D. Staphylococcus aureus infections. *N. Engl. J. Med.* **339**, 520–32 (1998).
74. Anderson, D. J., Sexton, D. J., Kanafani, Z. A., Auten, G. & Kaye, K. S. Severe surgical site infection in community hospitals: epidemiology, key procedures, and the changing prevalence of methicillin-resistant Staphylococcus aureus. *Infect.Control Hosp.Epidemiol.* **28**, 1047–1053 (2007).
75. Otto, M. Staphylococcus epidermidis--the 'accidental' pathogen. *Nat. Rev. Microbiol.* **7**, 555–67 (2009).
76. Villatte, G. *et al.* Photoactive TiO<sub>2</sub> antibacterial coating on surgical external fixation pins for clinical application. *Int. J. Nanomedicine* **10**, 3367–75 (2015).
77. Campoccia, D., Montanaro, L. & Arciola, C. R. The significance of infection related to orthopedic devices and issues of antibiotic resistance. *Biomaterials* **27**, 2331–2339 (2006).
78. Alhede, M., Jensen, P., Givskov, M. & Bjarnsholt, T. Biofilm of Medical Importance. *Eolss.Net* **XII**, (1999).
79. Abouelhassan, Y. *et al.* Discovery of quinoline small molecules with potent dispersal activity against methicillin-resistant Staphylococcus aureus and Staphylococcus epidermidis biofilms using a scaffold hopping strategy. *Bioorganic Med. Chem. Lett.* **24**, 5076–5080 (2014).

80. Stoodley, P., Sauer, K., Davies, D. G. & Costerton, J. W. Biofilms as complex differentiated communities. *Annu. Rev. Microbiol.* **56**, 187–209 (2002).
81. Hall-Stoodley, L. & Stoodley, P. Biofilm formation and dispersal and the transmission of human pathogens. *Trends in Microbiology* **13**, 7–10 (2005).
82. Srey, S., Jahid, I. K. & Ha, S. Do. Biofilm formation in food industries: A food safety concern. *Food Control* **31**, 572–585 (2013).
83. Abdel-aziz, S. M. & Aeron, a. Bacterial Biofilm: Dispersal and Inhibition Strategies. *SAJ Bio-technol* **1**, 1–10 (2014).
84. Sanchez, C. J. *et al.* Effects of local delivery of d-amino acids from biofilm-dispersive scaffolds on infection in contaminated rat segmental defects. *Biomaterials* **34**, 7533–7543 (2013).
85. Simões, M., Bennett, R. N. & Rosa, E. a S. Understanding antimicrobial activities of phytochemicals against multidrug resistant bacteria and biofilms. *Nat. Prod. Rep.* **26**, 746–757 (2009).
86. Paraje, M. G. Antimicrobial resistance in biofilms. *Sci. against Microb. Pathog. Commun. Curr. Res. Technol. Adv.* **2**, 736–744 (2011).
87. Bjarnsholt, T., Ciofu, O., Molin, S., Givskov, M. & Høiby, N. Applying insights from biofilm biology to drug development - can a new approach be developed? *Nat. Rev. Drug Discov.* **12**, 791–808 (2013).
88. Ewald, A. *et al.* Silver-doped calcium phosphate cements with antimicrobial activity. *Acta Biomater.* **7**, 4064–4070 (2011).
89. Kingshott, P., Wei, J., Bagge-Ravn, D., Gadegaard, N. & Gram, L. Covalent attachment of poly(ethylene glycol) to surfaces, critical for reducing bacterial adhesion. *Langmuir* **19**, 6912–6921 (2003).
90. von Eiff, C., Kohnen, W., Becker, K. & Jansen, B. Modern strategies in the prevention of implant-associated infections. *Int. J. Artif. Organs* **28**, 1146–1156 (2005).
91. Samuel P. Sawan, Tadmor Shalon, Sundar Subramanyam, A. Y. Contact-killing non-leaching antimicrobial materials. (1998).
92. Woo, G. L. Y. *et al.* Biological characterization of a novel biodegradable antimicrobial polymer synthesized with fluoroquinolones. *J. Biomed. Mater. Res.* **59**, 35–45 (2002).
93. Ginebra, M.-P. P., Canal, C., Espanol, M., Pastorino, D. & Montufar, E. B. Calcium phosphate cements as drug delivery materials. *Adv. Drug Deliv. Rev.* **64**, 1090–1110 (2012).
94. Lin, Y., Yang, Z., Cheng, J. & Wang, L. Synthesis, characterization and antibacterial property of strontium half and totally substituted hydroxyapatite nanoparticles. *J. Wuhan Univ. Technol. Mater. Sci. Ed.* **23**, 475–479 (2008).
95. Hobman, J. L. & Crossman, L. C. Bacterial antimicrobial metal ion resistance. *J. Med.*

- Microbiol.* **64**, 471–497 (2014).
96. Grace, M., Chand, N. & Bajpai, S. Copper alginate-cotton cellulose (CACC) fibers with excellent antibacterial properties. *J Eng Fiber Fabr* **4**, 24–35 (2009).
  97. Varaprasad, K., Raghavendra, G. M., Jayaramudu, T. & Seo, J. Nano zinc oxide-sodium alginate antibacterial cellulose fibres. *Carbohydr. Polym.* **135**, 349–355 (2016).
  98. Ray, S. *et al.* Anticancer and antimicrobial metallopharmaceutical agents based on palladium, gold, and silver N-heterocyclic carbene complexes. *J. Am. Chem. Soc.* **129**, 15042–15053 (2007).
  99. Ge, R. & Sun, H. Bioinorganic chemistry of bismuth and antimony: Target sites of metallodrugs. *Acc. Chem. Res.* **40**, 267–274 (2007).
  100. Garner, J. P. & Heppell, P. S. J. Cerium nitrate in the management of burns. *Burns* **31**, 539–547 (2005).
  101. Chitambar, C. R. Medical applications and toxicities of gallium compounds. *International Journal of Environmental Research and Public Health* **7**, 2337–2361 (2010).
  102. Porter, F., Silver, S., Ong, C. & Nakahara, H. Selection for mercurial resistance in hospital settings. *Antimicrob. Agents Chemother.* **22**, 852–858 (1982).
  103. Colwell, R. R. Toxic Effects of Pollutants on Microorganisms. *Princ. Ectotoxicology* **4**, 275–288 (1988).
  104. Taylor, D. E. Bacterial tellurite resistance. *Trends in Microbiology* **7**, 111–115 (1999).
  105. Aarestrup, F. M. & Hasman, H. Susceptibility of different bacterial species isolated from food animals to copper sulphate, zinc chloride and antimicrobial substances used for disinfection. *Vet. Microbiol.* **100**, 83–89 (2004).
  106. Dahl, S. G. *et al.* Incorporation and distribution of strontium in bone. *Bone* **28**, 446–453 (2001).
  107. Boivin, G. *et al.* Strontium distribution and interactions with bone mineral in monkey iliac bone after strontium salt (S 12911) administration. *J. Bone Miner. Res.* **11**, 1302–11 (1996).
  108. Reeve, J., Green, J., Maletskos, C. & Neer, R. Skeletal retention of <sup>45</sup>Ca and <sup>85</sup>Sr compared: Further studies on intravenously injected <sup>85</sup>Sr as a tracer for skeletal calcium. *Calcif. Tissue Int.* **35**, 9–15 (1983).
  109. Cohen-Solal, M. Strontium overload and toxicity: impact on renal osteodystrophy. *Nephrol. Dial. Transplant* **17 Suppl 2**, 30–4 (2002).
  110. Zhang, W. *et al.* Effects of strontium in modified biomaterials. *Acta Biomater.* **7**, 800–808 (2011).
  111. Bigi, A., Boanini, E., Capuccini, C. & Gazzano, M. Strontium-substituted

- hydroxyapatite nanocrystals. *Inorganica Chim. Acta* **360**, 1009–1016 (2007).
112. Neves, N. *et al.* Strontium-rich injectable hybrid system for bone regeneration. *Mater. Sci. Eng. C* **59**, 818–827 (2016).
  113. Marques, C. F. *et al.* Antibiotic-loaded Sr-doped porous calcium phosphate granules as multifunctional bone grafts. *Ceram. Int.* **42**, 2706–2716 (2016).
  114. Sampath Kumar, T. S., Madhumathi, K., Rubaiya, Y. & Doble, M. Dual Mode Antibacterial Activity of Ion Substituted Calcium Phosphate Nanocarriers for Bone Infections. *Front. Bioeng. Biotechnol.* **3**, 1–10 (2015).
  115. Roy, M., Fielding, G. a., Bandyopadhyay, A. & Bose, S. Effects of zinc and strontium substitution in tricalcium phosphate on osteoclast differentiation and resorption. *Biomater. Sci.* 74–82 (2013). doi:10.1039/c2bm00012a
  116. Romieu, G., Garric, X., Munier, S., Vert, M. & Boudeville, P. Calcium-strontium mixed phosphate as novel injectable and radio-opaque hydraulic cement. *Acta Biomater.* **6**, 3208–15 (2010).
  117. Bonnelye, E., Chabadel, A., Saltel, F. & Jurdic, P. Dual effect of strontium ranelate: Stimulation of osteoblast differentiation and inhibition of osteoclast formation and resorption in vitro. *Bone* **42**, 129–138 (2008).
  118. Brauer, D. S. *et al.* Bactericidal strontium-releasing injectable bone cements based on bioactive glasses. *J. R. Soc. Interface* 1–8 (2012). doi:10.1098/rsif.2012.0647
  119. Gentleman, E. *et al.* The effects of strontium-substituted bioactive glasses on osteoblasts and osteoclasts in vitro. *Biomaterials* **31**, 3949–3956 (2010).
  120. Hurtel-Lemaire, A. S. *et al.* The calcium-sensing receptor is involved in Strontium ranelate-induced osteoclast apoptosis new insights into the associated signaling pathways. *J. Biol. Chem.* **284**, 575–584 (2009).
  121. Marie, P. J. The calcium-sensing receptor in bone cells: A potential therapeutic target in osteoporosis. *Bone* **46**, 571–576 (2010).
  122. Yang, F. *et al.* Strontium enhances osteogenic differentiation of mesenchymal stem cells and in vivo bone formation by activating Wnt/catenin signaling. *Stem Cells* **29**, 981–991 (2011).
  123. Tat, S. K., Pelletier, J.-P., Mineau, F., Caron, J. & Martel-Pelletier, J. Strontium ranelate inhibits key factors affecting bone remodeling in human osteoarthritic subchondral bone osteoblasts. *Bone* **49**, 559–67 (2011).
  124. Armstrong, A. P. *et al.* A RANK/TRAF6-dependent signal transduction pathway is essential for osteoclast cytoskeletal organization and resorptive function. *J. Biol. Chem.* **277**, 44347–44356 (2002).
  125. Khosla, S. Minireview: The OPG/RANKL/RANK system. *Endocrinology* **142**, 5050–5055 (2001).



126. Rousselle, a. V. *et al.* Influence of metal ion solutions on rabbit osteoclast activities in vitro. *Histol. Histopathol.* **17**, 1025–1032 (2002).
127. Marie, P. J., Ammann, P., Boivin, G. & Rey, C. Mechanisms of action and therapeutic potential of strontium in bone. *Calcif. Tissue Int.* **69**, 121–129 (2001).
128. Morohashi, T., Sano, T. & Yamada, S. Effects of strontium on calcium metabolism in rats. I. A distinction between the pharmacological and toxic doses. *Jpn. J. Pharmacol.* **64**, 155–162 (1994).
129. Fu, Y.-F. & Chen, D.-M. The influence of Sr<sup>2+</sup> on the cytotoxicity of strontium substituted hydroxyapatite (Sr-HA). *Gongneng Cailiao/Journal Funct. Mater.* **39**, 645–646+650 (2008).
130. Fu, Y., Chen, D. & Zhang, J. Cytotoxicity of the strontium-substituted hydroxyapatite evaluated by MTT colorimetry. *Sheng Wu Yi Xue Gong Cheng Xue Za Zhi* **18**, 389–390, 415 (2001).
131. Qiu, K., Zhao, X. J., Wan, C. X., Zhao, C. S. & Chen, Y. W. Effect of strontium ions on the growth of ROS17/2.8 cells on porous calcium polyphosphate scaffolds. *Biomaterials* **27**, 1277–1286 (2006).
132. Gopi, D., Ramya, S., Rajeswari, D., Karthikeyan, P. & Kavitha, L. Strontium, cerium co-substituted hydroxyapatite nanoparticles: Synthesis, characterization, antibacterial activity towards prokaryotic strains and in vitro studies. *Colloids Surfaces A Physicochem. Eng. Asp.* **451**, 172–180 (2014).
133. Feng, Q. L. *et al.* A mechanistic study of the antibacterial effect of silver ions on Escherichia coli and Staphylococcus aureus. *J. Biomed. Mater. Res.* **52**, 662–668 (2000).
134. Zhang, L. *et al.* Antibacterial activities of mechanochemically synthesized perovskite strontium titanate ferrite metal oxide. *Colloids Surfaces A Physicochem. Eng. Asp.* **456**, 169–175 (2014).
135. Rajeswari, D., Gopi, D., Ramya, S. & Kavitha, L. Investigation of anticorrosive, antibacterial and in vitro biological properties of a sulphonated poly(etheretherketone)/strontium, cerium co-substituted hydroxyapatite composite coating developed on surface treated surgical grade stainless steel for orth. *RSC Adv.* **4**, 61525–61536 (2014).
136. Geng, Z. *et al.* Strontium incorporation to optimize the antibacterial and biological characteristics of silver-substituted hydroxyapatite coating. *Mater. Sci. Eng. C* **58**, 467–477 (2016).
137. O’Sullivan, C. *et al.* Deposition of substituted apatites with anticolonizing properties onto titanium surfaces using a novel blasting process. *J. Biomed. Mater. Res. - Part B Appl. Biomater.* **95**, 141–149 (2010).

138. Hu, C., Guo, J., Qu, J. & Hu, X. Efficient destruction of bacteria with Ti(IV) and antibacterial ions in co-substituted hydroxyapatite films. *Appl. Catal. B Environ.* **73**, 345–353 (2007).
139. A. Guida, M. R. Towler, J. G. W. Preliminary work on the antibacterial effect of strontium in glass ionomer cements. *J. Mater. Sci. Lett.* **22**, 1401–1403 (2003).
140. Dabsie, F., Gregoire, G., Sixou, M. & Sharrock, P. Does strontium play a role in the cariostatic activity of glass ionomer?. Strontium diffusion and antibacterial activity. *J. Dent.* **37**, 554–559 (2009).
141. Eisenberg, A. D., Oldershaw, M. D., Curzon, M. E. & Handelman, S. L. Effects of fluoride, lithium, and strontium on growth and acid production of mutants streptococci and *Actinomyces viscosus*. *Caries Res* **25**, 179–184 (1991).
142. Liu, J., Rawlinson, S. C. F., Hill, R. G. & Fortune, F. Strontium-substituted bioactive glasses in vitro osteogenic and antibacterial effects. *Dent. Mater.* 1–11 (2015). doi:10.1016/j.dental.2015.12.013
143. Greena, J. A. M., Shajan, X. S., Karuppasamy, K., Antony, R. & Kumaresan, and S. Biocidal action of metal (Mg/Cu/Ni/Zn) doped strontium formate dihydrate crystal against bacterial and fungal strains. *Der Chem. Sin.* **3**, 1229–1238 (2012).
144. Lee, D., Cohen, R. E. & Rubner, M. F. Antibacterial properties of Ag nanoparticle loaded multilayers and formation of magnetically directed antibacterial microparticles. *Langmuir* **21**, 9651–9659 (2005).
145. Slawson, R. M., Van Dyke, M. I., Lee, H. & Trevors, J. T. Germanium and silver resistance, accumulation, and toxicity in microorganisms. *Plasmid* **27**, 72–79 (1992).
146. Russell, A. D. & Hugo, W. B. 7 Antimicrobial Activity and Action of Silver. *Prog. Med. Chem.* **31**, 351–370 (1994).
147. Holt, K. B. & Bard, A. J. Interaction of silver(I) ions with the respiratory chain of *Escherichia coli*: An electrochemical and scanning electrochemical microscopy study of the antimicrobial mechanism of micromolar Ag. *Biochemistry* **44**, 13214–13223 (2005).
148. Hajipour, M. J. *et al.* Antibacterial properties of nanoparticles. *Trends in Biotechnology* **30**, 499–511 (2012).
149. Ribeiro, C. C., Barrias, C. C. & Barbosa, M. A. Preparation and characterisation of calcium-phosphate porous microspheres with a uniform size for biomedical applications. *J. Mater. Sci. Mater. Med.* **17**, 455–463 (2006).
150. Wiegand, I., Hilpert, K. & Hancock, R. E. W. Agar and broth dilution methods to determine the minimal inhibitory concentration (MIC) of antimicrobial substances. *Nat. protoc.* **3**, 163–175 (2008).
151. Monte, J., Abreu, A., Borges, A., Simões, L. & Simões, M. Antimicrobial Activity of

- Selected Phytochemicals against *Escherichia coli* and *Staphylococcus aureus* and Their Biofilms. *Pathogens* **3**, 473–498 (2014).
152. EAGLE, H. & MUSSELMAN, A. D. The rate of bactericidal action of penicillin in vitro as a function of its concentration, and its paradoxically reduced activity at high concentrations against certain organisms. *J. Exp. Med.* **88**, 99–131 (1948).
  153. Arciola, C. R., Campoccia, D., Ehrlich, G. D. & Montanaro, L. Biofilm-based implant infections in orthopaedics. *Adv. Exp. Med. Biol.* **830**, 29–46 (2015).
  154. Augst, A. D., Kong, H. J. & Mooney, D. J. Alginate hydrogels as biomaterials. *Macromol. Biosci.* **6**, 623–633 (2006).
  155. Kumar, R. & Münstedt, H. Silver ion release from antimicrobial polyamide/silver composites. *Biomaterials* **26**, 2081–2088 (2005).

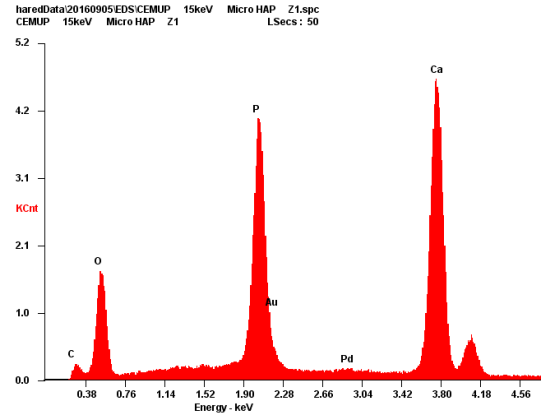
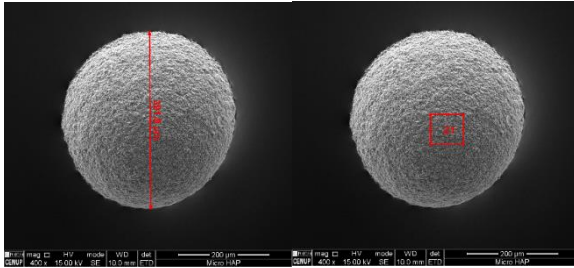


# Appendix

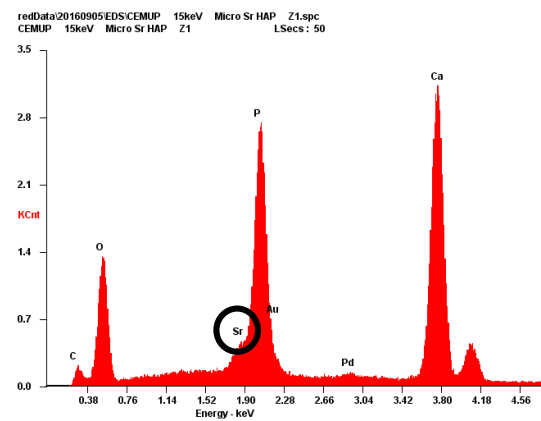
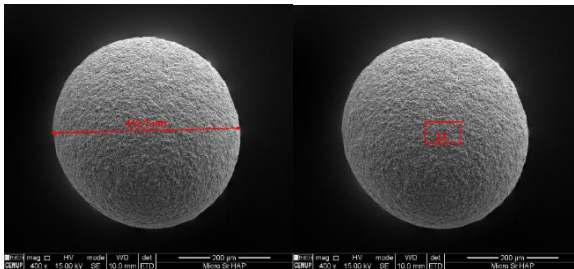
## Appendix 1

SEM/EDS analysis. Size (diameter) and EDS analysis of the produced microspheres.

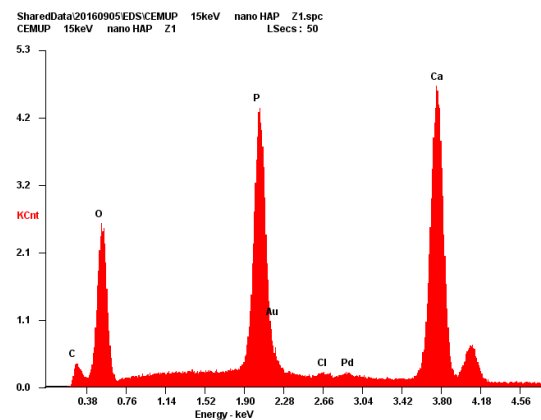
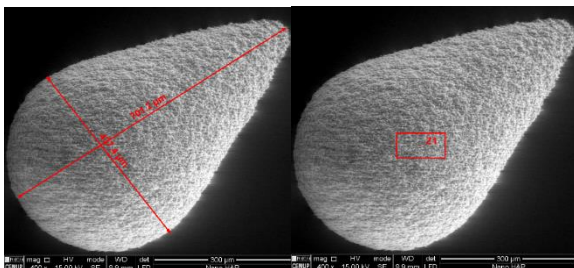
### $\mu$ HAp



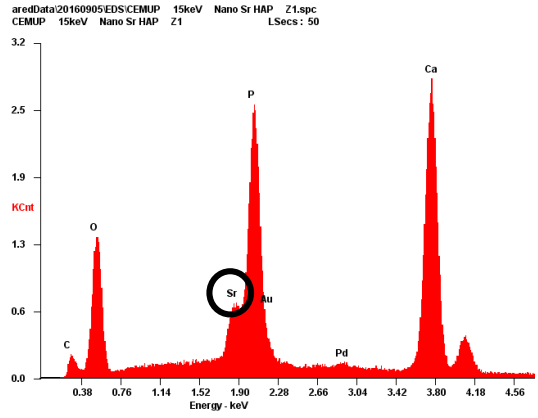
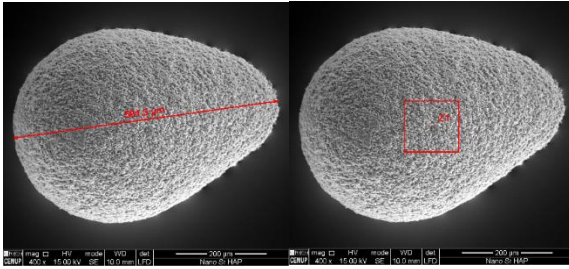
### $\mu$ SrHAp



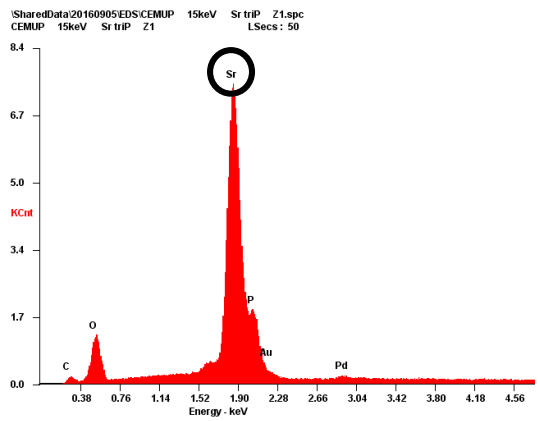
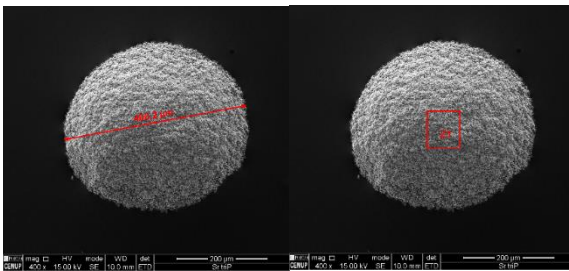
### nHAp



### nSrHAp

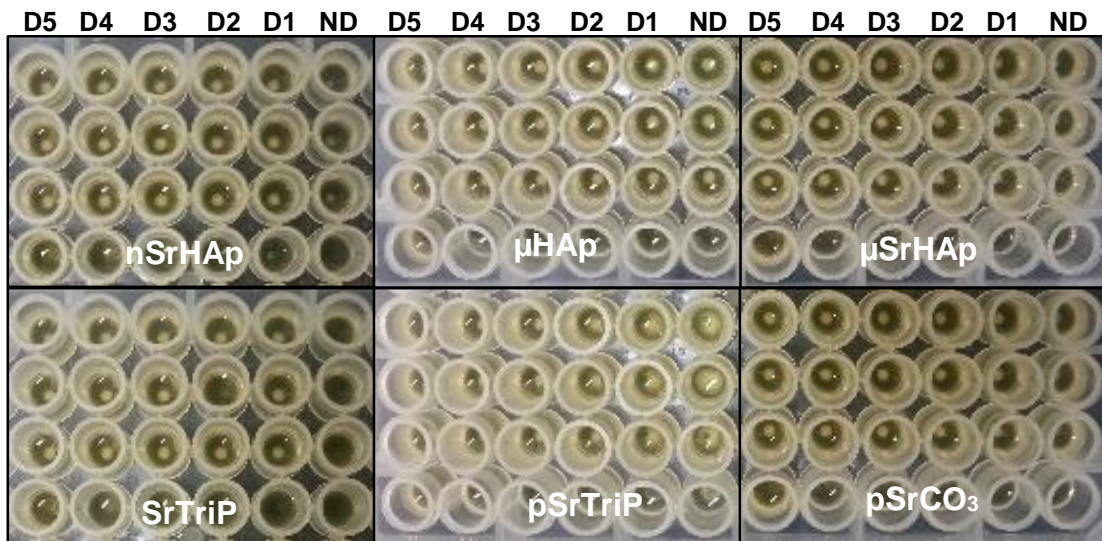


### SrTriP



## Appendix 2

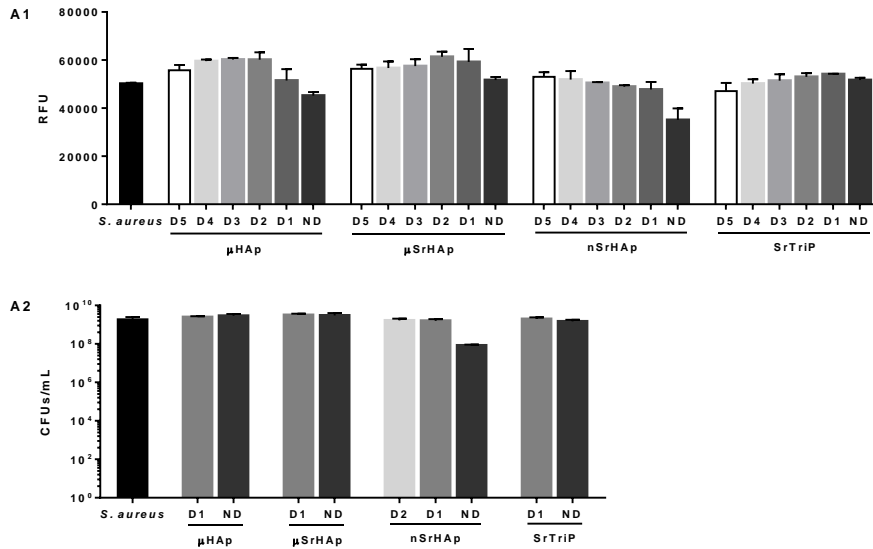
MIC after challenging *S. aureus* to 72h microspheres and powders extracts. A MIC was determined for the ND extract of SrTriP microspheres noticeable by visual inspection to inhibit bacterial growth. The ND extracts of nSrHAp microspheres did not reveal by visual inspection a MIC, however it is clear the inhibition of bacterial growth in some extent. No inhibition is visually observed for any of the extracts and its dilutions for  $\mu$ HAp,  $\mu$ SrHAp, pSrTriP or pSrCO<sub>3</sub>.



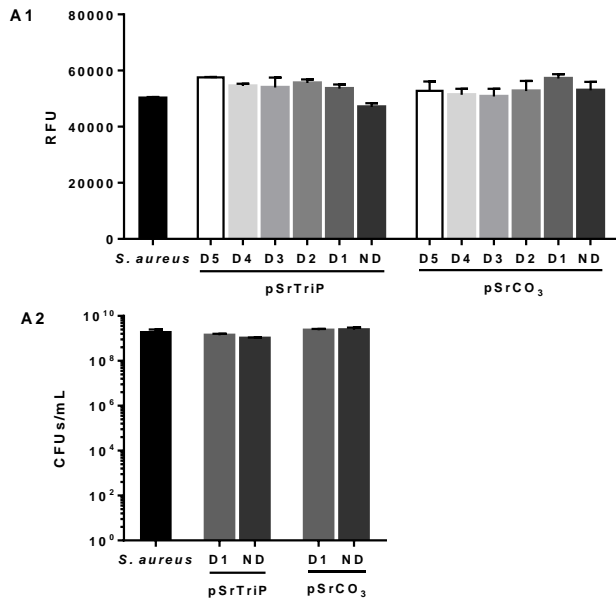


### Appendix 3

Evaluation of the bactericidal properties of 21 days extracts of the microspheres and powders against *S. aureus*. These results were excluded from the main text given to lack of confidence on the viability of the extract as described above.



**Antimicrobial evaluation of the 21 days microspheres extracts towards *S. aureus*.** **A1**– Metabolic activity evaluation. Relative fluorescence units (RFU) are presented as a function of the extract dilutions. **A2** – Bacteria culturability. CFUs count are presented as a function of the extracts dilutions used. *S. aureus* represents the negative control (no treatment). Mean values  $\pm$  standard deviation are illustrated.



**Antimicrobial evaluation of the 21 days powder extracts towards *S. aureus*.** **A1**– Metabolic activity evaluation. Relative fluorescence units (RFU) are presented as a function of the extract dilutions. **A2** – Bacteria culturability. CFUs count are presented as a function of the extracts dilutions used. *S. aureus* represents the negative control (no treatment). Mean values ± standard deviation are illustrated.

Percentages of metabolic activity inhibition and percentages of kill for *S. aureus* after exposure to 72 hr extracts of the microspheres and powders

Material		μHAp	μSrHAp	nHAp	nSrHAp	SrTriP	pSrTriP	pSrCO <sub>3</sub>
Extracts time (h-hours; d-days)		21d						
<b>Metabolic activity inhibition (%)</b>								
extracts dilutions	D5	10	0	-	0	6	0	0
	D4	3	0	-	0	0	0	0
	D3	0	0	-	0	0	0	0
	D2	0	0	-	3	0	0	0
	D1	0	0	-	5	0	0	0
	ND	0	0	-	32	0	7	0
<b>Percentage of kill (%)</b>								
Extracts dilutions	D2	-	-	-	0	-	-	-
	D1	0	0	-	1	0	1	0
	ND	0	0	-	14	1	3	0

#### Appendix 4

Gradual changes in turbidity of the medium after 24h direct exposure of increasing concentrations of SrTriP microspheres to *S. aureus*.

